UNIVERSITY OF NAPOLI FEDERICO II

Doctorate School in Molecular Medicine

Doctorate Program in
Genetics and Molecular Medicine
Coordinator: Prof. Lucio Nitsch
XXVIII Cycle

"Exploring the role of Fig4 and Synj1 in the membrane trafficking and neurodegenaration in Charcot Marie Tooth 4J and Parkinson neuropathies"

DOMINGA FASANO

Napoli 2016

Tutor
Prof. S. Paladino

“Exploring the role of Fig4 and Synj1 in the membrane trafficking and neurodegenaration in Charcot Marie Tooth 4J and Parkinson neuropathies”

TABLE OF CONTENTS

LIST OF ABBREVIATIONS

AD	Autosomal Dominant
AP2	Adaptor Protein complex 2
AR	Autosomal Recessive
CMAP	Compound Muscle Action Potentials
CMT	Charcot-Marie Tooth
CMT4J	Charcot-Marie Tooth disease 4J
DAG	Diacylglycerol
Eps15	Epidermal growth factor receptor pathway substrate 15
ER	Endoplasmic Reticulum
GABA	γ-aminobutyric acid
GAPs	GTPase activating proteins
GEFs	Guanine nucleotide Exchange Factors
Grb2	Growth factor receptor-bound protein 2
GWAS	Genome-Wide Association Studies
HMSN	Hereditary Motor and Sensory Neuropathy
Ins-1,4,5-P3	Inositol 1,4,5-trisphosphate
LRRK2	Leucine-Rich Repeat Kinase 2
NCV	Nerve Conduction Velocity
NGS	Next Generation Sequencing
NPF	Asparagineproline-phenylalanine domain
ORFs	Open Reading Frames
PD	Parkinson Disease
PI	Phosphoinositide
PI3Ks	PtdIns 3-OH kinases
PI4Ks	PtdIns 4-OH kinases
PI5K	PtdIns 5-kinase
PIPKs	Phosphoinositide-kinases
PLC	Phospholipase C
PLT	Pale Tremor
PRD	Proline-Rich Domain
PtdIns	Phosphatidilisosito
PIs	Phophoinositides

PTEN	Phosphatase and Tensin homolog
PTP	Protein Tyrosine phosphatase
Sac	Suppressor of Actin
Sac3	SAC domain-containing protein 3
SacN	SAC N-terminal sub-domain
SNCA	Alpha-synuclein
SNpc	Substantia Nigra Pars Compacta
Synj1	Synaptojanin 1
VPS35	Vacuolar Protein Sorting-Associated Protein 35

ABSTRACT

ABSTRACT

Homeostasis of eukaryotic cells is largely dependent on dynamic compartmentalization of the endo-membrane system. The membrane trafficking linking different organelles is essential to maintain a proper composition of various compartments as well as to transport various molecules to appropriate compartments. Thus, the molecular machinery regulating properly the intracellular membrane trafficking has a key role in the maintenance of organelle functionality and cell viability. It is not surprising that alterations in membrane trafficking can result in different pathologies. Respect to other cell types nervous system is more sensitive to disturbances of the membrane trafficking. Hence, to understand how alterations of the intracellular trafficking could lead to neurodegeneration, we focused our attention on two nervous system disorders, Charcot-Marie Tooth disease 4J (CMT4J) and Parkinson disease (PD), both caused by mutations of an inositol phospahatase (Fig4 and Synj1, respectively). Together with specific kinases, the activity of phospahatases control, the levels of phosphoinosities (PI), a class of phospholipids that even more is emerging to be involved in the regulation of membrane trafficking.

Numerous findings highlighted that the levels of PI might be finely regulated, in time and in the space, and are critical for membrane homeostasis. Specifically PI metabolism seems critical for nervous system functions.

Aim of my PhD project was to explore the role of Fig4 and Synj1 in the membrane trafficking and neurodegenaration in CMT4J and Parkinson neuropathies.

INTRODUCTION

INTRODUCTION

Homeostasis of eukaryotic cells is largely dependent on dynamic compartmentalization of the endo-membrane system. Intracellular compartments are designed so that they can exchange materials and undergo dramatic morphological changes in order to meet the demands of metabolism, growth, and environment. Hence, membrane trafficking linking different organelles is essential to maintain a proper composition of various compartments as well as to transport various molecules to appropriate compartments. Two pathways mainly achieve this: the biosynthetic secretion and the endocytic route. The anterograde flow is counterbalanced by retrograde transport, which is essential for the maintenance of organelle homeostasis and re-use of components of the trafficking machineries. The out-going and in-coming pathways communicate through bidirectional transport between the Golgi complex and endosomes. Strikingly, the endosomal system, which is a crossroads of distinct intracellular pathways, has emerged and is still emerging more as key player in the sorting of molecules throughout the cell.

Thus, the molecular machinery regulating properly the intracellular membrane trafficking has a key role in the maintenance of organelle functionality and cell viability. It is not surprising that alterations in membrane trafficking can result in different pathologies. Indeed, genetic defects of cargo proteins or components of the trafficking machinery (responsible for cargo sorting, tethering, docking and fusion of vesicles at the target membrane as for their motility) leading to abnormal trafficking have been found involved in a large number of different human diseases. Interestingly, respect to other cell types nervous system is more sensitive to disturbances of the membrane trafficking as supported by the fact that various neurodegenerative and neurological disorders are caused by mutations or dysfunction of trafficking machinery components.

Main goal of my laboratory is to unravel the role of membrane trafficking in the proper functions of nervous system as to understand how alterations of the intracellular trafficking could lead to neurodegeneration. In particular, during my PhD programme we focused our attention on two nervous system

disorders, Charcot-Marie Tooth disease 4J (CMT4J) and Parkinson disease (PD), both caused by mutations of a lipid phosphatase.

CHARCOT MARIE TOOTH (CMT)

Charcot Marie Tooth disease (CMT) is an inherited group of peripheral neuropathies bearing the name of the three doctors (Jean Charcot, Pierre Marie and Howar Henry Tooth) who described the disease for the first time in 1886. CMT, also referred to as hereditary motor and sensory neuropathy (HMSN), is the most common inherited degenerative disorder of the peripheral nervous system with a prevalence of about 1 in 2500 persons (Saporta et al, 2011; Patzko and Shy, 2011; Reilly et al, 2011; Tazir et al, 2013).

Clinically, CMT diseases are characterized by distal muscle weakness and atrophy, sensory loss affecting the feet and hands, hyporeflexia (Saporta et al, 2011; Patzko and Shy, 2011; Reilly et al, 2011). Additionally, deep tendon reflexes are often depressed and skeletal anomalies such as hammertoe deformity and pes cavus are present (Saporta et al, 2011; Patzko and Shy, 2011; Reilly et al, 2011). There can be a wide age of onset and severity range in CMT both inter- as well as intra-familial (Patzko and Shy, 2011; Reilly et al, 2011; Siskind et al, 2013). Most patients begin to show symptoms within the first two decades of life, while others develop few if any symptoms until adulthood. However, many patients are affected by severe forms developing in infancy or early childhood, which were also classified as congenital hypomyelinating neuropathy and Dejerine-Sottas neuropathy (Reilly et al, 2011; Saporta et al, 2011). Life span is not shortened, though quality of life may be decreased since patients usually remain ambulatory throughout their life and often need ankle-foot orthotics (Arnold et al, 2005).

The historical classification based on nerve conduction velocity (NCV) of median or ulnar nerve (Harding and Thomas, 1980) is fundamental and remains the cornerstone of modern diagnosis. By this electrophysiological parameter, CMT are classified in two main types: CMT1 (also defined demyelinating) characterized by NCV <38 m/s; CMT2 (also defined axonal) with a NCV> 38 m/s (Saporta et al, 2011; Reilly et al, 2011; Tazir et al, 2013).

Intermediate forms with intermediate values of NCV between 35 and 45 m /s were also identified (Saporta et al, 2011; Reilly et al, 2011; Tazir et al, 2013).

The current classification is based on the combination of the electrophysiological parameter, inheritance pattern and causative genes (Fig. 1). While intermediate forms of CMT are mainly dominant (AD), CMT1 and CMT2 are inherited both as an autosomal dominant trait as well as autosomal recessive (AR) and X-linked trait (Reilly et al, 2011; Siskind et al; 2013). The prevalence varies in different populations. In Western Europe, United States and Japan the dominant forms are by far the most frequent, whereas in the Mediterranean basin and Middle East communities, with high percentage of consanguineous marriages, autosomal recessive forms account for 30-50% of all CMT cases (Reilly et al, 2011; Siskind et al; 2013).

So far, there are at least 40 genes known to cause CMT when mutated (Fig. 1) and more than 44 distinct loci have been identified (Shy et al, 2005; Siskind et al, 2013). Nonetheless, more than 70% of patients with CMT in Western countries have genetic abnormalities associated with essentially four genes: PMP22, MPZ, MFN2 and GJB1 (Saporta et al, 2011). While most of the known CMT gens are strictly implicated either in axonal or demyelinating form, some others like GDPAP1, NEFL and MPZ may be mutated in both forms. Furthermore, while certain genes mutations are mainly of dominant inheritance and others recessive, some of them such as EGR2, PMP22, MPZ, NEFL, MFN2, GAPDP1 and HSPB1 mutations may be of both inheritance traits.

CHARCOT MARIE TOOTH 4J (CMT4J)

Charcot-Marie-Tooth 4J (CMT4J) is a rare recessive demyelinating form of CMT. The designation of CMT4 (instead of AR-CMT1) is applied to all autosomal recessive forms of demyelinating CMT (Fig. 2). Ten sub-types (from the CMT4A CMT4J; Fig 2) corresponding to the ten mutated genes have been identified to date (Tazir et al, 2013).

CMT4J is characterized by severe motor dysfunction with rapid clinical progression that results in weakness, often asymmetric, of proximal and distal muscles. Initially, the CMT4J phenotype was described as a severe early onset CMT (Chow et al., 2007), but further studies showed that the CMT4J

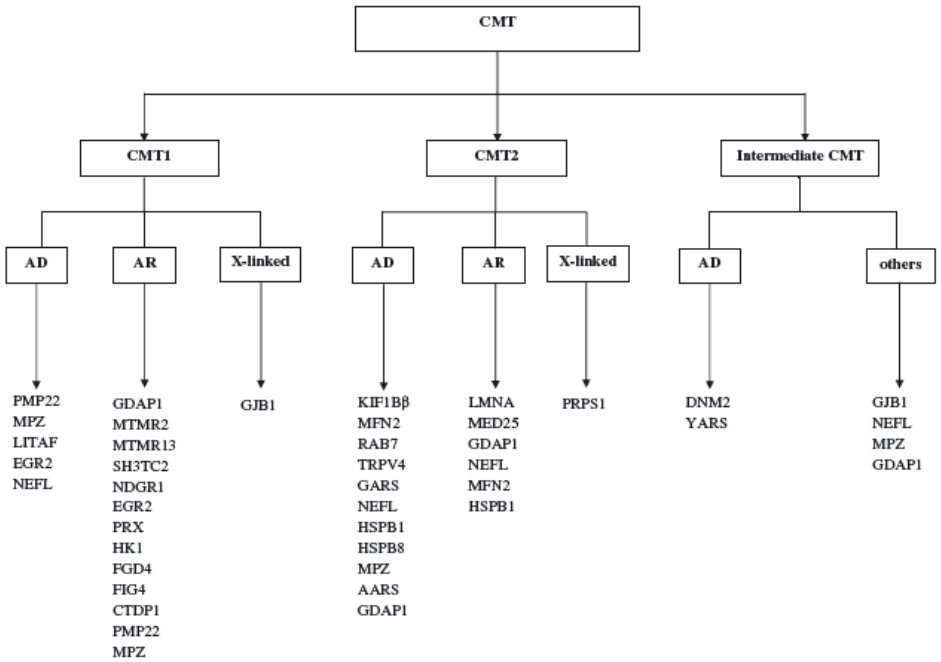

Fig. 1: Genetic classification of Charcot-Marie-Tooth (CMT). CMT are classified in CMT1, CMT2 and intermediate CMT on the basis of the nerve conduction velocity (NCV). CMT can be inherited as dominant, recessive and X-linked trait (from Reilly et al. 2011).

Type	Gene	Age of onset	Specific phenotype (Alleles)	Nerve biopsy
Autosomal recessive CMT1/CMT4				
CMT4A	GDAP1	Onset <2 years	Severe, progressive CMT1. Vocal cord and diaphragm paralysis.	Segmental demyelination. Onion bulbs (OB).
CMT4B1	MTMR2	3 years	SevereCMT1. Facial/bulbar weakness. Scoliosis.	Myelin outfolding. Loss of myelinated fibers (MF)
CMT4B2	MTMR13	4–13 years	Severe CMT1/glaucoma. Kyphoscoliosis.	Myelin outfolding. Loss of MF.
CMT4C	SH3TC2	Early onset. First to second decade	Severe CMT1/ Scoliosis. Deafness. Tongue fasciculation.	Long cytoplasmic extensions of unmyelinated fibers. OB
CMT4D	NDRG1	1–10 years	Severe CMT1. Deafness	Demyelination. Axonal loss. OB. Axonal inclusion
CMT4E	EGR2	Birth	Congenital hypotonia, respiratory failure. Arthrogryposis.	Severe loss of MF and unmyelinated fibers, OB formations
CMT4F	PRX	Birth	CMT1/prominent sensory involvement.	Severe loss of MF. Congenital hypomyelination.
CMT4G	HK1	8–16 years	Severe early-onset CMT1	Hypomyelination, regenerating clusters.
CMT4H	FDG4	<2 years	Delayed milestones. Severe CMT1 course. Scoliosis	Hypomyelination. Small OB.
CMT4J	FIG4	Congenital to sixth decade	Severe CMT1. Similarities to motor neuron disease.	Profound axonal loss, thin MF

Fig 2: Classification of autosomal recessive CMT4. The designation of CMT4 (instead of AR-CMT1) is applied to all autosomal recessive forms of demyelinating CMT. Ten sub-types (from the CMT4A to CMT4J) corresponding to the ten mutated genes have been identified to date.

was characterized by a highly variable onset, from early childhood through to the sixth decade, and severity (Tazir et al, 2013). Even, early loss of ambulation has been found in some patients. Moreover, it has been observed that, beyond the motor neurons, sensory neurons are also affected (Chow et al., 2007; Zhang et al., 2008). In fact, CMT4J patients exhibit, albeit slight, sensory abnormalities such as reducing the sensitivity of the distal limbs and decreased tendon reflex (Saporta et al, 2011; Tazir et al, 2013). On neurological examination, dysfunction of the cranial nerves is uncommon and these patients usually display normal cognitive function. Consistently, no abnormalities of the central nervous system have been observed in patients with CMT4J (Nicholson et al. 2011; Zhang et al. 2008). Mutations in the lipid phosphatase Fig4 causes CMT4J (Chow et al, 2007). Affected individuals are compound heterozygotes carrying one unique null allele of FIG4 in combination with the missense allele FIG4-I41T (more frequent) or FIG4-L17P (Chow et al. 2007; Nicholson et al. 2011).

The recessive mutations appear to result in a loss of function of Fig4. Homozygous “pale tremor” (plt) mice with a spontaneous mutation (through a transposon insertion) that eliminates the expression of Fig4 exhibit extensive and progressive neurodegeneration in the brain and peripheral ganglia (Chow et al, 2007; see also box1). In particular, extensive loss of neurons from sensory and autonomic ganglia is evident during the neonatal period. Peripheral nerves are also affected consistently with the observed reduction of nerve conduction velocities and CMAP (compound muscle action potentials) amplitude (Chow et al, 2007).

Histological phenotype

Sural nerve biopsies of CMT4J patients show extensive loss of large-diameter myelinated fibers and onion bulb lameallae surrounding some remaining demyelinating fibers (Fig. 3) (Zhang et al., 2008; Nicholson et al, 2011). There is relative sparing of moderate to small diameter fibers, which range from thinly myelinated to absent myelin. These features are also seen in sciatic nerve of plt mice (Chow et al, 2007).

Hence, the defects in myelin sheath formation could imply the involvement of glial cells in the pathogenesis of disease. This is supported by recent findings

Box 1: The 'pale tremor mouse' as model of CMT4J.

The pale tremor mouse recapitulates CMT4J phenotype therefore is a good model to study this desease. Mice exhibit severe tremors starting early in life, abnormal gait, motor dysfunction and reduced NCV. At postnatal day three (P3), affected homozygotes have reduced size. Intentional tremor develops during the second week after birth, and abnormal limb postures are evident by the third week. Furthermore the pale tremor mice have impaired motor coordination, muscle weakness and 'swimming' gait. There is a progressive loss of mobility, reduction in body weight and juvenile lethality. Within the brain, neuropathy is observed as early as P7 in the thalamus, pons, medulla, cortical layers V and VI, and the olfactory bulb. Many areas of them are involved in motor control, emphasizing similarity to CMT. Differently from humans, mice show diluted pigmentation suggesting that the loss of Fig4 affects melanosome functions. Furthermore at cellular level large vacuoles are observed in the trigeminal ganglia by post-natal day 1 (P1), the dorsal root ganglia by P7, and the spinal motor neurons by 6 weeks of age.

	CMT4J
Enlarged vacuoles	Enlarged vacuoles
Reduced PI(3,5)P2	Reduced PI(3,5)P2
Slowed nerve conduction velocities	Slowed nerve conduction velocities
Peripheral neuronopathy	Peripheral neuronopathy
Motor system defects	Motor system defects
CNS neuronal degeneration	Axonal loss
Diluited pigmentation	
Cell loss in spleen	
Survive 4-6 weeks	Little effects on lifespan

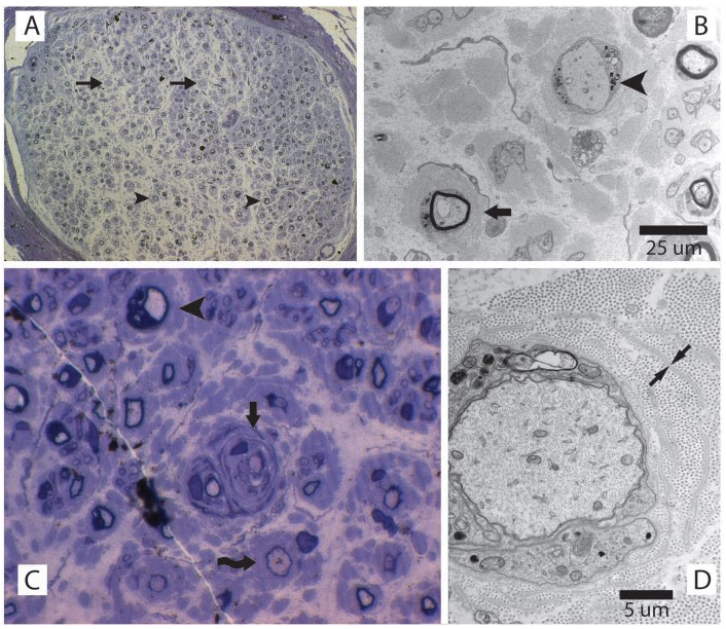

Fig. 3: Sural nerve biopsy of a patient with CMT4J. Anomalies in myelinated fibers are detected in a sural biopsy of CMT4J patient. (A) Cross section of a sural nerve fascicle with extensive loss of large myelinated fibers. There is relative sparing of moderate to small diameter fibers, which range from thinly myelinated (arrowheads) to absent myelin (arrows). (B) Electron microscopy demonstrating one naked axon with myelin breakdown products (arrowhead) and one thinly myelinated axon with surrounding onion bulb remnants and no clear Schwann cell processes (arrow). (C) Thinly myelinated axon with multiple thin myelin bands within the surrounding onion bulb (arrow). Also visible, a demyelinated axon (arrowhead) and a thinly myelinated axon (curving arrow). (D) Electron microscopy demonstrating a minimally myelinated axon with myelin breakdown products. Arrows indicate the cell remnants of a Schwann cell (from Nicholson et al. 2011).

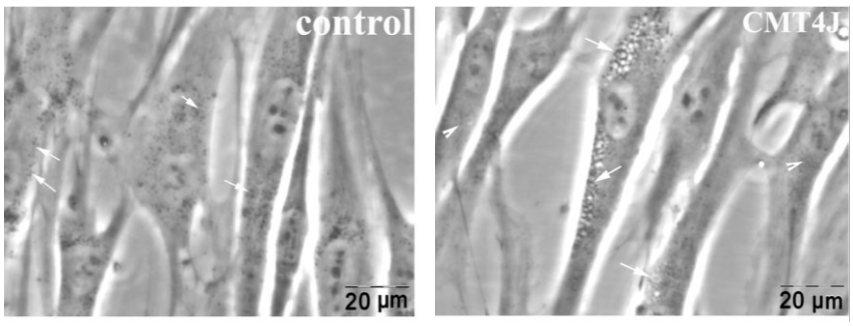

Fig. 4 : Vacuolation in FIG4-deficient human fibroblasts. Fibroblasts of normal (left) and CMT4J patient (right). Control fibroblasts contains occasional vacuoles, while there are excessive vacuoles in patients fibroblasts (arrows) (from Zangh et al. 2001).

showing that mice with conditional inactivation of Fig4 in Schwann cells display demyelination (Vaccari et al, 2014).

Cellular phenotype

At the cellular level, plt mice display: i) enlarged vacuoles with watery appearance immunoreactive for the late endosomes/lysosomes protein lamp2 in sensory neurons (Chow et al. 2007; Ferguson et al. 2009); ii) enlarged Lamp1/2 positive endo-lysosomes filled with electron dense material (Chow et al, 2007; Katona et al, 2011) in spinal motor/cortical neurons and glia. Lamp-2 reactive vacuoles accumulation is also observed in fibroblasts from patients with CMT4J (Zhang et al. 2008) (Fig. 4).

Thus, it appears that the deficiency of Fig4 leads to wide expansion and, probably, to dysfunction of the late endosome/lysosome compartments. Moreover, the observed differences of the cellular phenotype in the different types of neurons suggest that Fig4 might have different roles in the diverse cell types possibly by controlling specific cell pathways.

Furthermore, elevated levels of LC3-II and p62 have been detected in the brains and spinal cord of plt mice (Ferguson et al, 2009). Interestingly, this accumulation was not observed in liver or other non-neural tissues, suggesting that a defect of autophagy pathway could contribute to neurodegeneration phenotype. Moreover, in the brain homogenates there is no change in cytoplasmic LC3-I and in the levels of protein involved in the initiation of autophagy as Beclin-1 and mTOR (Ferguson et al, 2009), suggesting that a block in completion of autophagy rather than its up-regulation could be the defect of Fig4$^{-/-}$ mice.

FIG4

In humans FIG4 gene is located on chromosome 6 (from base pair 109,691,221 to base pair 109,825,43). It encodes a lipid phosphatase of 103 kDa comprised of 907 amino acids, the Fig4 protein, also known as SAC domain-containing protein 3 (Sac3) (Chow et al, 2007).

Fig4 belongs to the family of enzymes (from lower to higher eukaryotes) containing a conserved phosphoinositide (PI) phospahatase module termed Sac (suppressor of actin) domain (Hughes et al, 2000). Fig4 was originally

identified in a screen for genes induced by mating pheromone in Saccharomyces cerevisiae (Erdman et al, 1988). The mammal protein is closely related to the yeast one with overall amino acid sequence identity of 35% and similarity of 66% (Chow et al, 2007).

The Sac domain comprises about 500 amino acids and contains seven highly conserved motifs including the CX5R(T/S) catalytic motif, which is essential for catalytic activity (Hughes et al, 2000). Like in yeasts, also in humans there are five Sac phosphatase domain containing proteins, which appear to fall into two subfamilies (Fig. 5). Members of the first subfamily, including the trans-membrane protein Sac1, cytosolic proteins Sac2/INPP5f and Sac3/Fig4, have an N-terminal Sac phosphatase and no other recognizable structural domains. The second subfamily comprises two synaptojanin homologues, which have a PI 5-phosphatase domain immediately after the N-terminal Sac phosphatase module (Hughes ate al, 2000). Each Sac phosphatase prefers a specific sub-group of PIs as substrates, although how the substrate specificity is determined in still not well clear. Specifically, Fig4 removes the 5-phosphate from the phosphoinositide PI(3,5)P_2 to generate PI(3)P both in vitro and in vivo (Rudge et al, 2004; Duex et al, 2006).

Consistently with public expressed-sequence-tag and microarray databases, RT-PCR of tissues from wild type mice showed widespread expression of Fig4 (Chow et al, 2007). Moreover, transcript appears distributed throughout the brain as revealed by in situ hybridization (Chow et al, 2007).

Structure and enzymatic activity

Structural studies of Fig4/SAC3 have not yet been performed, but important information has been inferred through the crystal structure of the founding member of this family, the Sac1p, which is the only crystal structure solved in this family to this day (Manford et al, 2010). The Sac domain of yeast Sac1p comprises two closely packed sub-domains (Fig. 6): an N-terminal sub-domain (SacN domain; residues 1-182) and a C-terminal domain of about 320 residues in which is present the catalytic site CX5R(T/S) (Manford et al, 2010). The SacN domain comprises three layers of β-sheets and one long and three short α-helixes (Fig. 6). The SacN domain is closely opposed to the catalytic domain, but it takes some contacts through its third layer (Manford et

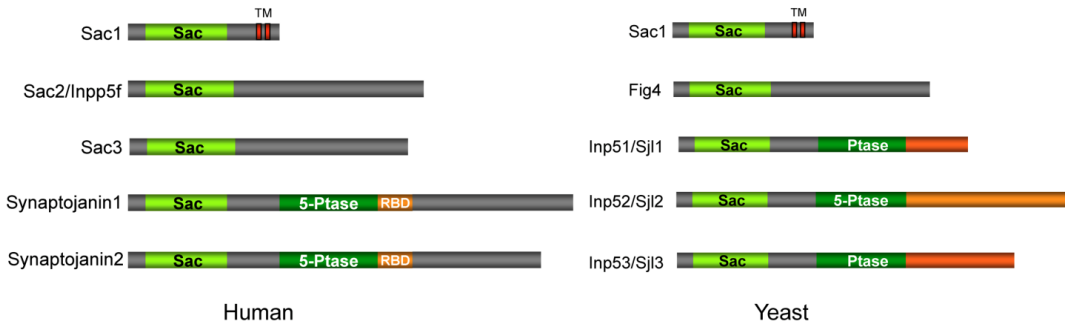

Fig. 5: Domain structures of the members of the Sac phosphoinositide phosphatase family. Both in human and yeast, there are five proteins containing the Sac phosphatase module (TM transmembrane module, RBD RNA binding module) (from Manford et al. 2010).

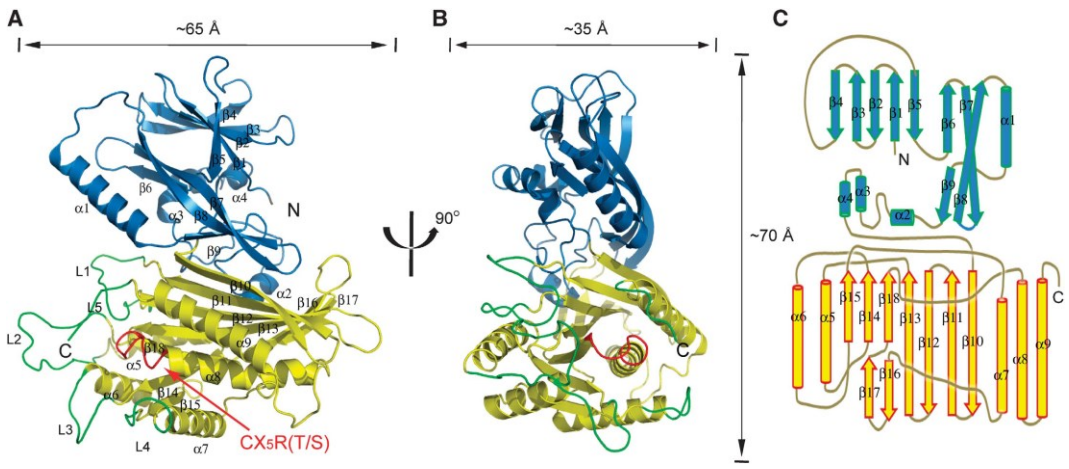

Fig. 6: Overall crystal structure of Sac1. (A) Ribbon diagram of the Sac PI phosphatase. The SacN domain is coloured blue and the catalytic domain yellow. The secondary structure elements (strands β1–β18 and helices α1–α9) are labelled. The catalytic CX5R(T/S) motif (P-loop) is coloured red and labelled. Five protruding loops (L1–L5) surrounding the catalytic site are coloured green. (B) a 90º rotated view of (A). (C) Schematic diagram of the secondary structure topologies of Sac1 (from Manford et al. 2010).

al, 2010). The function of this domain is still unknown, but it may control the enzymatic function through the interactions with other unknown factors. The catalytic domain consists of a nine-stranded and partially split β-sheet that is flanked by five α-helixes with two on one side and three on the other. The catalytic site (residues 392-399) is constituted by a conserved cysteine (Cys) followed by 5 amino acids and arginine (Arg) forming a conserved loop (termed P-loops; in red in Fig. 6). Finally, five protruding loops surrounding the catalytic site (Manford et al, 2010).

Moreover, the Sac domain is an electrostatic bipolar protein with one surface negatively charged and the opposite surface enriched with positive charges (Manford et al, 2010). The positive charged face is likely to interfaces with the lipid bilayer interacting with the negative charges of the phospholipids. Consistently, the catalytic motif CX5R (T/S) is localized on this positively charged surface.

Through a conserved mechanism in yeast and in mammals, Fig4 formed a ternary complex (Fig. 7) with PIKfyve (Fab1 in yeast) and the ArPIKfyve adaptor protein (Vac14 in yeast), which regulates both the kinase and phosphatase activities (Jin et al, 2008; Ho et al, 2011). Yet, it is not completely clear the dynamics through which this complex is formed and then performs its function, nor how it is regulated. Various studies suggest that Fig4 could bind Vac14/ArPIKfyve before to bind efficiently the kinase Fab1/PIKfyve (Botelho et al, 2008; Ikonomov et al, 2009; Sbrissa et al., 2007). This complex is responsible for the acute regulation of subcellular levels of PI(3,5)P2 (Botelho et al, 2008; Jin et al, 2008; Sbrissa et al, 2008). Similarly to the deficit of Fig4, the loss of Fab1, which is lethal in some eukariotes such as C. elegans and Drosophila, induces the formation of an enlarged, swollen vacuole in yeast cells (Efe et al, 2005) or the loss of ArPIKfyve in mice leads to massive neurodegeneration with accumulation of lamp2-positive vacuoles (Zhang et al, 2007). All together these findings indicate that the levels of $PI(3,5)P_2$ might be finely regulated and are critical for membrane homeostasis and specifically survival of neural cells.

How the function of Fig4 is impaired in the disease mutants is still not understood since both pathological mutations mapped outside of catalytic site (Fig. 7, 8). The pathological mutant Fig4I41T (presumably also Fig4L17P)

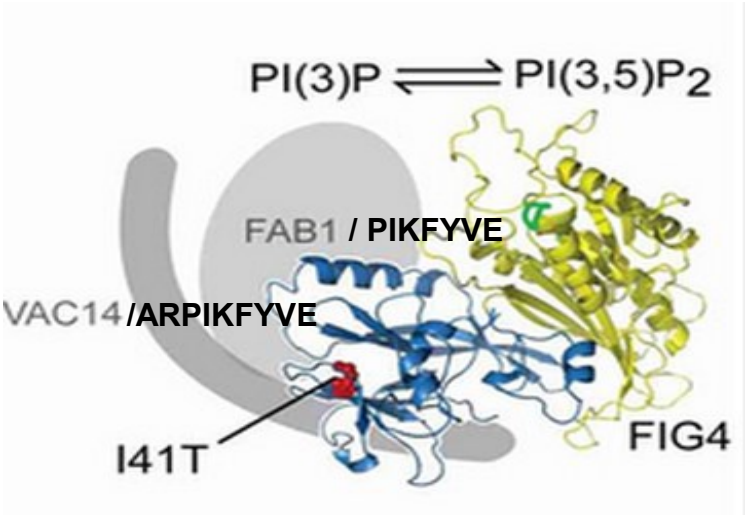

Fig. 7: The ternary complex containing Fig4, PIKfyve (FAB1) and ArPIKfyve (VAC14) regulates the overall concentration of PI(3,5)2P. Predicted orientation of Fig4 in complex is shown. The image shows the N-terminal domain (blue) and the catalytic domain (yellow) containing the active site (green). The I41T mutation of Fig4 is represented in red (from Lenk et al. 2011).

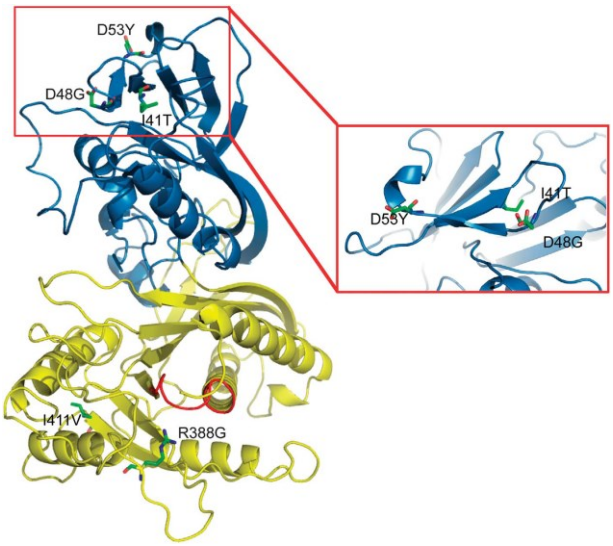

Fig. 8: I41T mutation is localized away from the catalytic site. The picture shows the localization of I41T predicted on the basis of crystal structure of yeast Sac1p. Together with residues D48G and D53Y (found mutated in ALS) I41T is clustered in a surface area on the top of the SacN domain. R388G and I411V are located in the catalytic domain and create a non-functional protein.

maintains its hydrolysing activity, but it appears to be unstable as consequence of the impairment of its interaction with ArPIKfyve, although there are conflicting data (Ikonomov et al, 2010; Lenk et al, 2011). ArPIKfyve seems to regulate the abundance of Fig4 by attenuating proteasome-dependent degradation (Ikonomov et al, 2010). Instead, through a mechanism still unclear ArPIKfyve would be unable to stabilize mutant protein, although it associates with Fig4I41T in similar manner to wild-type protein (Ikonomov et al, 2010).

Hence, these findings do not adequately explain the pathogenesis of CMT4J. Consistently, the overexpression of the mutant is unable to rescue all degenerative defects of plt mice (Lenk et al, 2011). This is also different to what occurs in yeast where Fig4 carrying a corresponding I59T mutation was able to produce normal levels of $PI(3,5)P_2$ and is sufficient to correct the vacuolar enlargement phenotype when this mutant was expressed in Fig4-/- cells (Chow et al. 2007). Although many similarities between yeast and mammals, these findings suggest that Fig4 can be differently regulate in these organisms or can be implicated in diverse cellular functions and this could be related to CMT4J pathogenesis.

Another hypothesis is that Fig4 could be essential for the function of the ternary complex as scaffold protein, thus implying that Fig4 could be involved both in the degradation (through its phosphatase function) and synthesis of $PI(3,5)P_2$. Hence, in the absence of Fig4 ArPIKfyve/Vac14 fails to exert its activity or, alternatively, Fig4 may be a direct activator of PIKfyve. This is in agreement with the fact that Fig4-deficient yeast cells and mice do not have higher $PI(3,5)P_2$, but instead, have lower basal levels (Chow et al, 2007; Duex et al, 2006). Moreover, in yeast the deletion of FIG4 impairs the localization of VAC14 and PIKfyve to the vacuole surface (Jin et al. 2008; Rudge et al. 2004). However, there are conflicting data in mammals: Fig4 is destabilized in mutant mice lacking VAC14, while VAC14 and PIKfyve are stable in mice lacking Fig4 (Lenk et al. 2011).

By computationally modelling of the structure of Sac domain based on the crystal structure of yeast Sac1p, the I41T localizes at c-terminal end of β3 in the SacN domain (Fig. 8) and is about 40 Å to the catalytic site confirming that mutation does not affect the catalytic activity of Fig4 (Manford et al, 2010).

The hydrophobic side chain of this isoleucine is buried in a hydrophobic core between the first two layers of β-sheets of the SacN domain (Fig. 6, 8). The mutation may affect the local folding or the stability of the protein because together with residues D48 and D53 the I41 residue is surface exposed and located in flexible loop regions (Fig. 8; Manford et al, 2010). In addition, this surface area of SacN domain may be involved in protein-protein interactions and therefore the I41T mutation could affect them.

PARKINSON'S DISEASE

Parkinson disease (PD) is the second most common neurodegenerative disorder with a prevalence of about 1% in people over 60 years of age to about 4% in people over the age of 85 (De Lau et al. 2006). It was first described in the essay entitled “n Essay of the Shaking Palsy” by James Parkinson in 1817.

Clinically, PD is characterized by a wide spectrum of symptomatology including motor symptoms such as resting tremor, bradykinesia, rigidity, postural instability, stooped posture and freezing (Fig. 9), as well as non-motor symptoms including cognitive and behavioural symptoms, sleep disorders, autonomic dysfunction, olfactory and other sensory deficits and fatigue (Polymeropoulos et al.1997; Hely et al., 2008).

The neuropathological hallmarks are characterized by progressive and profound loss of neuromelanin containing dopaminergic neurons in the substantia nigra pars compacta (SNpc) with presence of eosinophillic, intracytoplasmic, proteinaceous inclusions (mainly enriched of α-synuclein) termed as Lewy bodies (LB; Fig. 10) and dystrophic Lewy neurites in surviving neurons (MacPhee & Stewart, 2001; Thomas and Beal 2007). At the time of death, even middle affected PD patients have lost about 60% of their dopaminergic neurons (Zigmond and Burke, 2002; Jankovic et al, 2013). The depletion of striatal dopamine as a result of SNpc dopaminergic neuronal loss leads to an impaired nigro-striatal system that otherwise allows an individual to execute proper, coordinated movements. Indeed, dopamine is important for tuning down the cortical excitation of striatal neurons and therefore its loss may lead to an increase of corticostriatal glutamatergic transmission that in turn overactives striatal γ-aminobutyric acid (GABA) output (Robertson et al. 1990).

Moreover, although neuronal loss in substantia nigra is pronounced there is widespread neurodegeneration in the central nervous system (Thomas and Beal 2007).

While the neuropathological damage is clear and widely described, the PD aetiology remains currently unknown. Two forms of Parkinson’s disease are recognized (Fig. 11): a familial or early-onset Parkinson’s disease (<10% of all

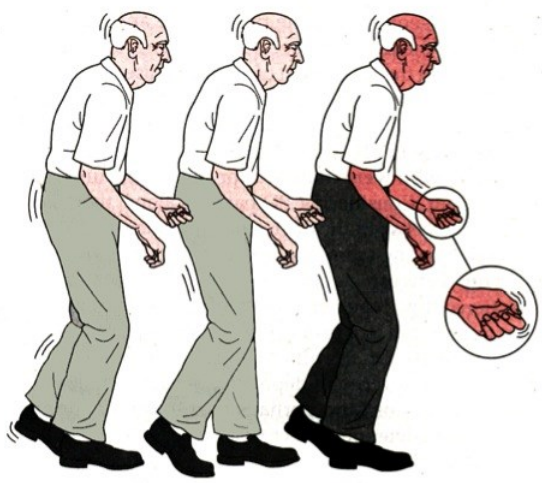

Fig. 9: Classic symptoms of late-stage Parkinson disease. Patients presents a stooped and rigid posture, shuffling gait and tremor (After Markey 1986).

Fig. 10: Lewy body in the substantia nigra are detected in brains of Parkinson's patients. Immunohistochemistry of brain slice of PD patient.

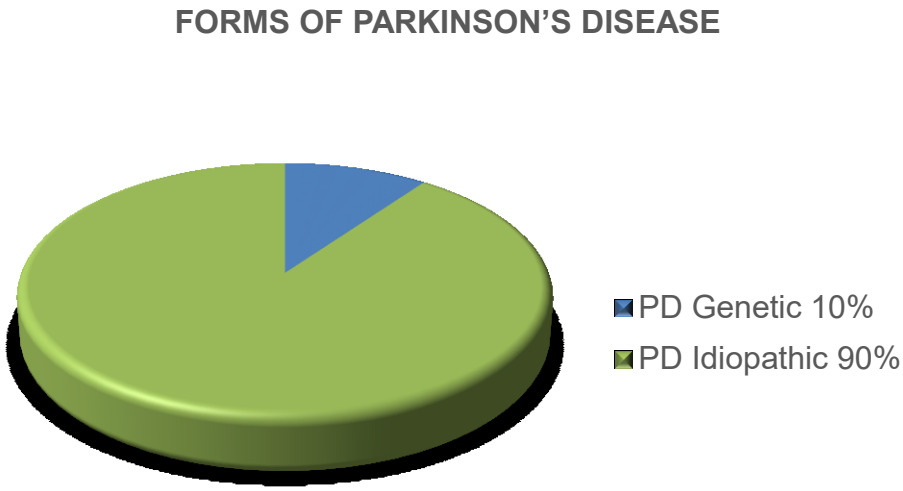

Fig. 11: Frequency of different forms of Parkinson's disease.

Symbol	Gene locus	Gene	Inheritance	Disorder
PARK1	4q21-22	SNCA	AD	EOPD
PARK2	6q25.2–q27	Parkin	AR	EOPD
PARK3	2p13	Unknown	AD	Classical PD
PARK4	4q21–q23	SNCA	AD	EOPD
PARK5	4p13	UCHL1	AD	Classical PD
PARK6	1p35–p36	PINK1	AR	EOPD
PARK7	1p36	DJ-1	AR	EOPD
PARK8	12q12	LRRK2	AD	Classical PD
PARK9	1p36	ATP13A2	AR	Kufor-Rakeb syndrome; atypical PD with dementia, spasticity, and supranuclear gaze palsy
PARK10	1p32	Unknown	Risk factor	Classical PD
PARK11	2q36-37	Unknown; not GIGYF2	AD	Late-onset PD
PARK12	Xq21–q25	Unknown	Risk factor	Classical PD
PARK13	2p12	HTRA2	AD or risk factor	Classical PD
PARK14	22q13.1	PLA2G6	AR	Early-onset dystonia-parkinsonism
PARK15	22q12–q13	FBX07	AR	Early-onset parkinsonian-pyramidal syndrome
PARK16	1q32	Unknown	Risk factor	Classical PD
PARK17	16q11.2	VPS35	AD	Classical PD
PARK18	3q27.1	EIF4G1	AD	Classical PD
PARK19	1p31.3	*DNAJC6*	AR	Juvenille onset, atypical PD
PARK20	21q22.11	*SYNJ1*	AR	Juvenille onset, atypical PD
PARK21	3q22.1	*DNAJC13*	AD	Late-onset PD

Fig. 12: Gene loci identified for Parkinson's disease.

patients) and idiopathic or late-onset Parkinson's disease (>85% of all cases) that does not appear to exhibit heritability. Notably, the clinical manifestations and neuropathology of familial parkinsonism can often be quite indistinguishable from sporadic cases, which fuelled the widely held assumption that the two forms of PD are likely to have shared pathogenic mechanisms.

Overall, the pathology of Parkinson's disease is complex and is most likely a consequence of a combination of genetic and environmental factors, which may induce a common pathogenic cascade of molecular events (Maguire-Zeiss and Federoff, 2003; Miller and Federoff 2005; Kalinderi et al, 2016). The molecular pathways leading to this pathological picture are still obscure. The discovery of several monogenic forms of PD substantially increased our knowledge of the neuodegeneration mechanisms in PD (Bonifati el al, 2007; Gasser et al; 2007 Dauer and Przedborsky, 2003; Lesage et al, 2009). For example abnormal protein processing, oxidative stress, mitochondrial dysfunction seems to be leading factors involved in the pathogenesis of PD (Gupta et al 2008; Greenamyre and Hastings, 2004). However, two decades after the detection of the first mutation associated with PD, the molecular basis of this neurodegenerative disease remains incompletely understood. Moreover, the precise relationship of familial linked genes to the sporadic illness is currently uncertain.

Epidemiology

Until the 1990s Parkinson's disease was the fourth most common neurodegenerative disease (Gray & Hildebrand, 2000), currently is the second in the world after Alzheimer's disease (Collins et al 2010). It is not possible to establish with certainty the age of disease development since mostly several years pass between the onset of symptoms and the diagnosis. Considering the total population, the prevalence is 1 in 100000, but the incidence increases to about 200 after 50 years, and nearly 1000 cases in the oldest age group (over 70 or 80 years) indicating that risk of PD increasing with advancing age (Korell and Tanner, 2013). Although less frequent, there are

also cases diagnosed earlier (around 40 years or below) as well as rare forms of juvenile parkinsonism (age onset around 20-25 years).

Gender-specific differences have been observed in PD incidence and prevalence studies (Korell and Tanner, 2013). However, there is variability across studies. A preponderance of PD among males has been reported, while a few studies have reported similar incidence or prevalence for males and females. In Japan, PD prevalence is higher in women, but it could reflect longer survival among females in Japan and differential access to medical service. In sharp contrast, the incidence of PD among men was approximately twofold higher than among women in the Northern California and Italian population (Korell and Tanner, 2013). If there are truly gender differences in PD across populations, this could be due to differential exposure to risk factors (such as occupational exposure to toxicants) in men and women.

Parkinson's disease is present in all countries with lower incidence in China and in Africa and seems affect all races (Korell and Tanner, 2013). Some studies showed a lower prevalence among Black as compared to Whites. A recent study investigating multi-ethnic population found that incidence rates were highest among Hispanics followed by non-Hispanic Whites, Asians and Blacks (Korell and Tanner, 2013).

GENETIC FORMS OF PARKINSON'S DISEASE AND INHERITANCE

The majority of PD cases are sporadic probably caused by a combination of genetic and environmental risk factors as aforementioned (Fig. 11). Approximately 10% of patients have monogenic forms of the disease, exhibiting a classical Mendelian type of inheritance (Lesage et al, 2009; Bonifati et al, 2013; Kalinderi et al, 2016).

The initial observations of positive familial histories in 10-20% of patients have shown that genetic factors might be involved in the pathogenesis of the disease. A lot of genetic association studies had later on implicated a number of genetic variants in the disease pathogenesis/protection. Then the major progress has been made with the advent of genome-wide association studies (GWAS) and the implementation of new technologies, like next generation sequencing (NGS) and exome sequencing.

Many chromosomal loci, termed PARK to denote their putative link to PD and numbered in chronological order, have been identified (Fig. 12). Nowadays, only six of these specific regions contain genes with mutations that conclusively cause monogenic typical PD (Singleton et al., 2013; Bonifati et al, 2013; Kalinderi et al, 2016). Both dominantly or recessively inherited mutations have been found (Bonifati et al, 2013; Kalinderi et al, 2016).

Autosomal dominant forms of PD

Mutations in three genes (SNCA, LRRK2, VPS35) are conclusively established as a cause of autosomal dominant forms of PD (Bonifati et al, 2013; Kalinderi et al, 2016). The evidence for a fourth gene, EIFAG1, remains inconclusive (Bonifati et al, 2013). Finally, heterozygous mutations in the GBA gene are important and strong risk factors for PD and diffuse Lewy-body disease (Bonifati et al, 2013).

Alpha-synuclein (SNCA) was the first gene associated with familial PD by linkage mapping and then confirmed by the identification of the missense mutation A53T in Italian and Greek families (Polymeropoulos et al. 1997).
Mutations in SNCA are rare and include point mutations and whole-locus multiplications (duplications or triplications). Beyond A53T, A30P and E46K mutations have been detected so far in single families of German and Spanish origin, respectively. The brain pathology is characterized by abundant α-synuclein-positive neuronal inclusions (LBs and Lewy neuritis), but the associated clinical spectrum is broad, ranging from classical PD to more atypical and aggressive phenotypes (including myoclonus, severe autonomic dysfunction and dementia in addition to parkinsonism). The patients with SNCA duplications display a classic PD phenotype, while the more rare cases carrying triplications have more severe phenotype, indicating a direct relationship between SNCA gene dosage and disease severity. Other point mutations (H50Q and G51D) have been recently identified in a sporadic English patient and in two independent families of French and British origin, respectively (Bonifati yet al, 2013). Interestingly all point mutations map at the

N-terminal of α-synuclein, suggesting that this domain could be critical for protein function.

Alpha-synuclein is an abundant protein in the brain, but to a lesser extent is also expressed in the heart, muscles and other tissues. In the brain α-synuclein was found mainly at the end of the pre-synaptic terminals, where it may interact with both phospholipids and proteins. In particular, it has been observed that α-synuclein binds to phospholipids via its amino-terminal end, while to synaptobrevin-2 via its carboxy-terminal end (Ben Gedalya et al., 2009; Nemani et al., 2010). Although its function is not yet fully elucidated, several studies suggest that α-synuclein, through the N-terminal domain, could be implicated in the regulation of synaptic vesicles trafficking and membrane fusion.

Increased expression of SNCA, both in its native or mutated form, or an incorrect degradation result in abnormal formation of insoluble aggregates, that can be deposited to form Lewy bodies after neuron demise. Misfolding and aggregation of the α-synuclein protein into neurotoxic species is at the centre of the current pathogenic theories for PD. The more recent discovery that α -synuclein aggregates develop in dopaminergic neurons transplanted in the brain of PD patients, suggest that misfolded a-synuclein may have prion-like properties, and could be able to induce a cascade of protein misfolding.

LRRK2 (Leucine-rich repeat kinase 2) mutations are the most common known cause of autosomal dominat PD. The LRRK2 gene encodes a large protein with two enzymatic domains (GTPase and kinases) and multiple protein-protein interaction domains. Seven mutations (Asn1437His, Arg1441Cys, Arg1441Gly, Arg1441His, Tyr1699Cys, Gly2019Ser, and Ile2020Thr) were considered to cause disease (Zimprich et al. 2004; Berg et al, 2005). Mutations of this gene have been found both in family and sporadic forms of Parkinson's disease.

VPS35 (Vacuolar protein sorting-associated protein 35) is a component of a large multimeric complex, termed the retromer complex, involved in retrograde transport of proteins from endosomes to the trans-Golgi network

(Bonifacino et al, 2008). In 2011 two groups reported the identification of the same missense mutation in VPS35 gene as novel cause of autosomal dominant PD (Vilarino-Guell et al, 2011; Zimprich et al, 2011).

Autosomal recessive forms of PD

To date, eight causative genes have been identified as cause of autosomal recessive parkinsonism.

Homozygous or compound heterozygous mutations in each of the following three genes, parkin (PRKN, PARK2), PINK1 (PARK6), and DJ-1 (PARK7) cause autosomal recessive forms of early-onset parkinsonism, usually without atypical clinical signs (Kitada et al, 1998; Valente et al, 2004; Bonifati et al, 2003). Mutations of these three geens are identified worldwide, including point mutations and large rearrangements leading to deletions or multiplications.

Mutations in Park2 gene are the most common and have been found both in familial forms (accounting up to half familial PD) and in sporadic PD (15% of the cases) with onset before 45 years (Lucking et al, 2000; Bonifati et al, 2013). Parkin is an ubiquitin E3 ligase. The loss-of-function effect of Parkin mutations result in inactivation of its E3 ligase function, failure of ubiquitination of the targeted proteins and therefore a toxic build-up of proteins that are no longer effectively degraded by the parkin dependent ubiqutin/proteosome pathway in the degradation system of proteasome (Shimura et al, 2000). Hence, it has hypothesized that he formation of these toxic aggregates to neurons of the substantia nigra have a crucial role to the pathogenesis of PD (Shimura et al, 2000).

Mutations in the gene PINK1 and DJ-1 are less common (1-2%; Valente et al, 2004; Bonifati et al, 2005; Ibanez et al, 2006). The PINK1 protein contains a kinase domain and is localized to the mitochondria. Recent studies indicate that PINK1 and Parkin are functionally linked, with PINK1 acting upstream of parkin (Narendra et al, 2010; Koyano et al, 2014). Indeed PINK1 has been found to phosphorylate parkin recruiting it onto depolarized mitochondria (Koyano et al, 2014). Together, they are important to tag damaged mitochondria for degradation by autophagy (Narendra et al., 2010; Koyano et al, 2014).

Recessive mutations in Park9 (ATP13A2), PARK14 (PLA2G6), PARK15 (FBXO7) are responsible of atypical forms of parkinsonism with very early (juvenile, <30 years) onset and other clinical signs (such as pyramidal, dystonic, ocular movement, and cognitive disturbances) in addition to parkinsonisms (Di Fonzo et al, 2009; Ramirez et al, 2006; Bonifati et al, 2013). Park9 encodes a lysosomal membrane transporter, ATP13A2, while PARK15 gene encodes two protein isoforms, which are part of larger ubiquitin-ligase complex, but have poorly characterized functions.

Recently, through exome sequencing approach combined with genome wide homozygosity mapping mutations in another two genes, DNAJC6 (encoding auxilin) and SYNJ1 (encoding synaptojanin 1) were identified as the cause of autosomal recessive, juvenile parkinsonism. DNAJC6 mutations have been identified first in Palestinian family and later confirmed in a Turkish family (Edvardson et al, 2012; Koroglu et al, 2013).

In the case of SYNJ1, the same homozygous mutation, Arg258Gln, was identified independently in two families of Iranian and Italian (consanguineous family from Sicily) origins (Quadri et al. 2013; Krebs et al. 2013). All four patients (2 siblings per family) display early onset parkinsonism with progressive bradykinesia and early development of tremors and other motor symptoms (at the age of 20). Additional clinical signs such as eyelid apraxia, generalized seizures, and dementia have been observed in some patients (Quadri et al, 2013; Krebs et al, 2013). One year later, the same homozygous mutation is found in two siblings of a third pedigree affected by progressive early-onset parkinsonism (Olgiati et al, 2014).

SYNJ1

Synaptojanin 1 (Synj1) is a lipid phosphatase belonging to the family of Sac domain containing proteins as aforementioned. It was discovered in 1994 as 145 kDa nerve terminal protein interacting with growth factor receptor-bound protein 2 (Grb2) (Mcpherson et al, 1994). Two decades later, Synj1 mutation was incriminated for the first time in autosomal recessive early-onset Parkinson's disease with atypical symptoms (Quadri et al, 2013; Krebs et al, 2013).

The SYNJ1 gene is located on chromosome 21q22.11 (Cremona et al. 2000) and spans 99.29 kb of genomic DNA. Two isoforms are generated from two open reading frames separated by an in-frame stop codon (Ramjaun and McPherson, 1996). The first open reading frame encodes a 145-kDa form of the protein (1350 amino acids), whereas a 170-kDa isoform appears to be composed of both open reading frames (1612 amino acids) (Ramjaun and McPherson, 1996). Whereas the 145-kDa isoform is highly enriched in adult brain, the 170-kDa isoform is excluded from this tissue (Ramjaun and McPherson 1996). Both isoforms harbor multiple functional domains (Fig. 13): a Sac domain on their N-terminal (typically of this enzyme family), a 5'-phosphatase domain in the centre, and a C-terminal proline-rich domain (PRD). The 170 kDa isoform contains an additional PRD translated from the second ORF (Ramjaun and McPherson, 1996).

There are two additional SYNJ1 isoforms: isoform c 1295 amino acids and isoform d 1526 amino acids, that are of unknown functional relevance. Despite isoforms c and d have a shorter N-terminus and a distinct C-terminus and are shorter than isoform a, they contain the same functional domains as isoforms b and a, respectively.

Furthermore, there is another form of synaptojanin, synaptojanin 2 (1248 amino acids), always identified by De Camilli's group (Nemoto et al, 1997). The two synaptojanin forms share 57.2 and 53.8% amino acid identity in their Sac and phosphatase domains, respectively, while their carboxyl-terminal PRD domain bear little homology. Synj2 has a broader tissue distribution and possess inositol 5-phosphatase activity (Nemoto et al, 1997). Protein binding assays demonstrated that among the proteins binding the proline-rich region only Grb2 binds to synaptojanin 2 (Nemoto et al, 1997). Furthermore, subcellular fractionation studies in transfected CHO cells revealed that synaptojanin 2 was predominantly associated with the membrane fraction, while synaptojanin 1 was mainly localized in the soluble fraction (Nemoto et al, 1997), suggesting that PRD domains of Synj1 and 2 are implicated in different protein-protein interactions.

Synj1 is an inositol 5-phosphatase and it converts $PI(1,4,5)P_3$ but not $PI(1,3,4)P_3$ to inositol bisphosphate (Mcpherson et al, 1996). In addition it dephosphorylates $PI(4,5)P_2$ to PI monophosphate (Mcpherson et al, 1996).

Protein domains

Respect to other inositol phosphatases Synj1 is peculiar because it contains two consecutive phosphatase domains, the Sac1 and the 5'-phosphatase domains. Specifically, it is composed of three domains (Fig 13):

1) at the N-terminus the Sac domain, homologous to the yeast Sac1p, dephosphorylates predominantly PI monophosphates present in cell membranes, including those of the Golgi apparatus and endosomes.
2) the central 5'-phosphatase domain dephosphorylates phosphatidylinositol bis- or trisphosphates localized in plasma membranes to activate downstream pathways (Perera et al, 2006; Mcpherson et al,1996; Cremona et al, 1999; Guo et al, 1999).
3) at the C-terminus, PRD domain comprises about 250 amino acid and contains at least five potential SH3 domain-binding consensus sequences (Mcpherson et al,1996).

   The 170 kDa isoform harbors an additional smaller PRD with at least three additional SH3 binding sites (Ramjaun and McPherson, 1996).

   Besides Grb2, the C-terminal region common to both SYNJ1 isoforms interacts with the SH3 domains of a variety of proteins implicated in endocytosis, subcellular targeting, and signalling such as endophilin, amphiphysin, syndapin/pacsin, intersectin, and many others (Heuvel et al, 1997; Itoh et al, 2005).

   The additional C-terminal tail of 170 kDa isoform contains binding sites for clathrin and AP2 via three types of binding motifs (WxxF, FxDxF, and DxF), and for Eps15 through asparagine-proline-phenylalanine (NPF) domain (Haffner et al,1997; Praefke et al, 2004).

The missense Arg258Gln mutation found in PD localizes in exon 5 within the Sac domain. This arginine in position 258 is conserved among 18 different orthologs, in Synj2 and three human proteins containing Sac domain (Sac1, Sac2 and Fig4/sac3) suggesting that it could be critical for its function. Consistently, it has been demonstrated that the mutation impairs the phosphatase activity of Synj1 against PI monophosphates (Krebs et al. 2013).

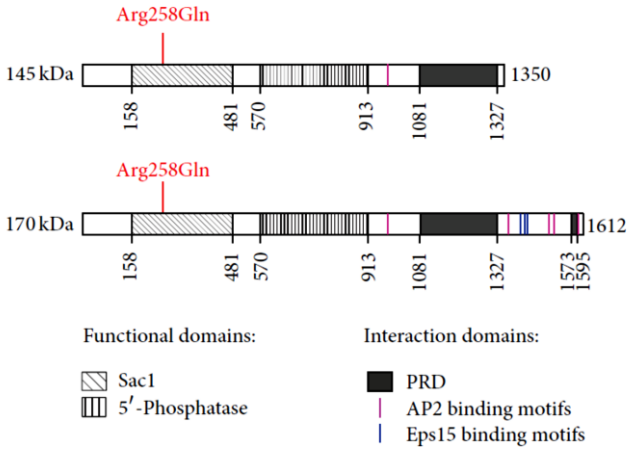

Fig. 13: Functional and interaction domains of the two major isoforms of SYNJ1. The 145 kDa (top) and the 170 kDa (bottom) SYNJ1 isoforms harbor two functional inositol phosphatase domains, an Nterminal Sac1 domain and a more central 5'-phosphatase domain. Several protein-protein interaction domains are found in the C-terminal part of the proteins: one or two PRD domains, AP2 binding motifs (WxxF, FxDxF, and DxF, in pink), and Eps15 binding motifs (NPF: asparagine-proline-phenylalanine, in blue). The homozygous mutation Arg258Gln, found in Parkinson's disease patients, is indicated in red. Numbers indicate the amino acid positions along the proteins (from Drouet and Lesage 2014).

Multiple functions

Thanks its different functional domains and overall to the capacity to interact with different proteins, Synj1 has been implicated in different cellular process both in nerve terminals where it has been first discovered and in other cell types (Drouet and Lesage, 2014).

First, Synj1 is implicated in synaptic vesicle recycling because it has been found localized in close proximity to clathrin- and dynamin coated endocytic intermediates in nerve terminals (McPherson et al.1994, David et al, 1996; Haffner et al. 1997). Further studies confirmed this role. Like dynamin Synj1 interacts with amphysin and undergoes dephosphorylation after nerve terminal depolarization (McPherson, Takei et al, 1994; McPherson et al, 1996). Moreover, it also interacts with endhophilin and together they are rapidly recruited to clathrin coated pits during prolonged stimulation (Heuwel et al, 1997; Perera et al, 2006). Recently, another study showed that upon endophilin-mediated recruitment (through an SH3-PRD interaction), SYNJ1 promotes dephosphorylation of PI(4,5)P2 to endocytic sites (Milosevic et al. 2011). Importantly, in neurons the dual phosphatase activity is required for efficient synaptic vesicle endocytosis and reavailability at nerve terminals (Mani et al. 2007).

Furthermore, it has been shown that through its Sac-phopshatase activity Synj1 participates in actin cytoskeleton polymerization/depolymerization and is mostly required during brief neuronal stimulation (Kim et al. 2002; Mani et al. 2007). Interestingly, it has been found that mutations in the homologues in C elegans (unc-26) and the inactivation of synaptojanin-like proteins in yeast, lead to increased levels of $PI(4,5)P_2$, an increased number of clathrin-coated vesicles, and a hypertrophy of the actin-rich matrix at endocytic zones (Gad et al, 2000; Stefan et al, 2002) indicating that that the activity of Synj1 is essential for proper vesicle trafficking and coating/uncoating of endocytic vesicles in different organisms.

In addition, another role has been identified for SYNJ1 post-synaptically: it is involved in the internalization of AMPA receptors in postsynaptic neurons (Gong and De Camilli, 2008) suggesting that Synj1 could participate in the signal transmission through postsynaptic reorganization.

Recent studies showed that Synj1 takes part in similar mechanisms in other cell types. Several studies in Zebrafish showed that Synj1 is required for vesicle recycling at ribbon synapses necessary for sensory transmission Indeed, in cone photoreceptors of Zebrafish vision mutant were found reduced numbers and abnormal distribution of synaptic vesicles within a dense cytoskeletal matrix have been found (van Epps et al, 2004). Moreover, Synj1 seems critical for proper membrane trafficking in cones (Holzhausen et al, 2009; George et al, 2014). This role has yet to be confirmed in mammalian cells. Like in neurons, in podocytes Synj1 participates in endocytosis with its interacting partners dynamin and endophilin by acting on phosphoinositides and actin filaments (Soda et al, 2012). Recently, Synj1 has been reported as a potential regulator of allogenic T cell responses (Sun et al, 2013).

All these data indicate that phosphoinositide metabolism plays an essential role in vesicle endocytosis and recycling. Hence, it is important to determine if the loss of Synj1 activity causes similar defects in humans as well as to understand if neurodegeneration in PD is caused by alteration of this process or by the lack of other pathways in which Synj1 could be involved.

PHOSPHOINOSITIDES

Phosphoinositides (PIs) are phosphorylated derivatives of phosphatidylinositol (PtdIns). Tough, these comprises less than 5% of total cellular lipids are essential components of cellular membranes and play key roles in many fundamental biological process (Di Paolo and De Camilli, 2006; Shewan et al, 2011; Mayinger et al, 2012).

PIs are concentrated on the cytosolic face of cellular membranes and rapidly diffuse within the plane of the membrane. Like other phospholipids, they consist of a glycerol backbone, which is esterified by two fatty acids and a phosphate that is attached to a polar head group, the cyclic polyol myo-inositol (Fig. 14A).

The PtdIns, the precursor of of phosphoinositides, is synthesized primarily in the endoplasmic reticulum (ER; Fig. 14B) and is then delivered to other membranes either by vesicular transport or via cytosolic PtdIns transfer proteins (Di Paolo and De Camilli, 2006). Reversible phosphorylation of the

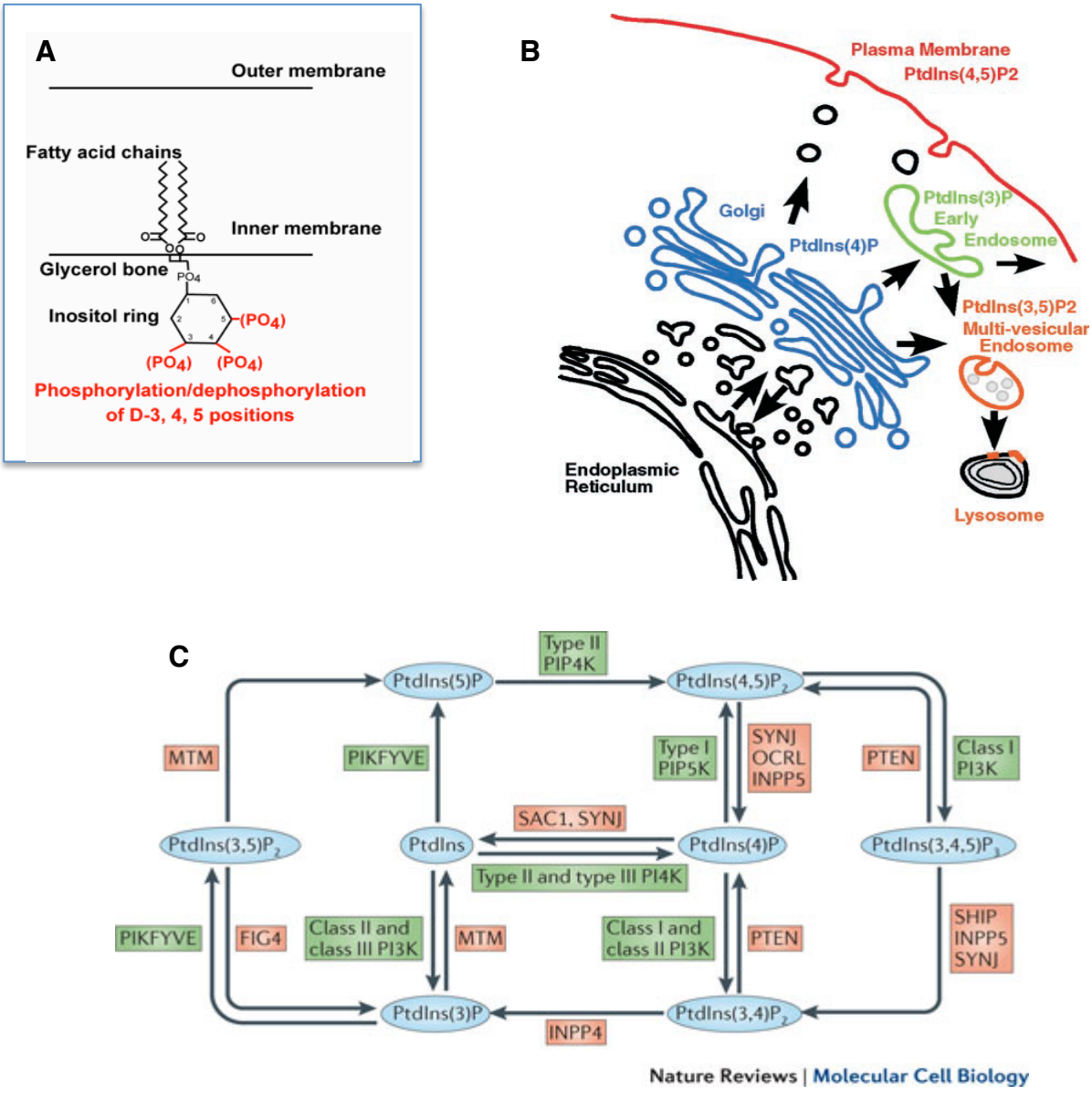

Fig. 14: Phosphoinositides synthesis and conversion. PtdIns and PIs contain an inositol head group linked to glycerol backbone, and two fatty acid chains. They are located in the inner leaflet of specific membranes and are reversibly phosphorylated at the D-3, 4, 5 positions of the inositol ring as indicated in red (A).
The PtdIns is synthesized primarily in the endoplasmic reticulum (ER) and is then delivered through the Golgi to the specific subcellular compartments (B).
Phosphoinositides can be interconverted between their many forms by the action of specific kinases (shown in green) and phosphatases (shown in red) (C). Phosphorylation of phosphatidylinositol can give rise to seven different phosphoinositide forms: three mono-phosphorylated forms [PI(3)P), PI(4)P and PI(5)P], three bi-phosphorylated forms [PI(3,4)P2, PI(3,5)P2 and PI(4,5)P2] and the single tri-phosphorylated form, termed PI(3,4,5)P3.

myo-inositol head group at position 3, 4 and 5 gives rise to seven PI isoforms identified in eukaryotes cells: PI(3)P, PI(4)P, PI(5)P, PI(3,4)P_2, PI(3,5)P_2, PI(4,5)P**2** and PI(3,4,5)P**3** (Fig. 14). Among them, PI(4)P and PI(4,5)P**2** are constitutively present in membranes and comprises the largest pool of cellular PIs, whereas is almost undetectable in most types of unstimulated cells (Lemmon and Ferguson, 2000; Saarikangas et al, 2010).

Conversion between these isoforms is controlled by specific phosphoinositide kinases and phosphatases that regulate the balance of these lipids (Fig.14C, 15). The concerted action of PI kinases and phosphatases, that attach or remove phosphate groups respectively, and phospholipases, that cleave lipids, results in the generation of unique PI enrichment in distinct intracellular membranes (Di Paolo and De Camilli, 2006; Kutateladze, 2010). Therefore, PIs can serve as a unique lipid signature or code, like Rab proteins, for cellular organelle identity (Fig. 15). Furthermore, within a given membrane, the localization of specific phosphoinositides can be heterogeneous, thus identifying specific sub-domains (Fig. 16). Hence, the differential intracellular distribution of phosphoinositides, together with their high turnover, makes these lipids optimal mediators of signalling events in all cellular compartments (Fig. 15, 16) (Di Paolo and De Camilli, 2006; Shewan et al, 2011). By acting as membrane designations for selective protein recruitment and assembly, PIs may trigger downstream signalling cascades. In particular, through the binding of their head groups to cytosolic proteins or cytosolic domains of membrane proteins they can regulate the function of integral membrane proteins (such as ion channels, and transporters, or recruit to the membrane cytoskeletal and signalling components (Di Paolo and De Camilli, 2006; Falkenburger et al, 2010; Zhang et al, 2012). Typically, binding of proteins to phosphoinositides involves electrostatic interactions with the negative charges of the phosphate(s) on the inositol ring. In some cases, adjacent hydrophobic amino acids strengthen the interaction (Lemmon, 2003). Protein that interacting with phosphoinositides can consist either of clusters of basic residues within unstructured regions, such as those found in many actin regulatory proteins (Yin and Jammey, 2003), or of folded modules, such as the pleckstrin homology (PH) domain (Lemmon, 2003; Balla et al, 2005). Whether these two types of interactions mediate different signalling cascades

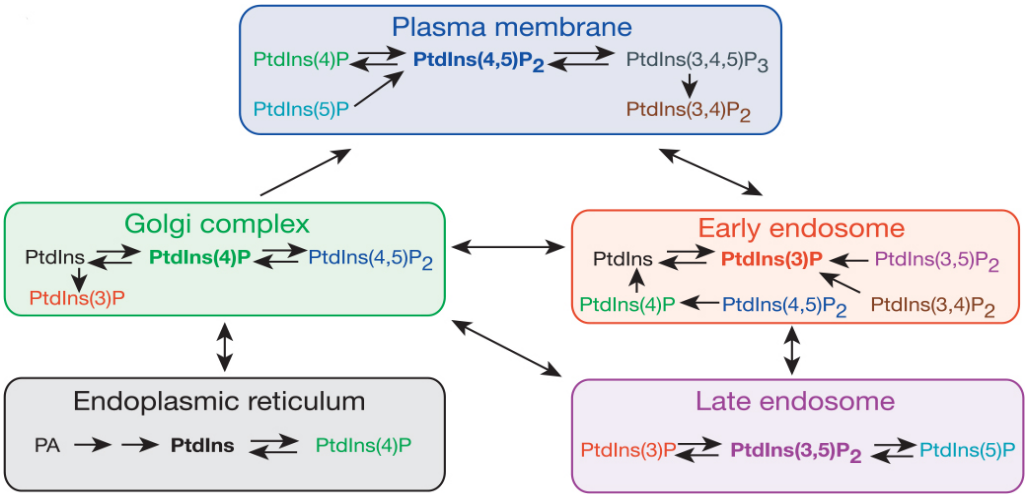

Fig. 15: Predominant subcellular localization of phosphoinositide species. PI(4,5)P2 and PI(3,4,5)P3 are concentrated at the plasma membrane. PI(3,4)P2 is mostly found at the plasma membrane and in the early endocytic pathway. PI(4)P is enriched at the Golgi complex, but also present at the plasma membrane. PI(3)P is concentrated in early endosomes and PI(3,5)P2 on late compartments of the endosomal pathway. The location of PI(5)P remains poorly characterized. Phosphorylation/dephosphorylation events occurring on each subcellular compartment are illustrated. In the ER, the conversion from phosphatidic acid (PA) to PtdIns involves more than one reaction (from Di Paolo and De Camilli 2006).

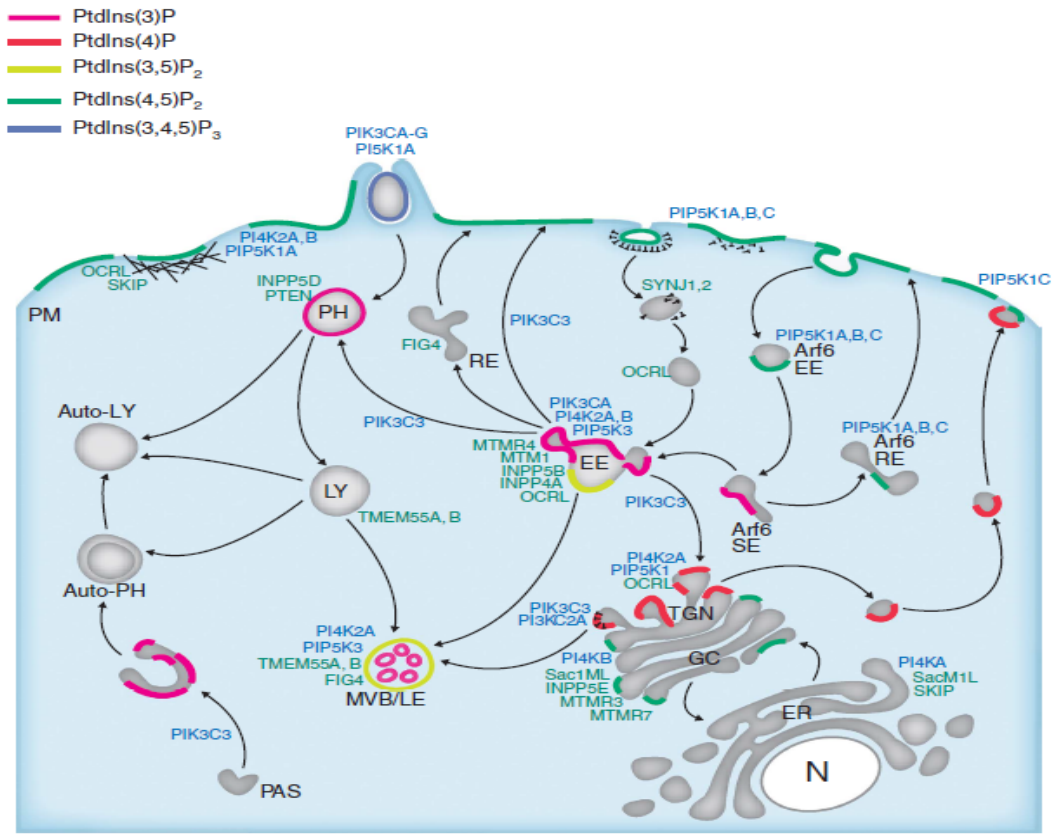

Fig. 16: Subcellular distribution of the PIs and PI-metabolising enzymes. The localization of the different PI kinases (blue) and PI phosphatases (green), as well as the predominant PI species (as visualized by PI-binding protein domains) in the different cell compartments. It is noted that many of the PI-metabolising enzymes are present in more than one cellular compartment. PM, plasma membrane; EE, early endosome; SE: sorting endosomes; RE, recycling endosome; LY, lysosome; MVB/LE, multivesicular body/late endosome; PAS, pre-autophagosomal structure; PH, phagosome; TGN, trans-Golgi network; GC, Golgi complex; ER: endoplasmic reticulum; N, nucleus.

are unknown. So far, 11 PI-binding modules are known interact with unique PIs with variable affinity (Kutateladze, 2010).

It is not surprising that the PI are emerging to be involved in many cellular processes such as membrane trafficking, cytoskeleton remodelling, signalling. The spatiotemporally regulated production and turnover of PIs is critical for PI functions. This is achieved by strict control of the subcellular distribution, membrane association and activity state of each of different kinases and phosphatases. Confirming their crucial role in cells, mice with mutation in the kinases or phosphatases that regulate levels of PI, die during embryonic life or develop severe neurological defects (Di Paolo and De Camilli, 2006; Vicinanza et al, 2008). An increasing number of human genetic diseases including myopathies and neuropathies are associated to mutations in enzymes regulating the turn over of PIs (Nicot and Laporte, 2008; Waugh 2015).

MULTIPLE ROLES OF PHOSPHOINOSITIDES

PI(4)P

PI(4)P is produced by the phosphorylation of PtdIns by the PI 4-kinases (PI4Ks). Four different PI4K isoforms have been identified so far in mammals, and two of them, PI4KIIa and PI4KIIIb, are localized to the Golgi complex. Indeed, PI(4)P is enriched in the Golgi complex, where it plays a direct role in controlling trafficking and Golgi morphology (De Matteis et al. 2007; D'Angelo et al, 2008). On the other hands, the deficiency of PI(4)P affects the function and the structure of Golgi complex. In yeast, mutations of the Golgi-localized PI 4-kinases PIK1 result in an accumulation of abnormal membrane intermediates ('Berkeley bodies') with impairment of transport to the plasma membrane (Odorizzi et al, 2004). Consistently, many PI4P-binding proteins have been identified at the Golgi complex, such as clathrin adaptors (AP1, GGAs, and epsin R) and lipid-transfer proteins (such as the four-phosphate-adaptor proteins, FAPPs; the ceramide transport protein, CERT; and the oxysterol-binding protein, OSBP). The fact that AP1, the GGAs, FAPP1 and FAPP2 bind not only PI(4)P, but also the small GTPase Arf1 ensures the correct recruitment of these PI4P-binding proteins to the TGN (De Matteis et al. 2007; Levine et al. 2002).

Spatial restriction of PI(4)P to the Golgi complex is ensured by phosphatases, one of which is likely to be Sac1 (Guo et al. 1999). This protein is an ER- and Golgi-complex-associated phosphoinositide phosphatase, which may thus dephosphorylate PI(4)P when retrograde traffic occurs from the Golgi complex to the ER (Guo et al. 1999). Mutant sac1 yeast cells have high levels of PI(4)P, including high levels at the plasma membrane (Roy et al. 2004), which may be the indirect consequence of the excessive PI(4)P in early secretory compartments.

PI(4,5)P_2

PI(4,5)P_2 is produced by the phosphorylation of either PI(4)P by type I PI kinases or PI(5)P by type II PI kinases (Fig. 14-16) (Yin et al. 2003; Roth et al. 2004).

PI(4,5)P_2 is mainly present at the plasma membrane (Falkenburger et al., 2010). Small fractions of PI(4,5)P2 were are also detected at the Golgi and the nuclear envelope (Watt et al. 2002).

Most cell surface PI(4,5)P_2 is generated from PI(4)P. This lipid is delivered to the cell surface by membrane carriers derived from the Golgi complex and from recycling organelles, but is also produced locally at the plasma membrane.

PI(4,5)P2 has an important role in endocytosis, because it functions as an important co-receptor for the recruitment and regulation of endocytic proteins selectively to the plasma membrane (Wenk and De Camilli 2004). Indeed, PI(4,5)P2 binds the endocytic clathrin adaptors (AP-2, AP180/CALM, epsin) and many other endocytic factors, including dynamin, which controls the vesicle fission (Wenk and De Camilli 2007; Owen et al. 2004).

Plasma membrane PI(4,5)P2 is directly implicated in exocytosis. Specifically, this PI acts in controlling docking of synaptic vesicles prior to fusion (Holz et al. 2002). Several PI(4,5)P2 binding proteins play a role in this process including CAPS (calcium-activated protein for secretion), Syt1 (Synaptotagmin-1) and rabphilin (Osborne et al. 2006).

The Golgi complex PI(4,5)P2 is dephosphorylated by the 5- phosphatase OCRL that has been found mutated in the Lowe syndrome (Loi, 2006). OCRL ineracts with clathrin, the adaptor protein APPL and several Rab proteins and

is involved in the endocytic pathway and in trafficking betwenn endosomes and the TGN (Choudhury et al, 2005; Hyvola et al, 2006; Erdmann et al, 2007). A recent report shows that OCRL deficiency causes accumulation of PI(4,5)P_2 in early endosomes and induces an increase in endosomal F-actin (Vicinanza et al, 2011).

PI(3)P

PI3P is synthetized by class III PI-3 kinase first discovered in yeast as essential component of vacuolar sorting pathway, Vps34 (Leevers et al. 1999). The mammalian homologues of VPS34 is also involved in endocytic sorting (Mayinger et al, 2012). Also class II PI-3 kinases phosphorylate Pins to generate PI(3)P and are activated upon stimulation of tyrosine kinases receptor or G-protein coupled receptors (Falasca et al, 2009). Several phosphatases belonging to the myotubularin and myotubulayn-related proteins dephosphorylate the PI(3)P (Begley et al. 2005).

PI3P is enriched on early endosomes (Fig 15) and participate to control the function of these organelles as sorting stations in the biosynthetic and the endocytic pathways (Efe et al. 2005, Di Paolo and De Camilli, 2006).

P(3)P-binding modules, mainly FYVE and PX domains, are present in a variety of endosomal proteins, such as EEA1 and Hrs (Lemmon et al. 2003, Balla 2005, Birkeland et al. 2004).

EEA1 is a Rab5 effector required for endosomal tethering and forms homo-dimers through a coiled-coiled domain. EEA1 also interacts with SNARE proteins such as syntaxin-6 and syntaxin-13 at early endosomes (Simonsen et al. 1999; McBride et al. 1999).

In contrast to EEA1, Hrs (hepatocyte growth factor-regulated tyrosine kinase substrate) binding to early endosomes independently of Rab5, but is dependnent on its FYVE domain (Raiborg et al. 2002). It is involved in the endosomal sorting of ubiquitinated membrane proteins through its clathrin-binding domain and ubiquitin-binding domain (Raiborg et al. 2002). Moreover, Hrs has also been found associated with phagosomes in a PI(3)P-dependent manner (Vieira et al. 2004).

PI(3,5)P2

PI 3,5)P2 was first described in yeast where its synthesis is strongly induced by osmotic stress, but was also discovered as minor lipid component in non-stimulated mammalian cells (Dove et al, 1997; Whiteford et al, 1997). Respect to other PIs, it is present in very low concentration (only 0.04/0.08% of total PI).

As aforementioned, the presence of this PI is dependent on the action of PI3P kinase PIKfyve and phosphatase Fig4 that form a ternary complex with the adaptor protein ArPIKfive (Jin et al. 2008).

The PI(3,5)P2 is enriched in the late compartments of endosomal pathway (late endosomes, multivesicular bodies, lysosomes) (Di Paolo and De Camilli 2006).

P(5)P

PI(5)P is the least characterized phosphoinositide. The mechanisms for PI(5)P biosynthesis are not well characterized. Theoretically, PI(5)P can be generated either by dephosphorylation of PI(3,5)P2 and PI(4,5)P2 or by phosphorylation of PI (Lecompte et al, 2008). The most established pathway is the generation of PI(5)P from PI(3,5)P2 by the 3-phosphatase myotubularin (Tronchere et al, 2004).

It is not yet clear whether the PI(5)P is present in cells stably or it is just a transitional product. Some studies suggest that it plays a regulatory role in the nucleus through binding ING2 (nuclear protein inhibitor of growth protein-2) (Gozani et al, 2003).

PI(3,4)P2 and PI(3,4,5)P_3

PI(3,4)P2 and PI(3,4,5)P3 are short-lived signalling molecules synthesized in response to extracellular stimuli and involved in cell proliferation and survival.

AIM OF THE STUDY

The proper membrane trafficking that connects different intracellular organelles is essential to ensure the transport of various molecules to the correct compartments as well as to maintain the specific composition of the various compartments. This is crucial for homeostasis of eukaryotic cells and their vitality. Hence, it is not surprising that genetic defects of the molecular machinery regulating membrane trafficking can result in the development of different diseases.

In this context, phosphoinositides (phosphorylated derivatives of phosphatidylinosititol) have emerged as important regulators of membrane trafficking by acting as membrane designations for selective protein recruitment and assembly, thereby triggering downstream signalling cascades. Thus, the levels of phosphoinositides might be finely regulated, in time and in the space, and they are critical for membrane homeostasis. This is achieved by strict control of the subcellular distribution, membrane association and activity state of each of different kinases and phosphatases. The proper balance between synthesis and degradation poses special challenges in nervous system, that indeed appears more sensitive to alterations of phosphoinositide metabolism as highlighted by the increasing number of human genetic diseases associated to mutations in enzymes regulating their turn over.

Aim of my PhD project was to explore the role of two inositol-phosphatases, Fig4 and Synj1, in membrane trafficking and neurodegenaration in CMT4J and Parkinson neuropathies (where they have been found mutated, respectively).

The rationale and the specific aims of each project are outlined below.

Project 1: molecular basis of Charcot-Marie Tooth disease 4J (CMT4J)

Fig4 removes the 5-phosphate from the phosphoinositide $PI(3,5)P_2$ enriched in the endo-lysosomal compartments. Mutation of Fig4 falls out of catalytic site and the pathological mutant maintains its hydrolysing activity. Typical cellular feature is the accumulation of enlarged lamp-2 positive vacuoles. Because endo-lysosomal system plays a crucial role in the cellular homeostasis, it is likely that its dysfunction could lead to neurodegeneration.

However it is unknown which pathway of endo-lysosomal axis is affected by the loss of Fig4.

Moreover, Fig4 seems play cell-specific role and this might contribute to CMT4J pathogenesis. However, the differential sensitivity of neuronal subtypes to Fig4 loss together with fact that Fig4 is expressed throughout development we could hypothesize that the Fig4 deficiency might affect some specific steps of neural differentiation.

Specific aims of my project were to study:

1) The localization and dynamics of Fig4 and its pathological mutants;
2) The role of Fig4 in the endo-lysosome axis;
3) The localization and the role of Fig4 in neural differentiation.

Project 2: molecular basis of Parkinson's disease

Synj1 is an inositol-phosphatase containing two consecutive phosphatase domains, the Sac and the 5'-phosphatase domain responsible of different functions. With its Sac domain dephosphorylates predominantly PI monophosphates present in the membranes of Golgi apparatus and endosomes, while the central 5'-phosphatase domain dephosphorylates phosphatidylinositol bis- or trisphosphates localized in plasma membranes to activate downstream pathways. Thus, with this double enzymatic activity Synj1 could be involved in different pathways in different cellular context. Indeed, so far it has been implicated in different process: Synj1 is required in synaptic vesicle recycling, participates in actin cytoskeleton polymerization/depolymerization and more recently it seems implicated in the regulation of proper membrane trafficking in cone phothoreceptors.

Pathological mutation is mapped in the Sac domain. However, the molecular mechanisms altered in the disease are still unknown.

Specific aims of my project were to study:

1) The expression and the localization of Synj1;
2) The role of Synj1 in the endocytic pathway.

METHODS

METHODS

REAGENTS AND ANTIBODIES

Primary antibodies used in this study include the following: rabbit polyclonal anti-Fig4 (Abcam) used for immunofluorescence and mouse monoclonal anti-Fig4 (NeuroMab) used for western blot. Rabbit polyclonal anti-Synj1 (Abcam). Mouse monoclonal anti-Lamp1 (BD Phamigen) used for human cell lines and rat monoclonal anti-Lamp1 (Santa Crutz) used for mouse cell lines. Mouse monoclonal anti-Rab7 (Santa Crutz), mouse monoclonal anti-eea1 (Abcam) and mouse β3-tubulin (Sigma).

Specifically for ESCs cells we used mouse Oct3/4 (Santa Cruz Biotechnology), rabbit Nanog (Calbiochem-EMD Biosciences) mouse GAPDH (Santa Cruz Biotechnology) and goat Sox1 (Santa Cruz Biotechnology).

The secondary antibodies used for immunofluorescence were Alexa Fluor 488 or 546 goat anti-mouse, rabbit, or rat IgG (Life Technologies).

The HRP conjugated secondary antibodies used for Western blot analysis were from GE Healthcare.

LysoTracker® Red DND-99 was from Molecular Probes. To stain nuclei we used DRAQ5® (1,5-bis{[2-(di-methylamino)ethyl]amino}-4, 8-dihydroxyanthracene-9,10-dione) or DAPI (4',6-diamidino-2-phenylindole) (Cell Signaling).

CELL CULTURES

Cell lines

MDCK cells were cultured in DMEM (Dulbecco's modified eagle medium) supplemented with 5% FBS (Fetal Bovine Serum) while NIH3T3 cells in DMEM 5% CS (Calf Serum).

HeLa and SH-SY5Y cells were maintained in RPMI-1640 with 10% FBS, 2mM L-glutamine. MO3.13 and NSC34 cells were cultured in DMEM 10% FBS, for NSC34 the medium was supplemented with 1mM L-glutamine and 1mM Sodium Pyruvate both from Life Technologies.

All cells lines were maintained at 37°C in a saturated humidity atmosphere containing 95% air and 5% CO2.

Stem Cells

E14Tg2a (BayGenomics) mouse ESCs were maintained on feeder-free, gelatin-coated plates in the following medium: Glasgow Minimum Essential Medium (GMEM, Sigma) supplemented with 2 mM glutamine, 1 mM sodium pyruvate, 1X non-essential amino acids (all from Invitrogen), 0.1 mM β-mercaptoethanol (Sigma), 10% FBS (Hyclone Laboratories) and 103 U/ml Leukemia Inhibitory Factor (LIF, Millipore).

ESCs were maintained at 37°C in a saturated humidity atmosphere containing 95% air and 7% CO2

Human fibroblasts

Patients and control fibroblasts, obtained from skin biopsies, were given from De Michele and Bonifati laboratory. They were cultured in DMEM supplemented with 10% FBS and penicillin/streptomycin at 37 °C and 5% CO2**.**

DIFFERENTIATION OF SH-SY5Y

For differentiation of SH-SY5Y cells were seeded at an initial density of 10^4 cells/cm^2 in culture dishes. All trans-Retinal (Sigma) was added the day after plating at a final concentration of 10 μM in RPMI-1640 with 5% FBS to induce differentiation for seven days. The culture medium, supplemented with fresh additives, was changed every 2 days.

DIFFERENTIATION OF ESCs

Neural differentiation

ESC differentiation into neuroectoderm was induced though SFEB formation. SFEBs were induced by placing 1x106 ESCs in 100-mm Petri dishes in the following differentiation medium: GMEM supplemented with 2 mM glutamine, 1 mM sodiumpyruvate, 1 × nonessential amino acids, 0.1 mM β-mercaptoethanol and 10% KSR. After 4 days, SFEBs were dissociated with trypsin and seeded in polylysine-coated dishes for neural differentiation.

Mesoderm differentiation

Mesoderm differentiation was obtained through Embryoid-body (EB) formation. EBs were induced by placing 4x105 ESCs in 100-mm Ultra Low attachment dishes for 5 days in the following differentiation medium: GMEM supplemented with 2 mM glutamine, 1 mM sodiumpyruvate, 1 × nonessential amino acids, 0.1 mM β-mercaptoethanol and 15% FBS.

GENE SILENCING

Short hairpin RNAs (shRNAs) in the pLKO.1-puro vector (Thermo Scientific) were used for stable suppressing Fig4 and Synj1 (specific sh-RNA sequences are shown in the table below).

Cells were transfected with shRNAs using Lipofectamine 2000 (Invitrogen) according to the manufacturer's protocol.

Transduced cells lines were selected with 0.6 μg/ml of puromycin (Sigma), while ESCs with 2 ug/ml of puromycin.

Specific Sh-RNA sequences of GFP, Fig4 and Synj1.

sh-GFP		GGCACAAGCTGGAGTACAACTA	
sh-2555	Fig4	AACTTATGAGTTCTTGTTA	human
sh-2441	Fig4	CTCCAAGAGTAGACAGAAA	mouse
sh-2409	Fig4	TTGCTCAGATGGAGTTATA	mouse
sh-2542	Synj1	TGAACATATGCTAAGTAAAT	mouse
sh-2269	Synj1	AAATACTCTGAATAGTGATT	mouse

We silencing transiently ESCs with selected Stealth RNAi™ named MSS272220 and Stealth RNAi™ siRNA Negative Control, Med GC (used as negative control) using Lipofectamine 2000 (Invitrogen), according to the manufacturer's protocol. Stealth RNAi™ were from Life Technologies.

PLASMIDS CONSTRUCTION AND MUTAGENESIS

GFP-Fig4 and mutants

The plasmid encoding human GFP-tagged Fig4 (RG207192) (GenBank accession number NM_014845) was purchased from Origene Technologies and was used also as template to generate the Fig4_I41T and Fig4-L17P mutants. Mutagenesis was performed by using the QuickChange Site-Direct

mutagenesis kit (Stratagene/Agilent Technologies). Primers were designed according QuickChange Site-Direct mutagenesis instruction and synthesized by the Ceinge Core Service Unit (Naples, IT). The mutations were confirmed by DNA sequencing performed by Ceinge Core Service Unit.

WESTERN BLOT ANALYSIS

Cells lines was grown on 100 mm petri dishes for 2 or 3 day, lysed with JS lysis buffer (Hepes pH 7.5 50mM, NaCl 150mM, glycerol 1%, Triton X-100 1%, MgCl2 1.5mM, EGTA 5mM) with 15 µg/ml of protease inhibitor (Antipain, Pepstatin and Leupeptin all from Sigma).

Undifferentiated and differentiated ESCs were lysed in a buffer containing 1 mM EDTA, 50 mM Tris-HCl (pH 7.5), 70mMNaCl, 1% Triton and protease inhibitor cocktail (Sigma), and analyzed by western blot.

Protein extracts was separated by SDS-PAGE and transferred onto PVDF membranes. Then were probed with the primary antibodies and proteins of interest were detected with HRP-conjugated secondary antibodies, visualized with the Pierce ECL Western blotting substrate (Thermo Scientific), according to the provided protocol.

NUCLEAR/CYTOSOL FRACTIONATION

Nuclear and cytoplasmic fractions were prepared with this method:

The cells grown on petri dishes was scraped with buffer A (10 mM HEPES, 1.5 mM MgCl2, 10 mM KCl, 0.5 mM DTT and 0.05% Igepal pH 7.9) leaved on ice for 10 min and centrifugated at 3000 rpm for 10 min then we removed supernatant and keep it (this contain everything except large plasma membrane pieces, DNA, nucleoli).

Then, the pellet was resupended in buffer B (5 mM HEPES, 1.5 mM MgCl2, 0.2 mM EDTA, 0.5 mM DT, 26% glycerol, pH 7.9; 300mM NaCl) and homogenized with Dounce. After 30 min on ice the sample was centrifuged at 24,000 g for 20 min and we took the supernatant.

INTERNALIZATION ASSAY

Transferrin receptor recycling assay

For transferrin receptor recycling assay cells we used two approaches:

In the first approach cells were washed twice with serum-free medium, incubated with 10 µg/ml Alexa-Fluor-546 (Invitrogen) or FITC (Molecular Probes) conjugated transferrin at 37°C in RPMI 5% BSA and fixed at 5, 10, 15 or 30 minutes. In the second approach the cells were first incubated transferrin for 10 min (pulse) at 37°C, the pulse medium was aspirated, and the cells were washed twice with serum-free medium to remove excess of unlabeled transferrin and then incubate with culture medium (chase), and fixed at 10, 20 and 30 min.

EGFR internalization assay

The cells was transiently transfected with an EGFR–GFP plasmid, after 48 hours starved for 3h and stimulated at with EGF (100 ng/ml) at 37°C and fixed at 10, 20 and 30 minutes with 4% PFA.

FLUORESCENCE MICROSCOPY

Cells lines grown on coverslips, were washed with PBS, fixed with 4% paraformaldehyde and quenched with 50 mM NH4Cl. Primary antibodies were detected with Alexa Fluor 488 or Alexa Fluor 546 conjugated secondary antibodies.

Undifferentiated ESCs and differentiate neurons were fixed in 4% paraformaldehyde and permeabilized with 0.2% Triton X-100 in 10% FBS (Invitrogen)/1% BSA in 1X PBS for 15' at room temperature. Thus, the samples were incubated with primary antibodies and with an appropriate secondary antibody. SFEBs were collected at the indicated differentiation day fixed in 4% paraformaldehyde and dehydrated with increasing percentages of ethanol. Samples were embedded in paraffin, sectioned in 7-µm slices and mounted on glass slides. After rehydration and permeabilization, the samples were treated as previously described.

For lysosome staining, cells were incubated for 1 h with Lysotracker (1:1000) in complete medium before fixing.

Images were collected using a Zeiss Laser Scanning Confocal Microscope (LSM 510) equipped with a planapo 63× oil-immersion (NA 1.4) objective lens. In silencing experiments we used the same settings (laser power, detector gain).

RNA ISOLATION AND QUANTITATIVE REAL-TIME PCR (qPCR)

For quantitative PCR total RNA was extracted by using TRI-Reagent (Sigma). The first-strand cDNA was synthesized according to the manufacturer's instructions (M-MLV RT). qPCR was carried out with the 7500 Real-Time PCR System instrument and the Sequence Detection Systems (SDS) 1.4 software (Applied Biosystems) using Power SYBR Green PCR Master mix (Applied Biosystems). The housekeeping GAPDH mRNAwas used as an internal standard for normalization, using 2-ΔΔCt method.

Primers used for Real-Time PCR

Name[a]	**Forward primer**	**Reverse primer**
Sox1	CGCCATGCAAATCACCGCCG	GGGCCCGGGCTGCCATTAAA
Gapdh	GTATGACTCCACTCACGGCAAA	TTCCCATTCTCGGCCTTG
Nanog	TCAGAAGGGCTCAGCACCA	GCGTTCACCAGATAGCCCTG
Oct3/4	AACCTTCAGGAGATATGCAAATCG	TTCTCAATGCTAGTTCGCTTTCTCT
Fig4	CGACCAGTGTATGTGACCCT	ATTTGCAACGTCACCCTCAC

RESULTS

RESULTS

PROJECT 1: MOLECULAR BASIS OF CMT4J

AIM 1. LOCALIZATION AND DYNAMICS OF FIG4 AND ITS PATHOLOGICAL MUTANTS

Fig4 is expressed in different cell types and is mainly localized in the cytosol

The intracellular localization of proteins has been proven to be important for their biological function and, regarding Fig4, it seems even more relevant since the precise regulation of PI levels, both in time and space, is achieved by strict control of their sub-cellular distribution and membrane association of kinases and phosphatase.

Because Fig4 has a widespread expression and it could control different pathways in diverse cell types we decided to use as cellular model both neural and non-neural cells. Specifically we performed our analysis in:

i) in HeLa cells and NIH3T3 cells (mouse embryonic fibroblasts) as non-neural cells;

ii) SH-SY5Y cells (from human neuroblastoma), MO3.13 cells (human glial oligodendrocytic hybrid), CAD (mouse cathecolaminergic neuronal cell line) and NCS34 (immortalized motor neurons) because the deficiency of Fig4 leads to distinct pathogenic changes in different neuronal cell subtypes (Ferguson et al. 2009, Katona et al. 2011, Vaccari et al. 2015).

Firstly, we analyzed the expression of Fig4 in these different cell lines by western blotting assay using an anti-Fig4 antibody (Fig. 17). As you can see in the figure, Fig4 migrates in the gel according to the estimated molecular weight (about 103 kDa). As expected, Fig4 is expressed in both neural and non-neural cell lines. Furthermore, by indirect immunofluorescence assay, we analyzed the localization of Fig4 in the different cell lines. We found that in all cell lines Fig4 is localized mainly in the cytoplasm, preferentially in discrete punctate structures, which could be the compartments where the

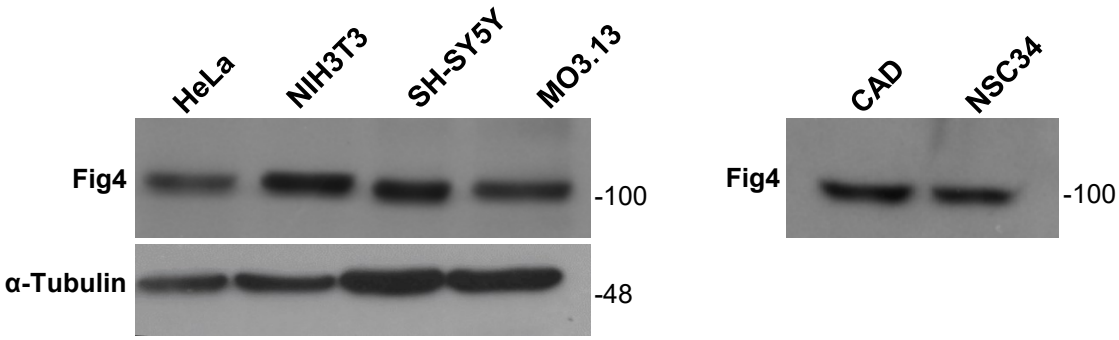

Fig. 17: Fig4 is expressed in different cell lines. HeLa, NIH3T3, SH-SY5Y and MO3.13 cells were lysed with JS buffer (see methods) and resolved by SDS-PAGE followed by immunoblotting with anti-Fig4 antibody. We used α-tubulin as loading control. Molecular weights of standard proteins are indicated.

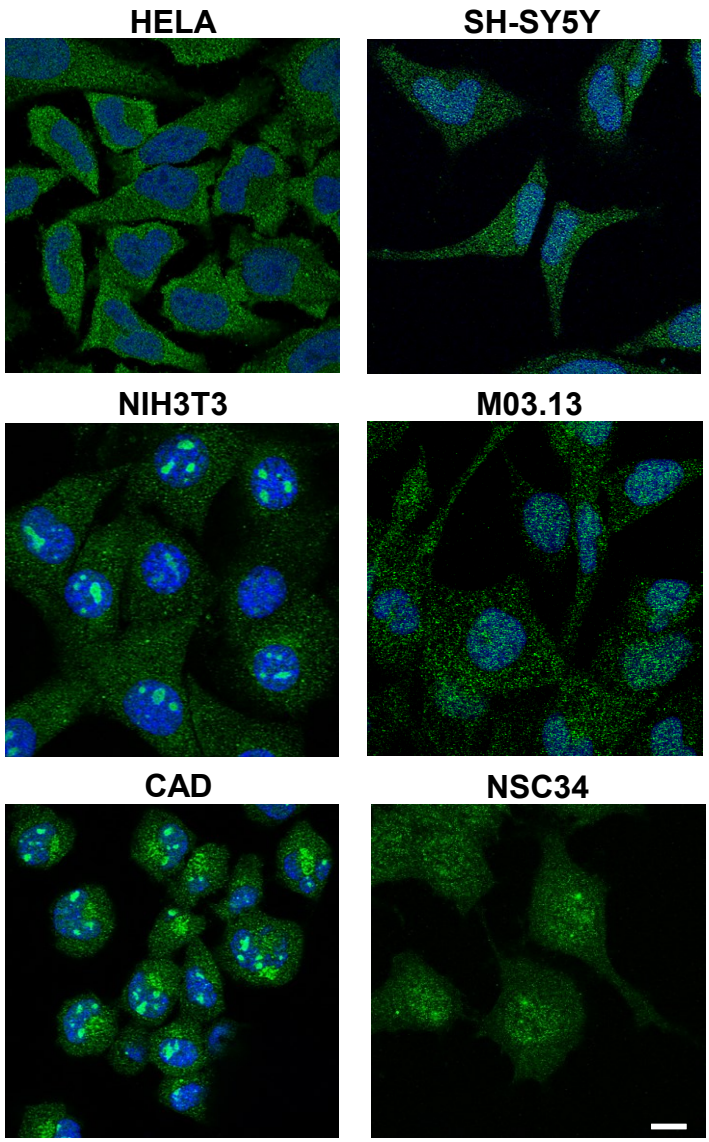

Fig. 18: In neural and non neural cells Fig4 is localized mainly in the cytosol in discrete punctate structures. HeLa, SH-SY5Y, NIH3T3, MO3.13, CAD and NSC34 cells were fixed with 4% PFA, permeabilzed with 0.2% Triton X-100 and stained with a specific anti-Fig4 antibody revealed with Alexa-488 conjugated secondary antibody. Nuclei were labelled with DRAQ5 dye. Images were acquired by confocal microscopy. Scale bar 5 µm.

phosphatase is working (Fig. 18). Interestingly, beyond to the cytosolic signal, in NIH3T3 and CAD cells Fig4 appears also distributed in a nuclear structure that resembles the typical nuclear bodies (Fig. 18). The fact that these cell lines derives from embryonic tissues where nuclear bodies are numerous supports that this signal is specific. We observed the same distribution in MEF (mouse embryonic fibroblast; data not shown) reinforcing this hypothesis. Moreover by a careful analysis of many images (as in the pictures in in Fig. 18) a faint and diffuse nuclear signal of Fig4 is also evident in the other cells. We confirmed these results by biochemical nuclei/citosol fractionation assays (Fig. 19). Indeed, Fig4 is purified also in nuclear fraction at different extent in the different cell lines (Fig. 19). Hence, it will be important to understand whether this distribution is related to Fig4 functions and whether nuclear and cytosolic pool has different roles. Further, we will investigate this issue.

Fig4 is enriched in Rab-7 positive compartments

To better determine the intracellular localization of FIG4 we performed double immunofluorescence experiments labelling the different organelles of exocytic and endocytic pathway with specific markers.

From morphological point of view, we observed that Fig4 signal is completely different from that of the exocytic compartments indicating the exclusion of the protein from these organelles (Fig. 20). Instead, Fig4-positive spots are localized in the areas occupied by the endocytic compartments and are in close proximity with these organelles (Figs 21-23). In particular, we found that both in neural and non-neural cells Fig4 does not partition either in early endosome (labelled with GFP-Rab5 or GFP-Rab4) or in recycling endosomes (labelled with GFP-Rab-11), while it is enriched in GFP-Rab7 compartments (Fig. 21). Similarly, about 5-7% of Fig4 co-localizes with Rab7 compartments labelled with a specific antibody (Fig. 22). Moreover, Fig4 results in close proximity with lamp1-compartments, but there is no co-localization (Fig. 23).

Altogether these data indicate that Fig4 is recruited on Rab7-enriched compartments suggesting that Fig4 could controls their activity.

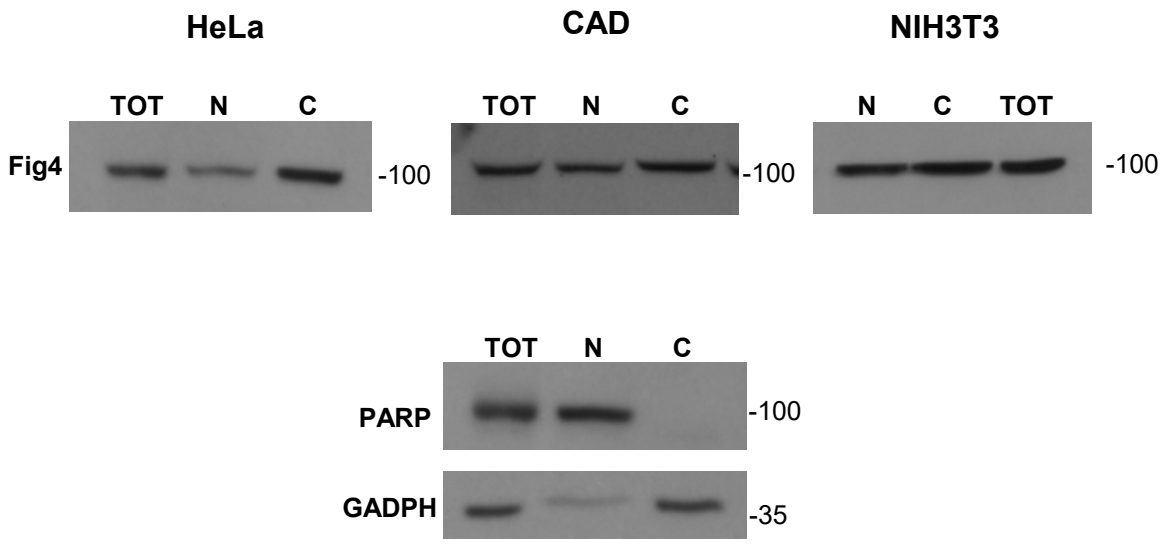

Fig. 19: Fig4 is purified both in cytosol and nuclear fraction in different cell lines. Nuclear are separated from cytosol by two sequential centrifugation (as described in detail in methods). Total cell lysates (T), cytosolic fraction (C) and nuclear fraction were analyzed by SDS-PAGE and western blotting by using an antibody anti Fig4. GAPDH were used as cytosolic and nuclear marker respectively. Molecular weights of standard proteins are indicated.

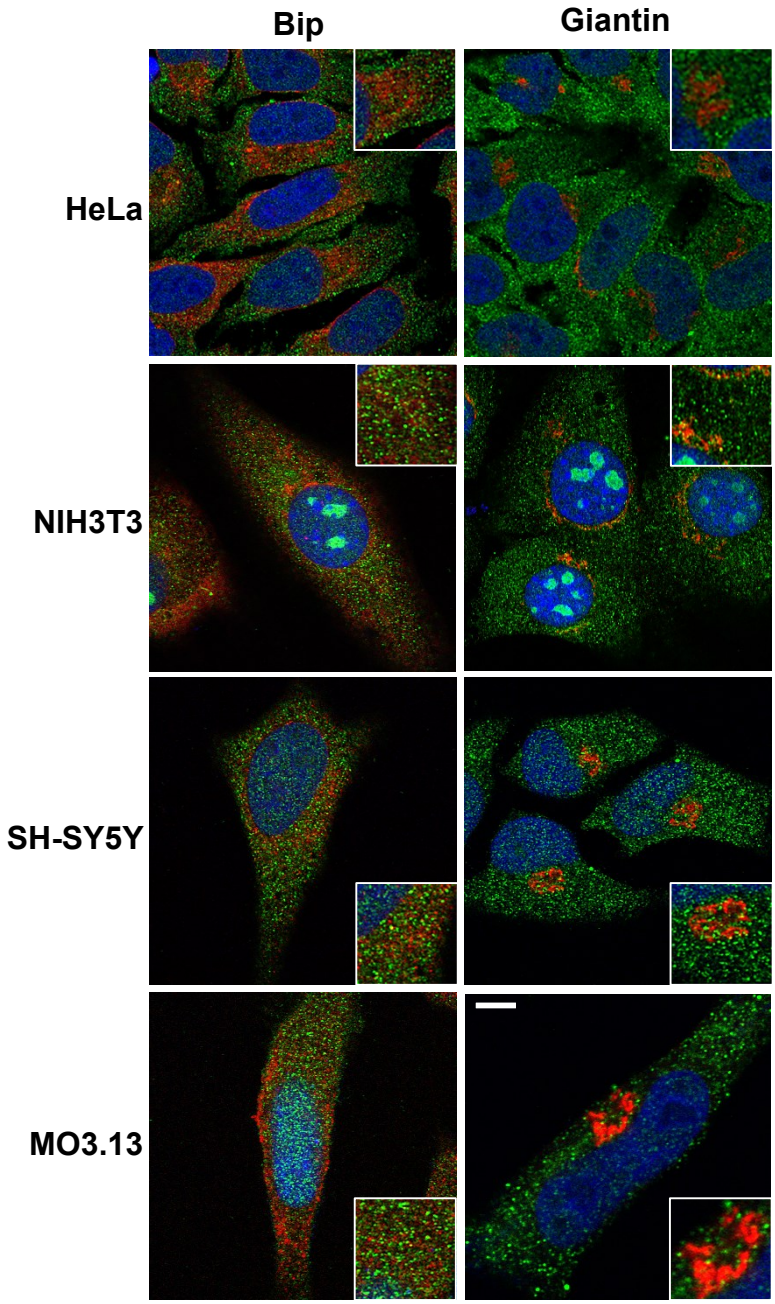

Fig. 20: Fig4 is excluded from Endoplasmic Reticulum and Golgi. Cells were fixed with 4% PFA, permeabilized with 0.2% Triton X-100, and stained by using specific antibodies against Fig4 (green), Bip or Giantin (red) revealed with Alexa Fluor 488 and 546 secondary antibodies, respectively. Nuclei were labelled with DRAQ5 dye. Images were acquired by confocal microscopy. Scale bar 5 μm. Insets show higher-magnification.

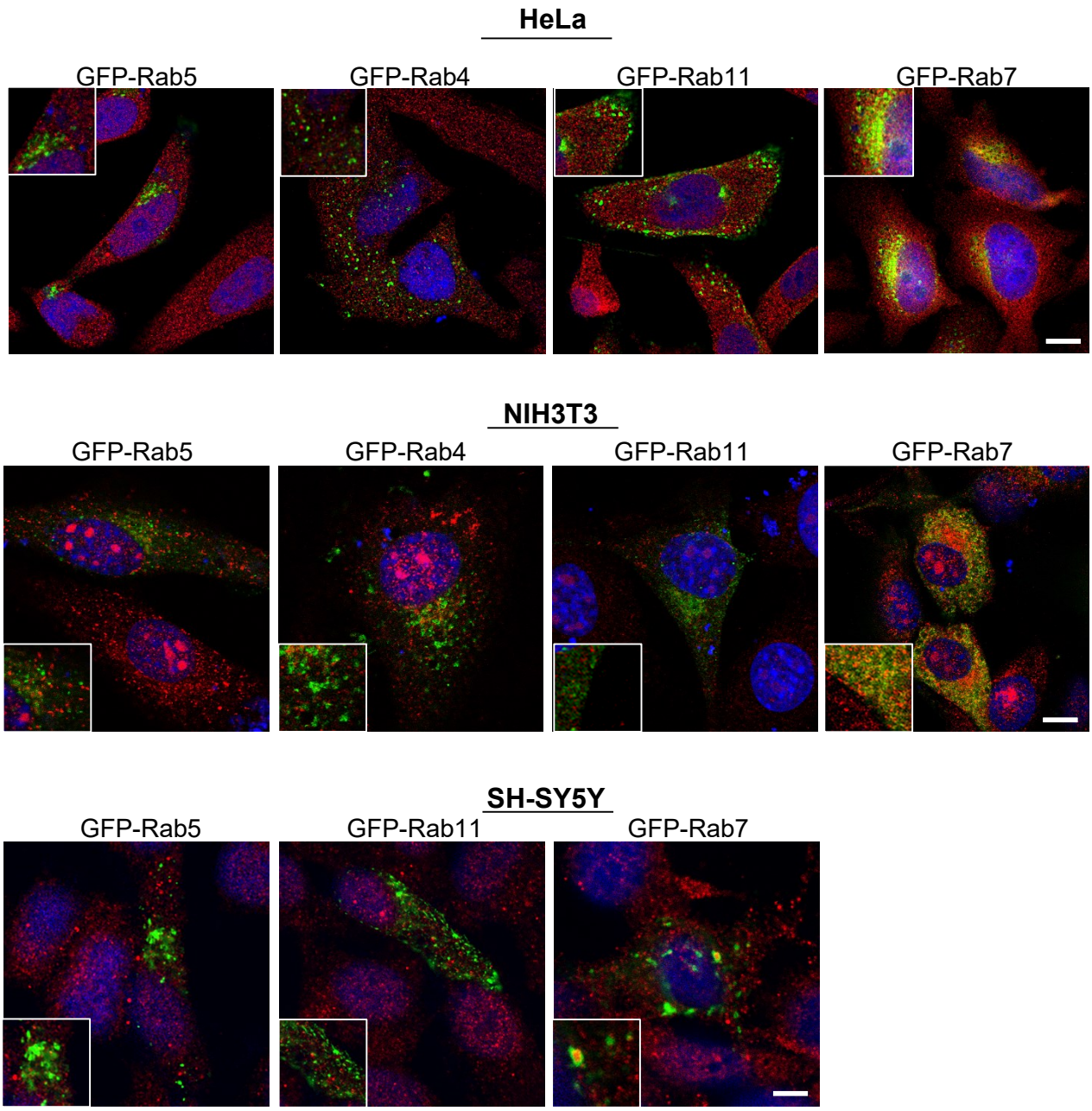

Fig. 21 : Fig4 partially colocalize GFP-Rab7 but not with GFP-Rab5 , GFP-Rab4 and GFP-Rab11. HeLa, NIH3T3 and SH-SY5Y were transiently was transfected with cDNA coding for different GFP-tagged Rab proteins. 48h after transfection the cells was fixed with 4% PFA, permeabilized with 0.2% Triton X-100 and stained with the anti-Fig4 revealed with Alexa Fluor 546-conjugated secondary antibody. Nuclei were labelled with DRAQ5 dye. Images were acquired by confocal microscopy. Scale bar 5 µm. Insets show higher-magnification.

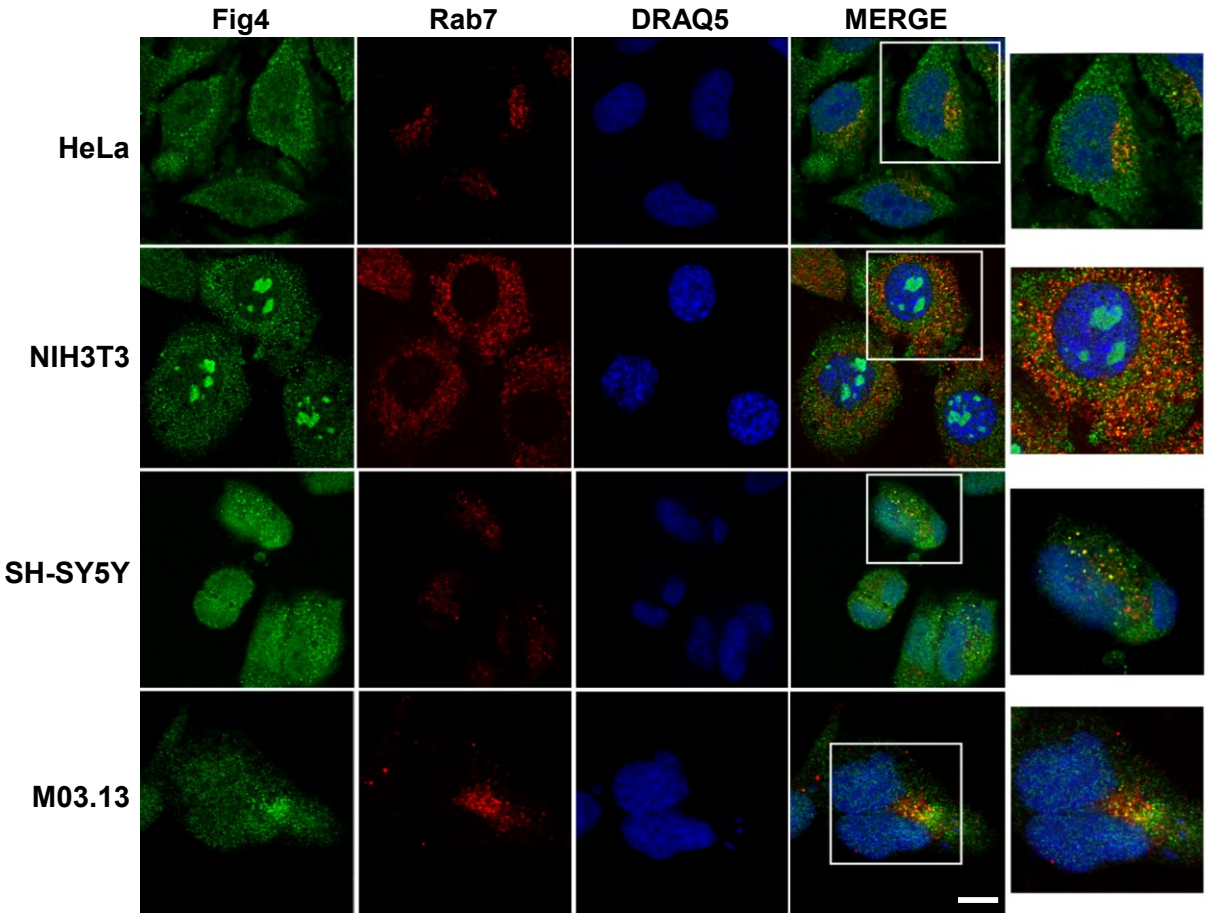

Fig. 22: Fig4 results enriched in Rab7-positive compartments in different cell lines. Cells were subjected to double immunofluorescence assay by using specific antibodies against Fig4 (green) and Rab7 (red). Cells were fixed, permeabilized with 0.2% TX-100 and stained with primary and secondary antibodies. Nuclei were labelled with DRAQ5 dye. Images were acquired by confocal microscopy. Squares show higher-magnification. Scale bar 5 μm.

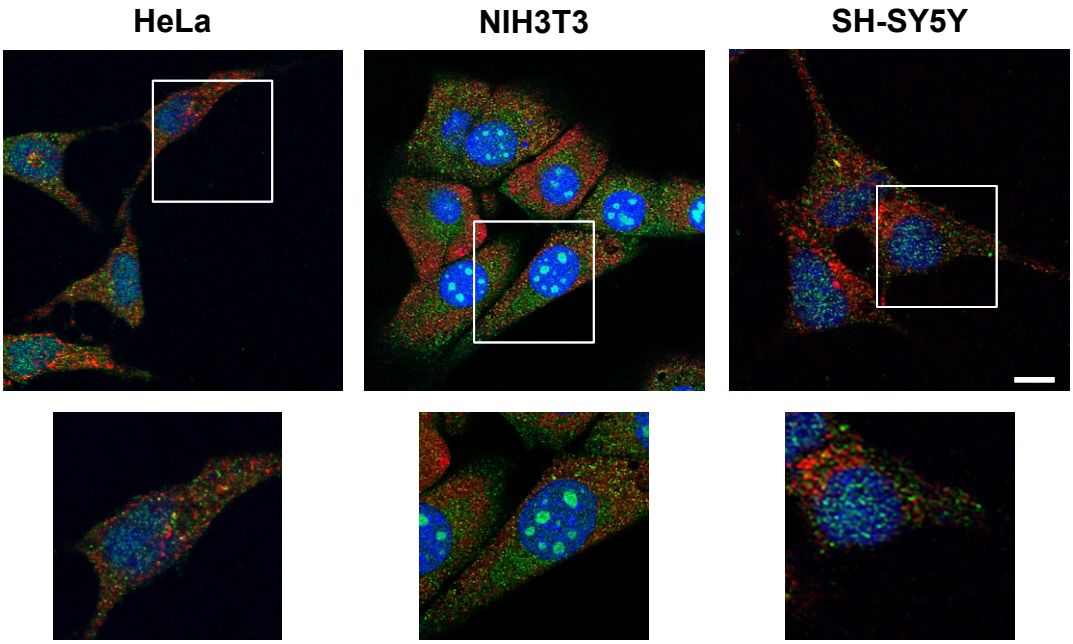

Fig. 23 Fig4 does not co-localize with Lamp1. HeLa, SH-SY5Y, NIH3T3 and MO3.13 cells were subjected to double immunofluorescence by using specific antibodies against Fig4 (green) and Lamp1 (red). Cells were fixed, permeabilized with 0.2% TX-100 and stained with primary and secondary antibodies. Nuclei were labelled with DRAQ5 dye. Images were acquired by confocal microscopy. Scale bar 5 μm. The squares show the magnification of image.

Pathological mutants appears unable to be recruited on intracellular compartments

So far, how the function of Fig4 is impaired is unknown. As aforementioned, the pathological mutant Fig4I41T maintains its hydrolysing activity (Chow et al, 2007). To understand the molecular defect of pathological mutants we decided to investigate their localization and dynamics. To this purpose, we engineered two chimeric proteins, Fig4I41T and Fig4L17P, by site-directed mutagenesis of a GFP-tagged version of the wild-type Fig4 (from Origene). After transfection, we obtained stable clones of HeLa, NIH3T3 and SH-SY5Y cells expressing the chimeric proteins.

As endogenous protein, GFP-Fig4 is localized in the cytosol in punctate structures indicating that GFP tag does not alter the behaviour of protein. Interestingly, we observed that both in HeLa and in SH-SY5 cells the two pathological mutants displayed a more diffuse intracellular signal (Fig. 24). These results suggest that mutants are unable to be recruited on intracellular compartments. Additionally, they suggest that the activity of Fig4 is strictly regulated through its localization.

AIM 2. ROLE OF FIG4 IN THE ENDO-LYSOSOME AXIS

Fig4 expression was silenced in HeLa, NIH3T3 and SH-SY5Y cells

Various studies have reported that fibroblasts of CMT4J patients and plt mice display enlarged Lamp1/2 positive vacuoles (Chow et al, 2007; Zhang et Zhang et al, 2008; Katona et al, 2011), suggesting that the deficiency of Fig4 leads to wide expansion and, likely, to dysfunction of the late endosome/lysosome compartments. Thus, to unravel how the specific pathway/pathways of the endo-lysosomal axis is/are regulated by Fig4 we decided to analyse the effects of its silencing on these compartments.

To this purpose we used specific short hairpin RNAs (SH-2441 and SH-2409 specific for mouse and SH-2555 specific for human, so called because of the position number in the library of short hairpins) and we stably transfected them in HeLa, NIH3T3 and SHSY5Y cells. As control we used an shRNA directed against GFP (SH-GFP, scramble).

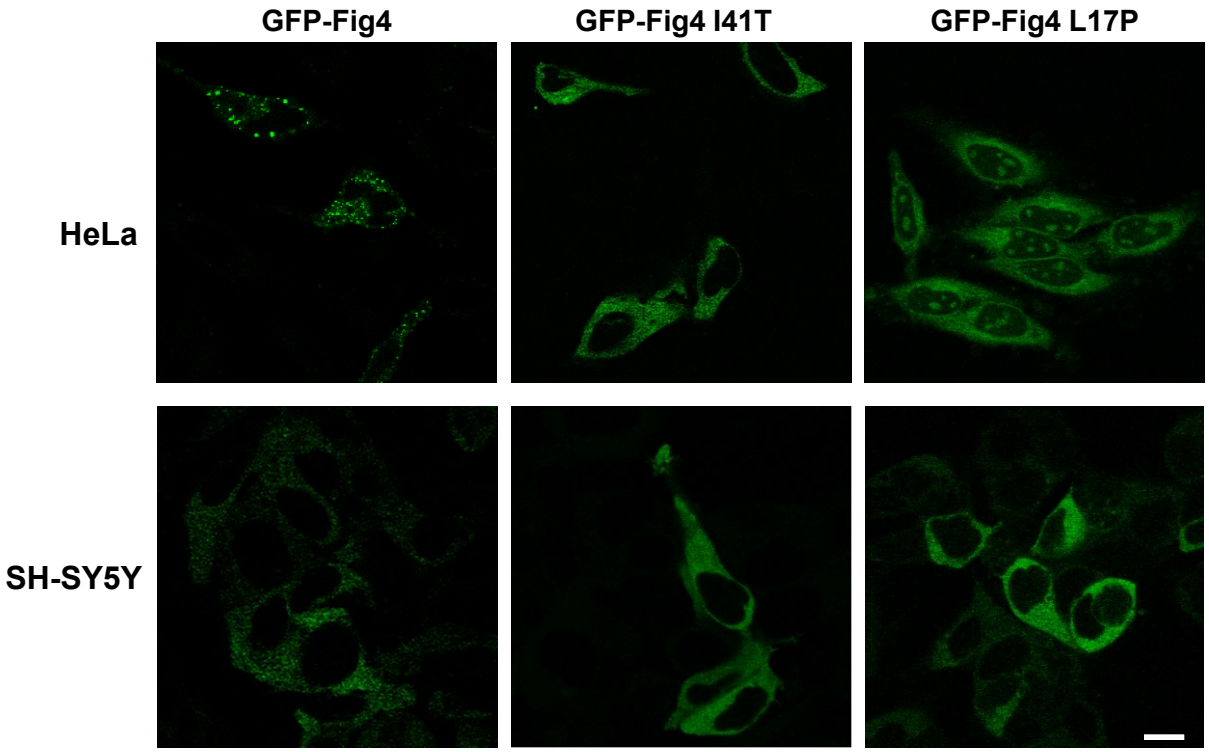

Fig. 24: Mutants of Fig4 display diffuse intracellular signal. Hela and SH-SH5Y stably expressing Fig4-GFP, Fig4I41T-GFP and Fig4L17P-GFP were fixed and images were acquired by confocal microscopy. Scale bar 5 µm.

After puromycin selection we collected several pools and clones for each cell line. We evaluated the efficiency of silencing by western blotting and real-time PCR (data not shown). For each cell line we obtained pools and some clones with different degree of silencing (from 30 to 70%) (Figs. 25-26). As expectable, clones resulted more silenced than pools. In particular, in HeLa cells the cl1 was the most silenced since Fig4 expression is reduced by approximately 65% (Figs. 25, 26), while in SH-SY5Y cells the cl8 displayed the best for the 42% of reduction (Figs. 25, 26). In NIH3T3 cells (2441 and 2409) we got clones with a high degree of silencing with both shRNA (86% and 40%, respectively) (Figs. 25, 26). In addition, by immunofluorescence assay we confirmed these results and we found that not only in the clones, but also in the pool all the cells are homogenously silenced (data not shown). Moreover, by western blot analysis we verified that the silencing is stable (data not shown) and is maintained in the cells in culture until at least the fourth passage (we have not tested later ones) and we have always performed the experiments no later than the third passage in culture.

The loss of Fig4 affects the endosome-lysosome compartments in different cell types

Once obtained the Fig4-silenced cells, we investigated whether and how the loss of Fig4 affects the endo-lysosomal compartments. To this aim, firstly we analyzed the morphology and properties of endo-lysosomal compartments by immunofluorescence assays using different markers of the endocytic route (Figs. 27, 28).

We have observed that in all three silenced cell lines lysosomal compartments are altered (Figure 27). In fact, in Fig4-depleted cells lysosomes, labelled either with the Lysotracker dye or with lamp-1 antibody, are increased in number and appear as large dots with strong fluorescent signal (Figure 27). These results are in agreement with observations made in the fibroblasts of plt mice and patients (Chow et al, 2006; Zhang et al, 2008).

Furthermore, we found that the absence of Fig4 also causes an alteration of early and late endosomes labelled with EEA1 and Rab7 antibodies, respectively (Fig. 28). Again they result more enlarged and the fluorescent signal of both markers are more intense (Fig. 28). Interestingly, in the NIH3T3

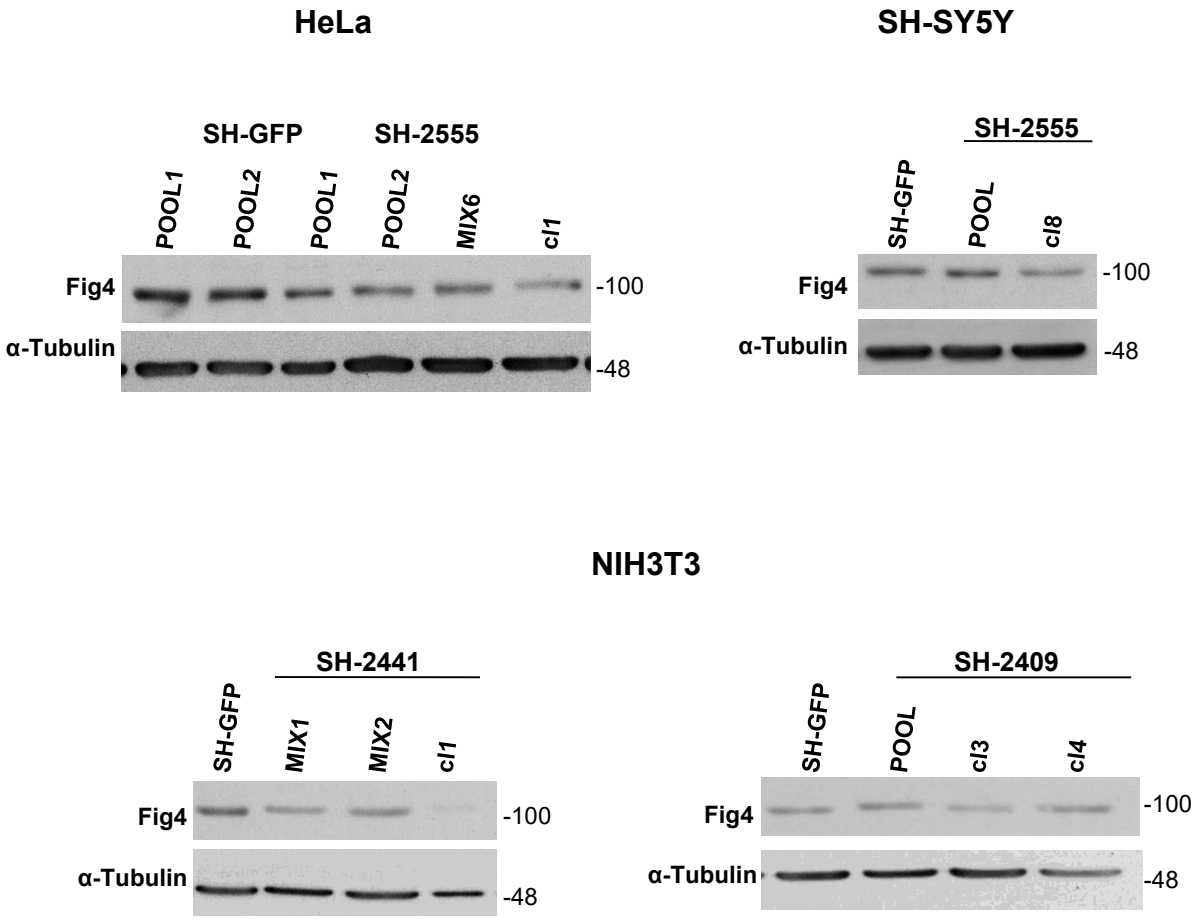

Fig. 25: Fig4 expression is silenced by using short hairpin RNAs in different cell lines. Lysates of NIH3T3, Hela and SH-SY5Y cells transfected with shRNA anti Fig4 (SH-2441, SH-2409, SH-2555), shRNA scramble (SH-GFP) were immunoblotted with an anti-Fig4 antibody. We used α-tubulin as loading control. Molecular weights of standard proteins are indicated.

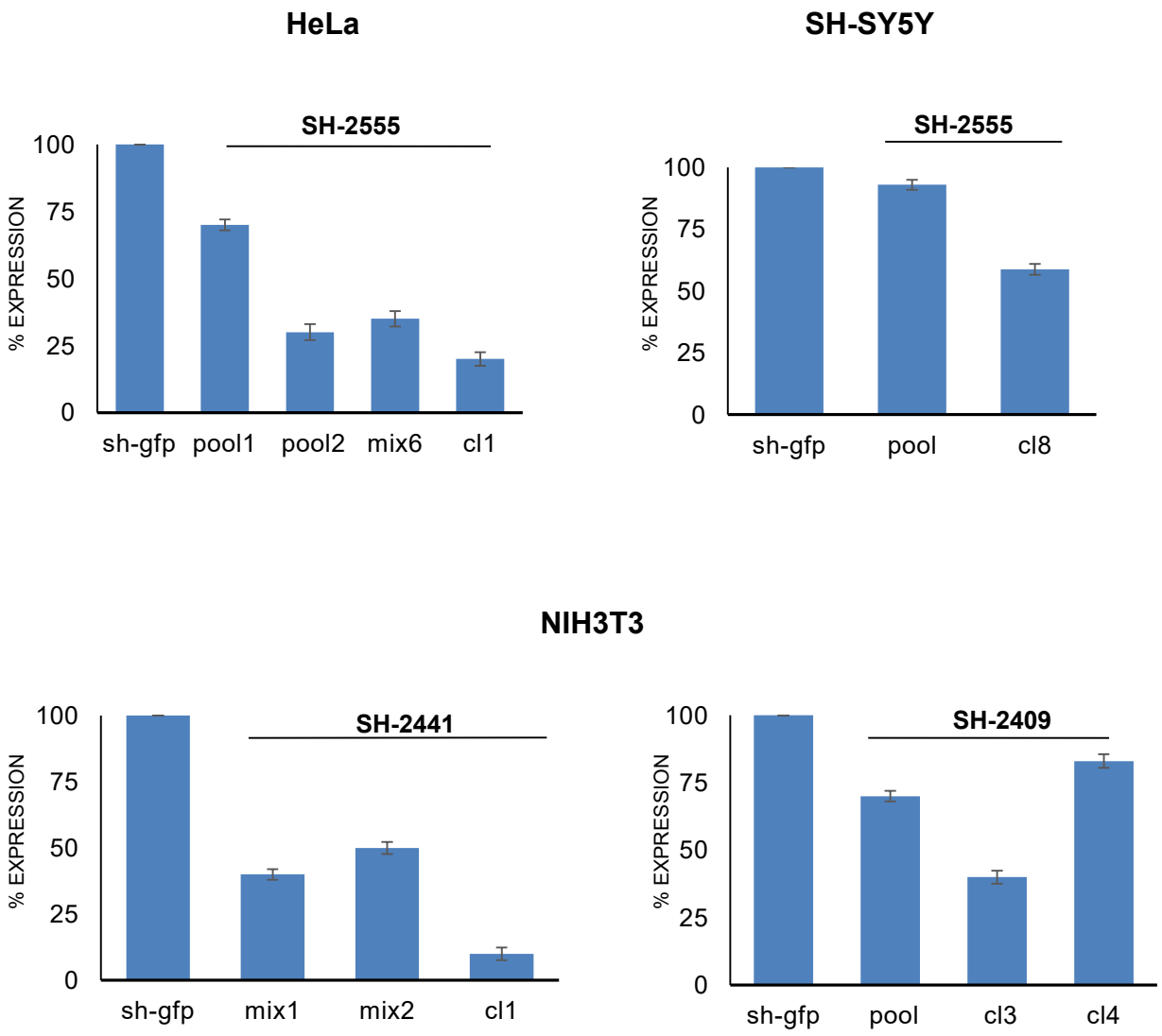

Fig. 26: Quantitation of silencing of the pool or clones in different cell lines. Densitometric analysis of bands was performed with ImageJ. Percentage of Fig4 expression in the different pools and clones respect to the amount of protein in scrambled cells (placed equal to 100). Quantification of three independent experiments are shown (Error bars ± SD).

cells, which have a major degree of silencing, EEA1-compartments appear as longer tubular elements in comparison to the punctate dots of control cells (Fig. 28).

In contrast, the morphology of exocytic organelles (e.g. ER, Golgi) is unchanged in all Fig4-depleted cells (Fig. 29). All these data indicate that the loss of Fig4 affects the homeostasis of the whole endosome-lysosome axis both in neural and non-neural cells.

The loss of Fig4 affects the intracellular trafficking along the endocytic pathway

Beyond to be fundamental to counterbalance the anterograde flux of membranes, endosome-lysosome system connects different cell compartments and is an important station of sorting: internalized molecules from cell outside are recycled back to plasma membrane, targeted to degradation or transported toward early secretory compartment (as Golgi apparatus, ER).

The above results highlight that Fig4 is critical for the homeostasis of the endo-lysosomal system; next, we asked whether Fig4 is also crucial for the function of these organelles. To this purpose, through endocytosis assays we assessed the trafficking of the transferrin receptor (TfR) and the EGF receptor (EGFR) that, after internalization from the plasma membrane, follow two different distinct itineraries: the recycling and degradation, respectively (Maxfield and McGraw, 2004; Thomas et al, 2013). We set up the best experimental conditions to monitor the trafficking of the two receptors.

In the case of TfR cells were incubated with transferrin (conjugated to Alexa Fluor 546 or FITC) at 37°C for different times and then fixed and observed. We found that in Fig4-depleted HeLa cells the transferrin is internalized as in scrambled cells (Fig. 30). Albeit less drastic than at 30 minutes, at early timepoints (5 and 10 min) in silenced cells the signal of transferrin is more intense than in scrambled cells (Fig. 30). At 30 min, we appreciated a strong intracellular accumulation of the transferring and even more the Tf-positive compartment seems collapsed toward the centre of cells (Fig. 30).

We obtained similar results when transferrin was added to cells for 10 minutes at 37°C (pulse), washed out and then cells were incubated for different times

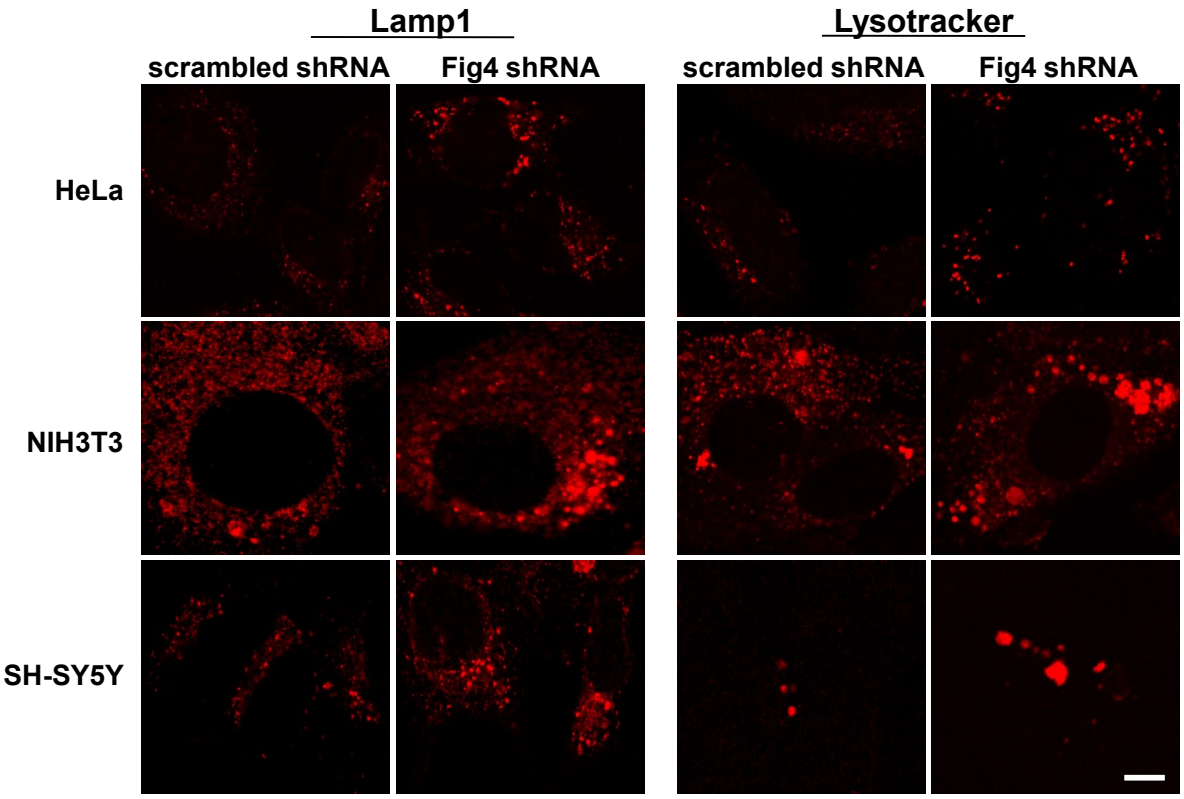

Fig. 27: The loss of Fig4 leads to an enlargement of endo-lysosomal compartments. Scrambled and silenced cells were subjected to immunofluorescence assay by using anti-Lamp1 antibody (left panel). Alternatively, cells were incubated with lysotracker for 1h at 37°C and then fixed. Images were acquired by confocal microscopy by using the same settings (laser power, detector gain). Scale bar 5 μm.

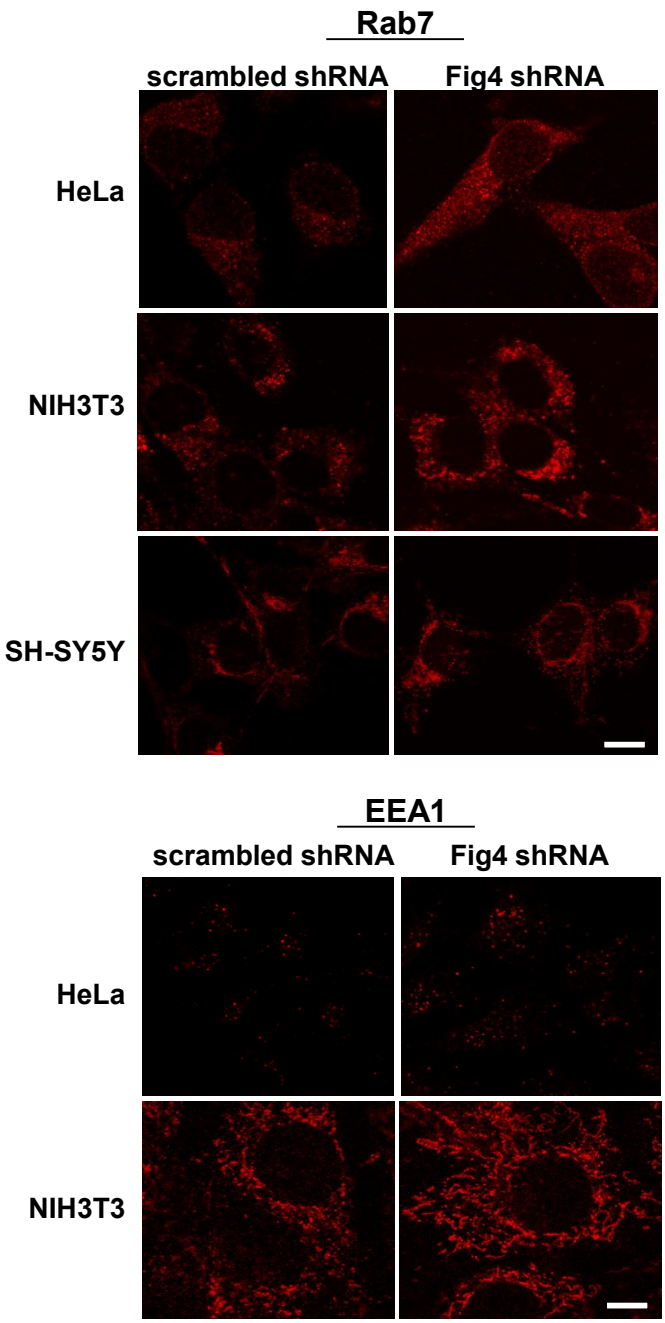

Fig. 28: The loss of Fig4 affects the morphology of both early and late endosomes. After fixation scrambled and silenced cells cells were permeabilized and stained with EEA1 (early endosome antigen 1) or Rab7 revealed with Alexa Fluor 546-conjugated secondary antibody. Images were acquired by confocal microscopy by using the same settings (laser power, detector gain). Scale bar 5 µm.

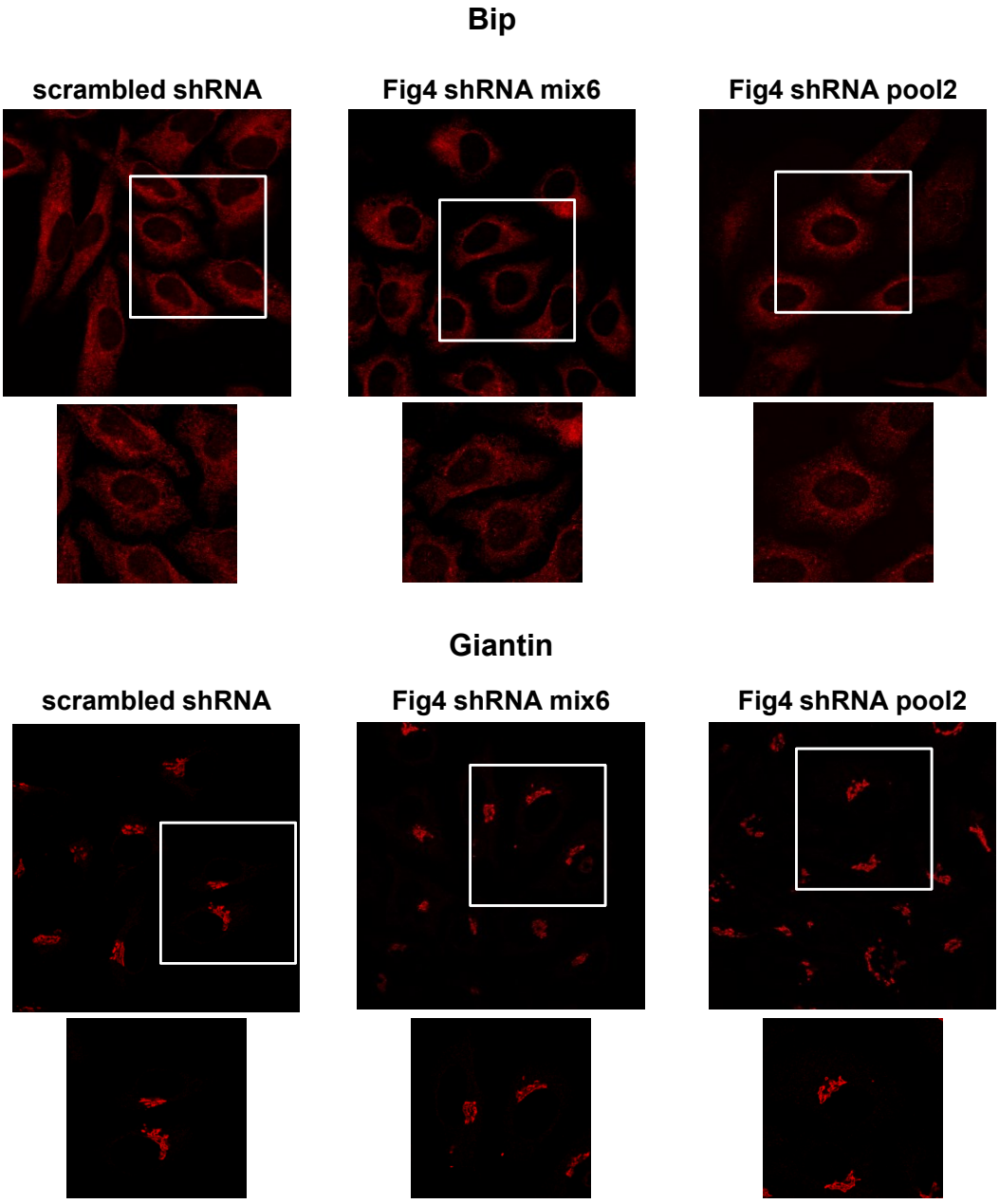

Fig. 29: The loss of Fig4 in Hela cells does not affects the morphology of Golgi and Endoplasmic Reticulum. Scrambled and silenced Hela cells were subjected to immunofluorescence assay. After fixation were permeabilized and stained with Giantin or Bip primary antibodies revealed with Alexa Fluor 546-conjugated secondary antibody. Images were acquired by confocal microscopy by using the same settings (laser power, detector gain). Scale bar 5 μm. The squares show the magnification of image.

(chases) in fresh medium (data not shown). Thus, all these data indicate that the loss of Fig4 alters the recycling of TfR, which is internalized but does not recycle back to the surface.

In addition, we observed the accumulation of transferrin also in SH-SY5Y cells as evident in single confocal sections and in 3D reconstruction (Fig. 31). This indicates that the regulation of the function of these compartments by Fig4 is a general mechanism active in all cell types.

To monitor the intracellular traffic of the EGF receptor (EGFR) we used a chimeric protein in which the GFP (green fluorescent protein) is fused to the EGF receptor. For this purpose, scrambled or Fig4-silenced cells were transiently transfected with cDNA coding for GFP-EGFR and 48 hours after transfection, the cells were serum starved for 3h (as previously described, Dinnen and Ceresa, 2004; Puri et al, 2005) in order to prevent its ligand-dependent internalization. As consequence, receptor accumulates at plasma membrane and indeed, as shown in Fig. 32, after starvation (time 0) the GFP signal is only present on the cell surface. Then cell were stimulated with EGF (100 ng/mL) at 37°C for different times.

It is important to note that at time 0 the fluorescent signal is comparable in control and silenced cells indicating that the absence of Fig4 does not alter the biosynthetic transport of the receptor on the surface (Fig. 32). As expected, upon EGF stimulation EGFR is internalized, but in Fig4-depleted cells it progressively accumulates at the intracellular level as shown by the intense intracellular GFP signal respect to control cells (Fig. 32). These data indicate that the absence of Fig4 also alters the fate of the EGF receptor. The intracellular accumulation may be due to the dysfunction of lysosomes, which could be unable to degrade proteins.

AIM 3. ROLE OF FIG4 IN NEURAL DIFFERENTIATION

Fig4 is expressed in all the stages of neural and mesodermal differentiation

The fact that in plt mice the loss of Fig4 leads to distinct pathogenic changes in different neuronal cell subtypes (Ferguson et al, 2009; Katona et al, 2011)

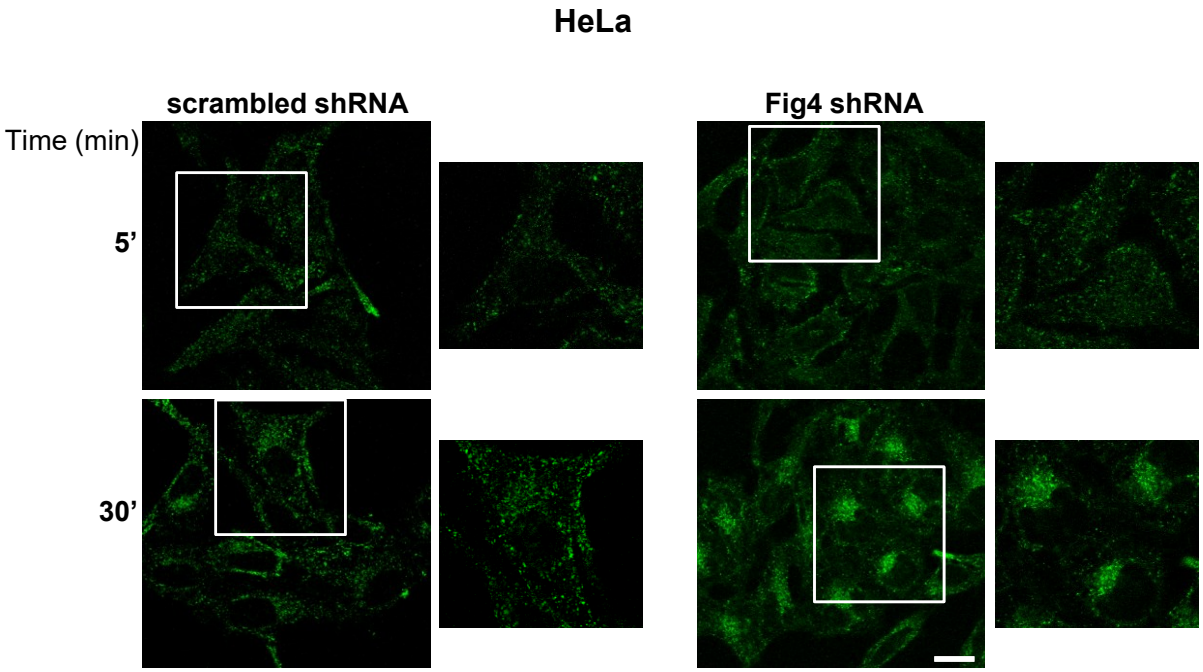

Fig. 30: The loss of Fig4 affects the trafficking of TfR in HeLa cells. Scrambled and silenced cells were incubated at 37°C with FITC- conjugated transferrin (Tf) for each time, cells were fixed with 4% PFA. Images were acquired by confocal microscopy by using the same settings (laser power, detector gain). Scale bar 5 μm. The squares show the magnification of image.

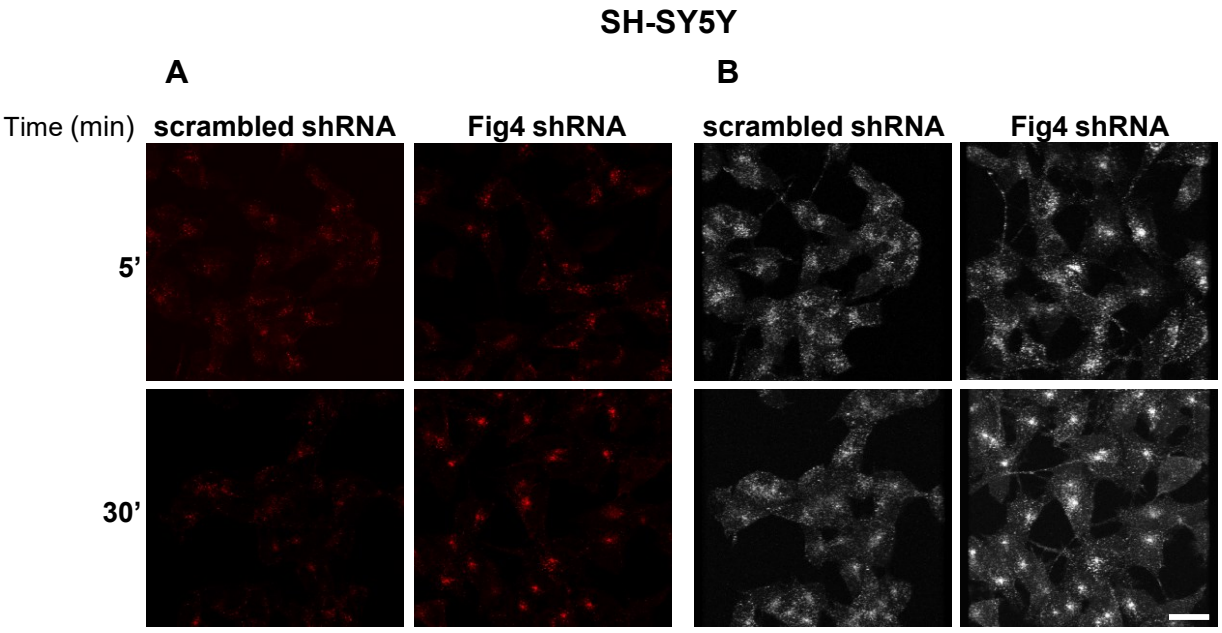

Fig. 31: **The loss of Fig4 affects the trafficking of TfR in SH-SY5Y cells.** Internalization assay of Alexa Fluor 546 conjugated transferrin (Tf) in scrambled and Fig4 silenced SH-SY5Y cells was carried out as in Fig. 30. An xy section toghether the 3D reconstruction are shown. Confocal images were acquired from the top to the bottom of cells by using the same settings (laser power, detector gain). Scale bar 5 μm.

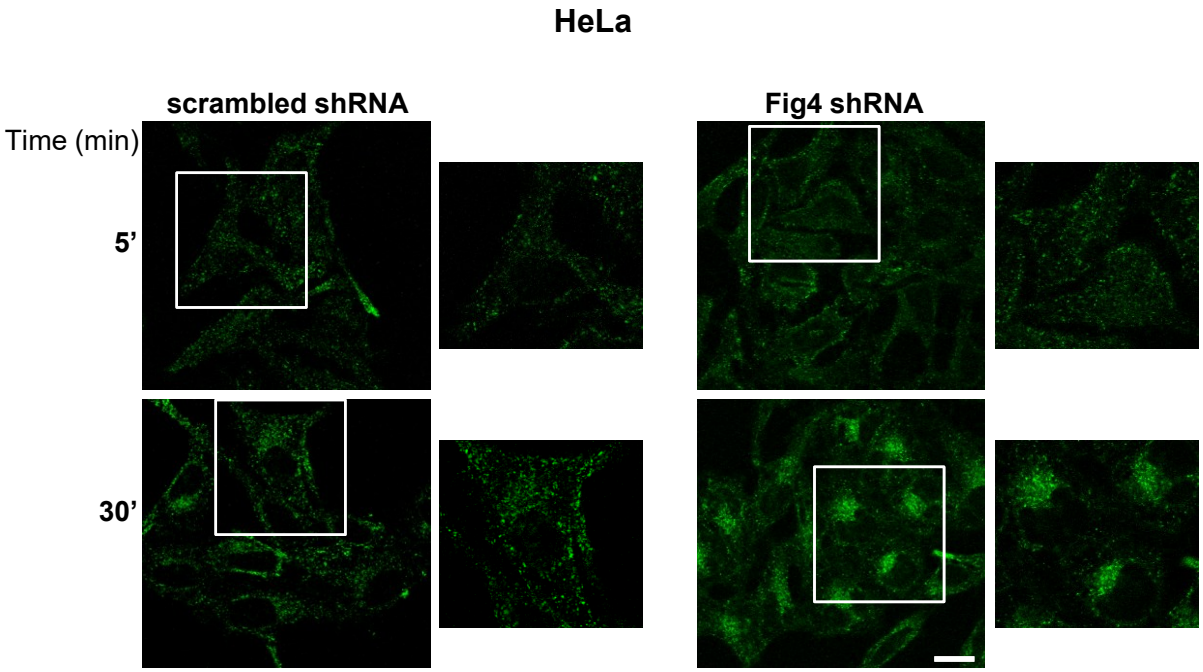

Fig. 30: The loss of Fig4 affects the trafficking of TfR in HeLa cells. Scrambled and silenced cells were incubated at 37°C with FITC- conjugated transferrin (Tf) for each time, cells were fixed with 4% PFA. Images were acquired by confocal microscopy by using the same settings (laser power, detector gain). Scale bar 5 μm. The squares show the magnification of image.

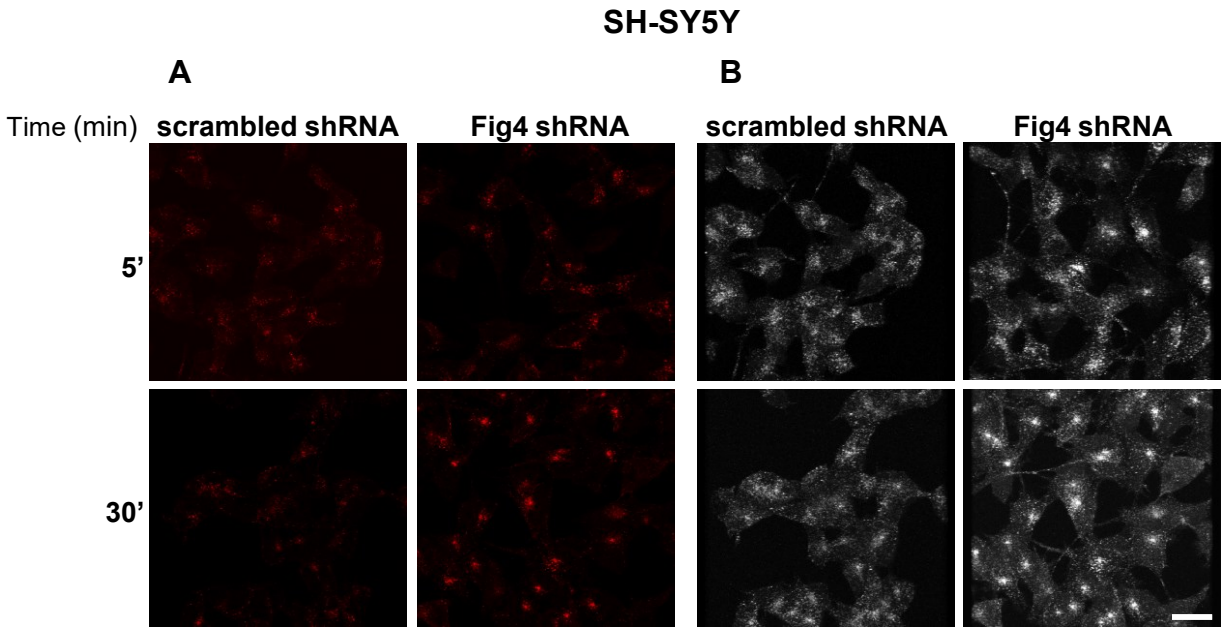

Fig. 31: **The loss of Fig4 affects the trafficking of TfR in SH-SY5Y cells.** Internalization assay of Alexa Fluor 546 conjugated transferrin (Tf) in scrambled and Fig4 silenced SH-SY5Y cells was carried out as in Fig. 30. An xy section together the 3D reconstruction are shown. Confocal images were acquired from the top to the bottom of cells by using the same settings (laser power, detector gain). Scale bar 5 μm.

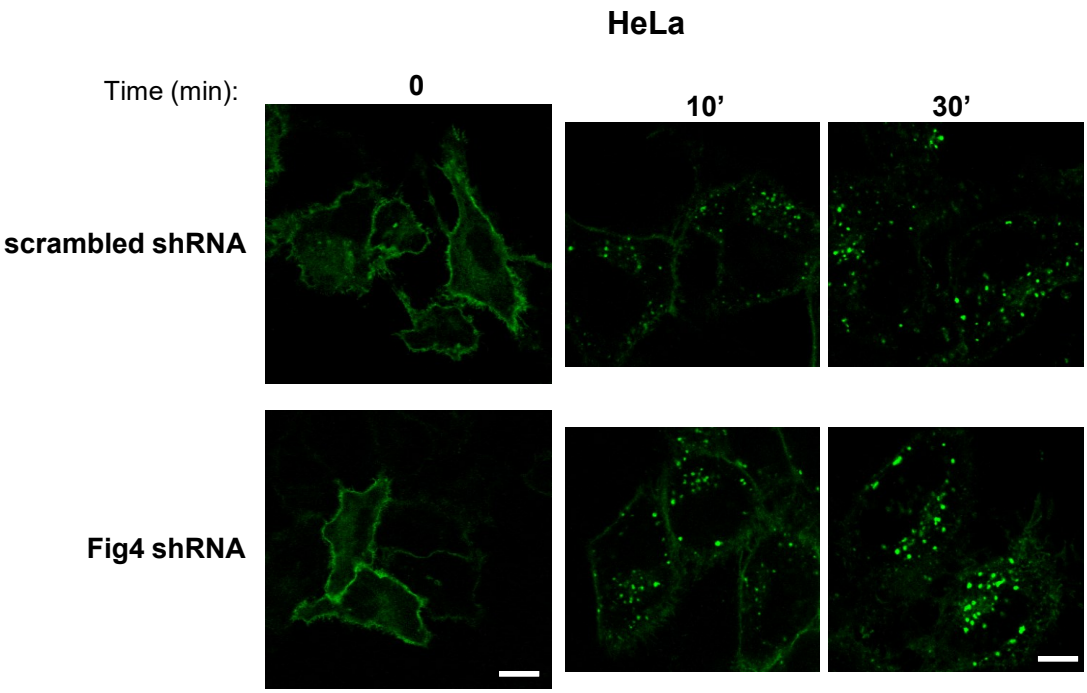

Fig. 32: The loss of Fig4 affects the trafficking of EGFR. Scrambled and Fig4-silenced HeLa cells were transiently transfected with cDNA coding for GFP-EGFR. 48 h after transfection, cells were serum starved for 3h, then treated with EGF (100 ng/mL) and fixed at the indicated times. Images were acquired by confocal microscopy by using the same settings (laser power, detector gain). Scale bar 5 μm.

and the loss of Fig4 is implicated in the defects of myelin sheath formation (Vaccari et al, 2014) suggesting that Fig4 might play cell-specific role and, likely, this might contribute to CMT4J pathogenesis. However, the molecular basis for the differential sensitivity of neuronal subtypes to loss of Fig4 is unclear.

To understand the role of Fig4 in neural differentiation we will take advantage of mouse embryonic stem cells (ESCs) differentiation, which are able, under specific conditions, to differentiate in any type of cell of an adult organism. In collaboration with Dr. Silvia Parisi, who set up protocols to specifically differentiate ESCs cells (Parisi et al, 2010) we analyzed the expression and distribution of Fig4 in stem cells and during neuronal differentiation by using double or triple immunofluorescence assays (Fig. 33).

We found that Fig4 is expressed in ESCs as wells as during the early stages of differentiation (SFEBS, serum free embryoid bodies) and in terminally differentiated neural subtypes (Fig. 33). Indeed, Fig4 is present in the Oct3/4 (stemness markers) positive cells, indicating that Fig4 gene is already expressed in stem cells (Fig. 33). We obtained similar results in Human embryonic stem cells (Fig. 33). Moreover, we found that Fig4 is expressed in all cells of SFEBS programmed toward neuorectodermal differentiation (which contain about 90% neuroectodermal cells, 8% mesodermal cell, 1-2% stem cells) at comparable extent. Indeed it is present both in Oct3/4 and Sox1 (marker of early neural differentiation) positive cells. Altogether these data indicate that Fig4 is expressed in the early stages of neural differentiation (Fig. 33).

Fig4 is localized mainly in the cytoplasm of ESCs and SFEBS preferentially in discrete punctate structures (Fig. 33). Interestingly, in ESCs it is also evident signal of Fig4 in nuclear areas (Fig. 33) resembling the nuclear structures also observed in cell lines of embryonic origin (Fig. 18).

Finally, in post-mitotic-neurons (after 13 days of ESCs differentiation) labelled with β3-tubulin (neuron marker) and GFAP (astrocyte marker) we found that Fig4 is expressed both in neurons and in astrocytes. In both cell types it is localized on the cell body and in neural extensions.

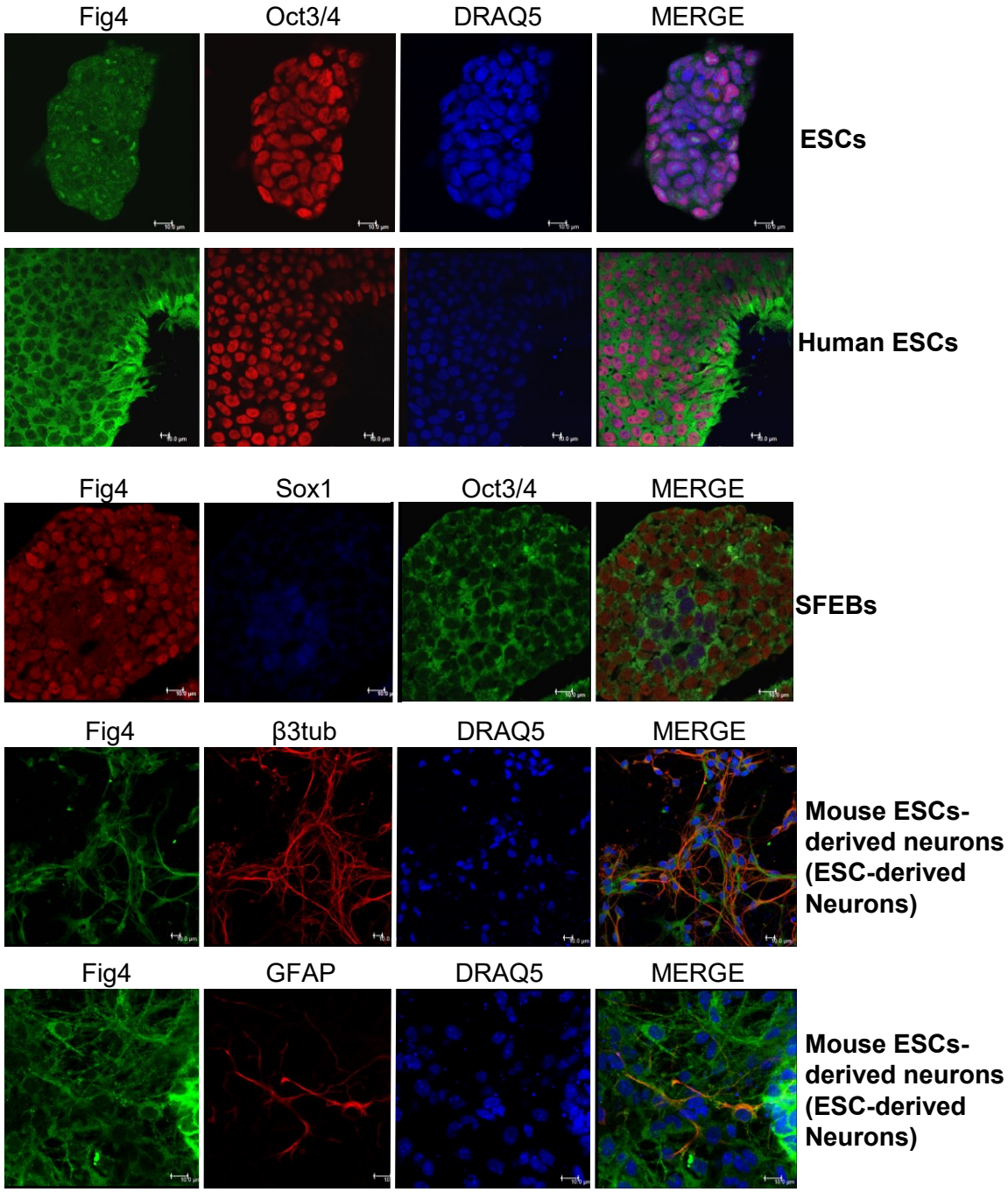

Fig. 33: Fig4 is expressed in Embryonic stem cells and during all the stages of the neural differentiation. Double or triple immunofluorescence was carried out in mouse and human Embryonic stem cells (ESCs) as well as in SFEBs and in mouse ESC-derived neurons by using specific markers of stemness (Oct3/4) or neural differentiation (Sox1 and β3tubulin). To identify astrocytes, differentiated neurons were labelled with GFAP. Nuclei were stained with DRAQ5. Images were acquired by confocal microscopy. Scale bar 10 μm.

We also evaluated the expression levels of Fig4 during the neural differentiation by western blotting (Fig. 34A). We found that the expression follows a peculiar kinetic: the levels of FIG4 are high in ESCs, decrease in SFEBS, and then increase again when the cells differentiate into neurons (Fig. 34A). Same kinetic was found by analyzing the levels of Fig4 transcripts by real-time PCR (Fig 34B). Interestingly, differently from neural differentiation, during mesodermal differentiation the levels of Fig4 decrease respect to the ESCs and then both transcripts and proteins remain stable over time (Fig. 35). In addition, the Fig4 expression during the diverse stage of mesodermal differentiation is lower than we observed during neural differentiation (Fig. 35).

Fig4 is essential in the early phases of neural differentiation

At this point, we asked in which steps of differentiation Fig4 could play a critical role. To this aim, we silenced the FIG4 expression in ESCs cells by using specific shRNAs, which are stably transfected in the cells. We collected a pool of ESCs transfected with a good degree of silencing (about 60-65%, Fig. 36 upper panel).We investigated the effect of loss of Fig4 in neural differentiation by analyzing the expression of Oct4 and Sox1 assayed by real-time-PCR (Fig 36, middle panel). Interestingly, the loss of Fig4 correlates with altered expression of stemness and and early neural markers (OCT4 and SOX1, respectively). Indeed, we found that in Fig4-depleted ESCs the levels of Oct4 are lower than in control cells, indicating a rapid loss of stemness (Fig. 36). Consistently, the expression of Sox1 increases earlier upon Fig4 silencing (Fig. 36). Although the silencing of Fig4 is lost over time, its absence in ESCs is sufficient to alter the equilibrium between stemness and differentiated proteins. These results suggest that the loss of Fig4 induces earlier differentiation.

Because of technical limit that ESCs lost the silencing of Fig4 during the culture, we decide to silence transiently the expression of Fig4 by using Stealth RNA and analyzed the effect of Fig4 absence in the early stage of neural differentiation. As shown in Fig. 37, the expression of Nanong, another marker of stemness, is reduced in Fig4-depleted cells, in agreement with results obtained with stable interference (Fig. 36).

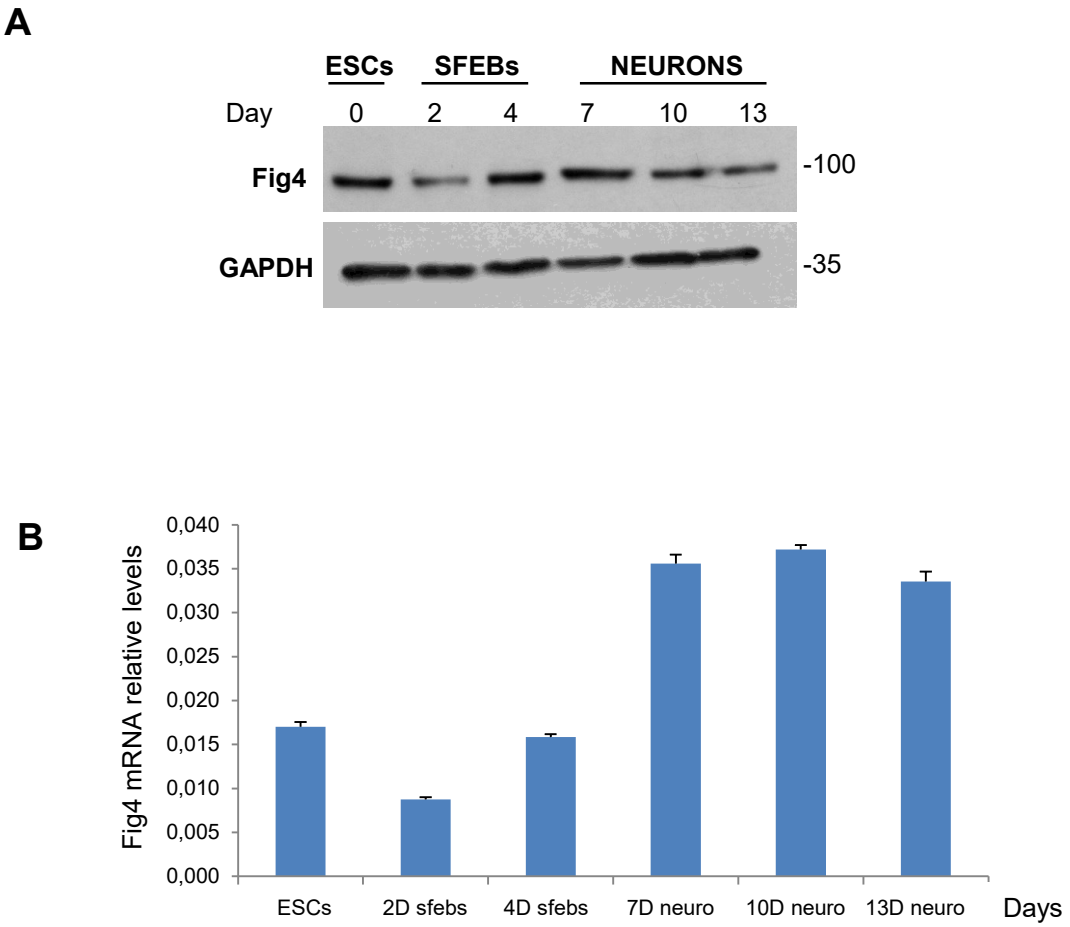

Fig. 34: Both Fig4 proteins and transcripts were expressed at different extent during all stages of neural differentiation. ESCs were induced to neural differentiation (see methods). After each time point cells were collected and processed for western blot (A) or for RT-PCR analysis (B). Samples were revealed with a specific anti-Fig4 antibody. We used GAPDH as loading control. Molecular weights of standard proteins are indicated (A). RT-PCR analysis (B) shows the mRNA expression levels of Fig4 (B). Error bars represent standard deviation of experimental triplicates.

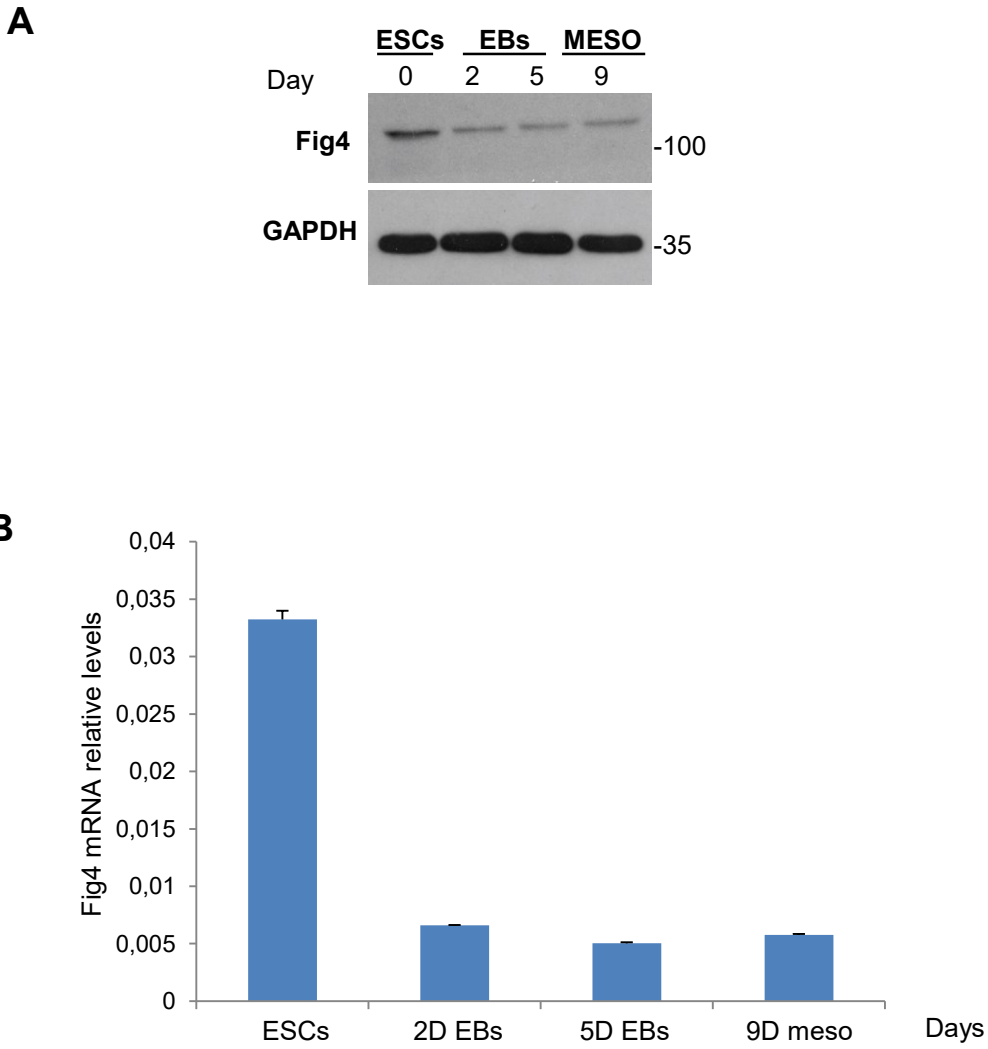

Fig. 35: Fig4 is expressed at low level during mesodermal differentiation. ESCs were induced toward mesodermal differentiation (see methods). At each time point, cells were processed for western blot and RT-PCR analysis as described in Fig.34 Molecular weights of standard proteins are indicated (A). Real time PCR shows the mRNA expression levels of Fig4 (B). Error bars represent standard deviation of experimental triplicates. EBs: Embryoid bodies; meso: mesoderm.

.

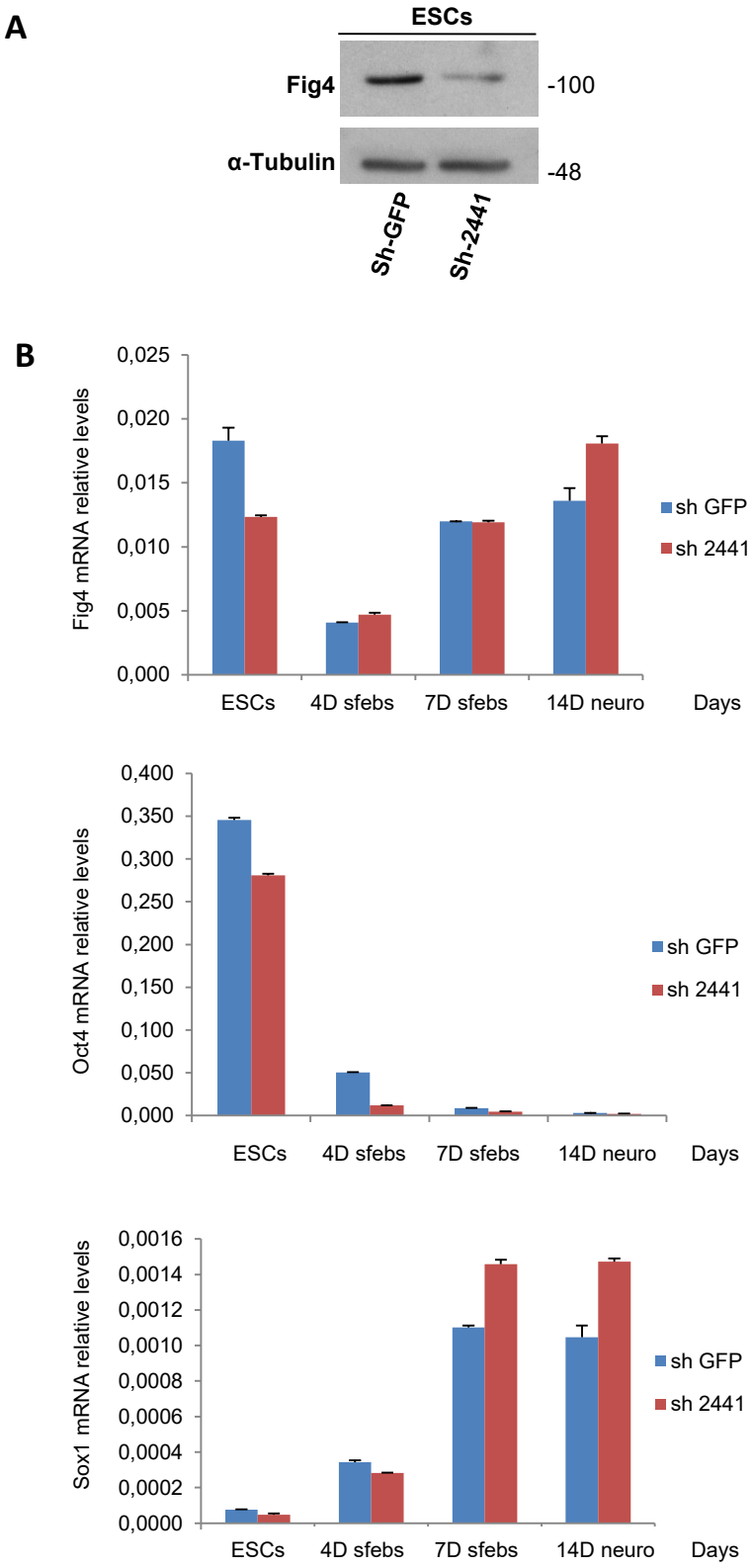

Fig. 36: The depletion of Fig4 in ESCs correlates with the altered expression levels of stemness and neural differentiation markers. ESCs were stably transfected with a short hairpin RNA against Fig4 (sh-2441) or anti-GFP as control (sh-GFP). Western blot analysis shows that Fig4 is silenced at great extent (A). α-tubulin was used as loading control. Molecular weights of standard proteins are indicated (A). Real time PCR (B) show the mRNA expression levels of Fig4, stemness (Oct4) and early neural differentiation (Sox1) markers. Error bars represent standard deviation of experimental triplicates.

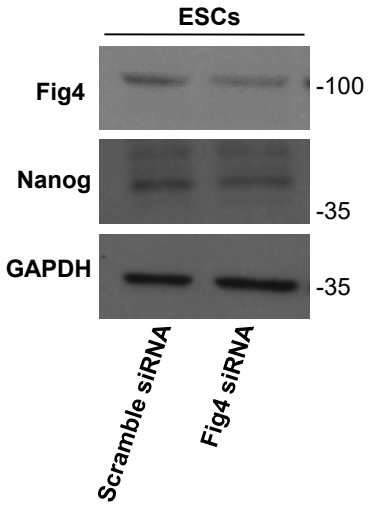

Fig. 37: Fig4 depletion in ESc correlates with an alteration of the expression levels of Nanog. ESCs were transiently transfected with specific Stealth against Fig4 (Fig4 siRNA) or with an unspecific sequence as control (scramble siRNA). The level of Fig4 and Nanog (stemness marker) were analyzed. GAPDH was used as loading control. Molecular weights of standard proteins are indicated.

All these data suggest that Fig4 is essential in the early phases of neural differentiation.

Unfortunately, because the silencing of Fig4 is lost over time, so far we did not get any data on the role of Fig4 in the late stages of neural differentiation. We are currently set up the best conditions to silence Fig4 expression later (already during neuroectodermal differentiation) by using Stealth RNA to analyse this issue.

PROJECT 2: MOLECULAR BASIS OF PARKINSON'S DISEASE

AIM 1. SET UP CELLULAR MODELS

Synj1 is expressed in different cell lines

First aim of project 2 was to set up the good cellular model to subsequent studies. To this purpose, first we analysed, by western blotting, the expression of Synj1 in various cell types (neural and non-neural) because the protein has a broader tissue distribution (Ramjaun and McPherson, 1996) as also confimed by recent analysis of mRNA expression profiles made on human and mouse tissues (GeneAtlas).

As shown in Figure 38, Synj1 migrates in the gel as two bands (slower and faster) corresponding to the molecular weight of the two isoforms of the protein (170 and 145 kDa, respectively). In agreement with previous data (Ramjaun and McPherson, 1996; Haffner et al, 1997), in neuronal cells only the 145 kDa isoform is present, while in the other cell types both isoforms are present at different extent (Fig. 38).

Since the expression is quite comparable in the different cell lines, for the following studies we used as cell model: i) Hela cells as a non-neural cell because they are easy manipulate (e.g., easy to transfect, etc.); ii) SH-SY5Y cells as neural type, constituting also a good model of the disease because these cells have many features of dopaminergic neurons (such as they produce dopamine).

Synj1 is localized in the cytoplasm mainly along the plasma membrane

By indirect immunofluorescence assay, we analysed the localization of Synj1 in Hela and SH-SY5Y. We found that in both cells lines, Synj1 is localized in the cytoplasm mainly along the plasma membrane (Fig. 39) in agreement with the fact that it is involved in synaptic vesicle endocytosis (McPherson et al, 1994; McPherson, Takei, et al, 1994). In addition, Synj1 is also present in intracellular discrete punctate structures more distant from surface (Fig. 39), which could be other sites where the enzyme acts. Moreover, it is interesting to note that in both cells lines there is a weaker signal at the level of the

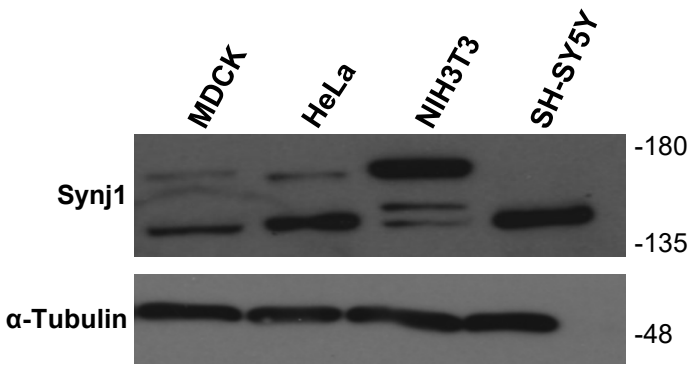

Fig. 38: Synj1 is expressed in different cell lines. MDCK, HeLa, NIH3T3 and SH-SY5Y cells were lysed and resolved by SDS-PAGE. Samples were revealed by using an specific antibody anti- Synj1. α-tubulin was used as loading control. Molecular weights of standard proteins are indicated.

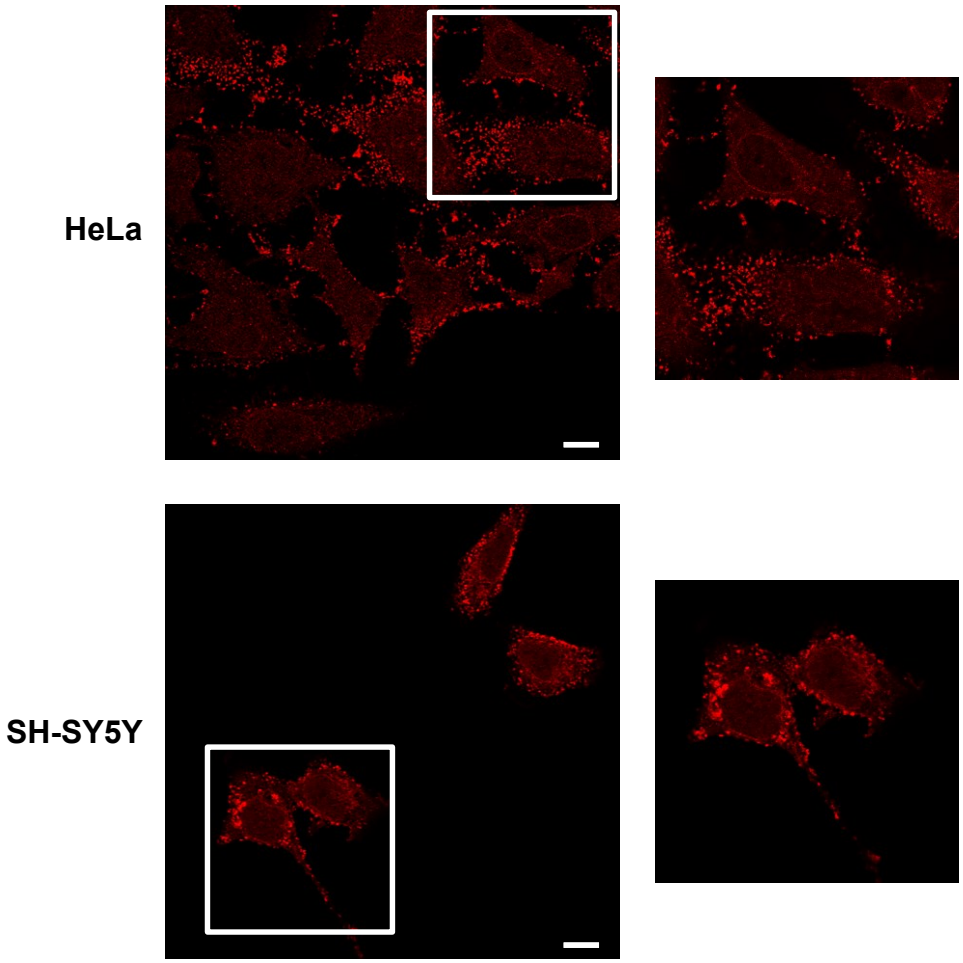

Fig. 39: Synj1 is localized mainly in the cytoplasm along the plasma membrane both in HeLa and SH-SY5Y cells. Cells were fixed, permeabilzed with 0.2% Triton X-100 and stained with an anti-Synj1 antibody revealed with Alexa Fluor 546-conjugated secondary antibody. Images were acquired by confocal microscopy. Scale bar 5 µm. Squares show the magnification.

endoplasmic reticulum as demonstrated by the nuclear envelope positivity (Fig. 39).

Furthermore, we analysed the localization of Synj1 in SH-SY5Y cells induced to differentiation by treatment with retinoic acid or its analogue (such as retinal) as previously described (Xie Hong-Rong et al, 2010). Although SH-SY5Y cells have the characteristics of neuronal cells, following to the treatment they can differentiate even more assuming the distinctive morphological and biochemical properties of the neurons in the human brain. The cells, cultured in low-serum medium (5% instead of 10 %) and in the presence of retinoic acid (or retinal, 10 μM), cease to proliferate and start to differentiate as shown by the formation of long neurites (Fig. 40A). We monitored the cells day by day evaluating their morphological characteristics over time (some representative images in Figure 40A). As it can observe, the cells change morphology over time by acquiring the peculiar neuronal morphology showing long neurites (Fig. 40A). In according to previous studies (Xie Hong-Rong et al, 2010), we also found that seven days after treatment cells reach the maximum differentiation state and at this time cells were subjected to double immunofluorescence assay using an anti-Synj1 antibody (in green) and an anti β3-tubulin (red), which is a typical marker of post-mitotic neruons. We found that in differentiated cells Synj-1 is localized in discrete punctate structures mainly along neurites (Fig. 40B).

AIM 2. ROLE OF SYNJ1 IN THE ENDOCYTIC PATHWAY

Synj1 expression was silenced in HeLa and SH-SY5Y cells

Various studies demonstrated that Synj1 together with its interacting partners dynamin and endophilin is implicated in synaptic vesicle endocytosis (McPherson, Takei et al, 1994; McPherson et al, 1996; Milosevic et al, 2011; Soda et al, 2012). Moreover, recent findings carried out in cone photoreceptors of Zebrafish highlighted that Synj1 could be also critical for proper membrane trafficking (Holzhausen et al, 2009; George et al, 2014), but this new role has yet to be confirmed in mammalian cells. Thus, to better understand the cellular pathways in which Synj1 could be involved and to

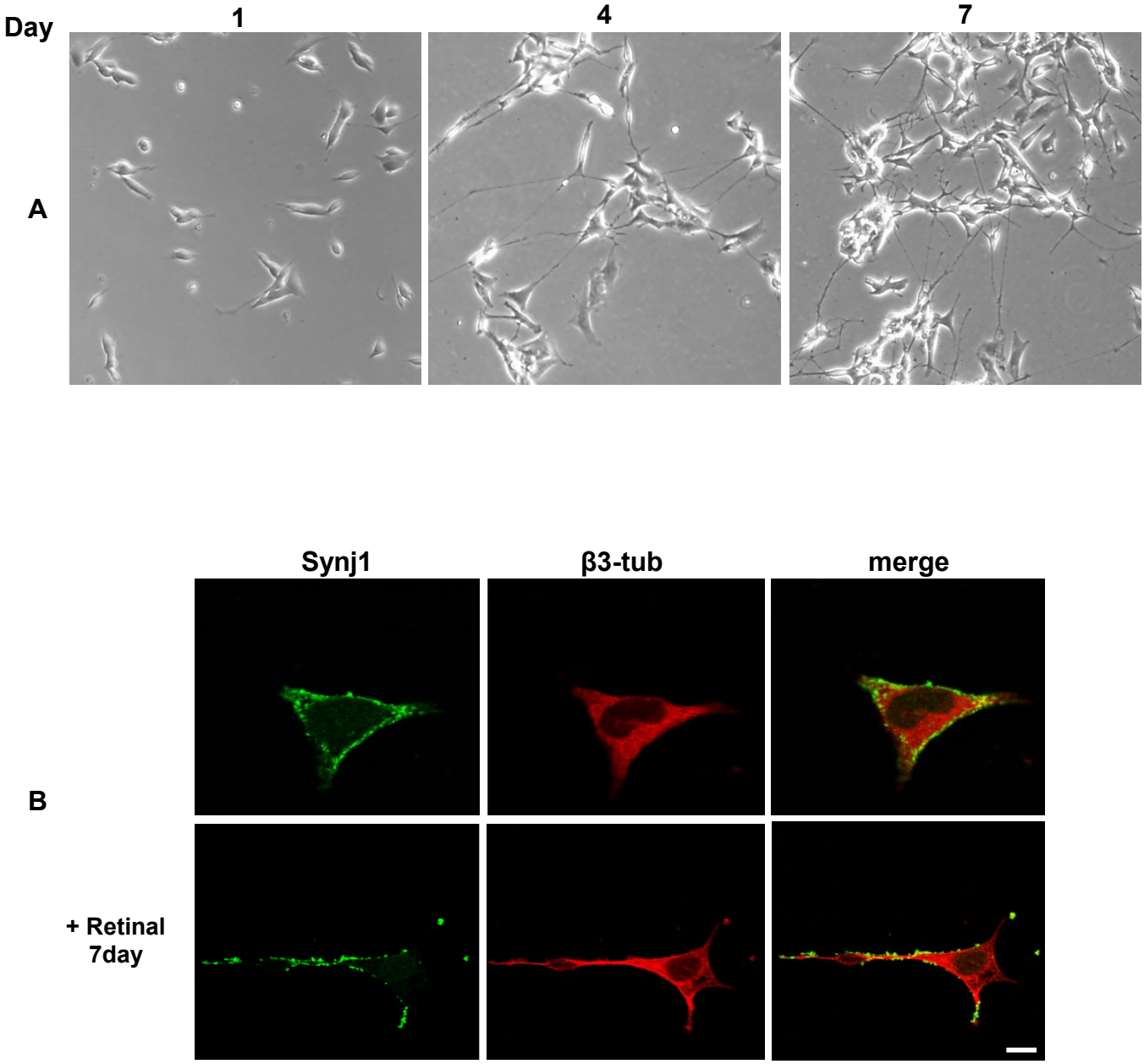

Fig. 40: Synj-1 is localized mainly in the cytoplasm along neurites in differentiated SH-SY5Y. Cells were coltivated in low-serum medium (5%) with all trans-Retinal (10 µM) for one week and observed under phase-contrast microscope. The photos show the differentiation state at 1, 4 and 7 days (A). After 7 days of all trans-Retinal treatment, the cells were fixed and subjected to double indirect immunofluorescence using antibodies against Synj1 and β3-tubulin revealed respectively with Alexa-488 and Alexa-546 conjugated secondary antibodies. Images were acquired by confocal microscopy. Scale bar 5 µm.

.

identify which of these putative pathways is altered in the PD, we decided to silence the expression of Synj1 by stable transfection of specific sh-RNAs (2269, 2542, 2231, and 2372) in HeLa cells and in SH-SY5Y cells. After puromycin selection we collected several pools and clones for each cell line and we evaluated the efficiency of silencing by western blotting. The sh2231 and sh2372 resulted not efficient because cells were not silenced or to a very low percentage (data not shown). We have obtained pools and clones with different degree of silencing (from 30 to 80%) in the case of 2269 and 2542 shRNA for both cell lines (Figs. 41, 42). In particular, in the case of sh2269 pool 1 and 2 were the most silenced (75-80%), while in the case of sh2542 cl1 resulted the most silenced because Snj1 expression was reduced of about 70% (Figs. 41, 42). In most of the experiments we used the pool with best degree of silencing because more representative of the cell population. In addition, it is important to note that it is reduced the expression of both isoforms of the protein. In SH-SY5Y cells the silencing was less efficient than in HeLa cells (Figs. 41, 42) and this is probably due to the considerable difficulties to transfect these cells. In subsequent studies We used pool 2 in the successive studies.

As in the case of Fig4 silencing, we found that cells are homogenously silenced and the silencing of Synj1 expression is maintained in the cells in culture over time (at least the fourth passage in culture).

The loss of Synj1 drastically affects the early endosomes, but not the late endosomes

Once obtained Synj1 silenced cells, we asked whether the absence of Synj1, and therefore the loss of its activity, affects the endo-lysosomal compartments and on which of these compartments. To this purpose, we analyzed the morphology and properties of endo-lysosomal compartments by immunofluorescence assays using different markers of the endocytic route (Figs. 43-45).

We found that both in HeLa and SH-SY5Y cells the loss of Synj1 drastically affects the morphology of early endosomes labelled with EEA1 (Fig. 43 and 44, respectively). Indeed these compartments appear enlarged and more abundant (Figs. 43, 44). Furthermore, in both cell lines the fluorescent signal

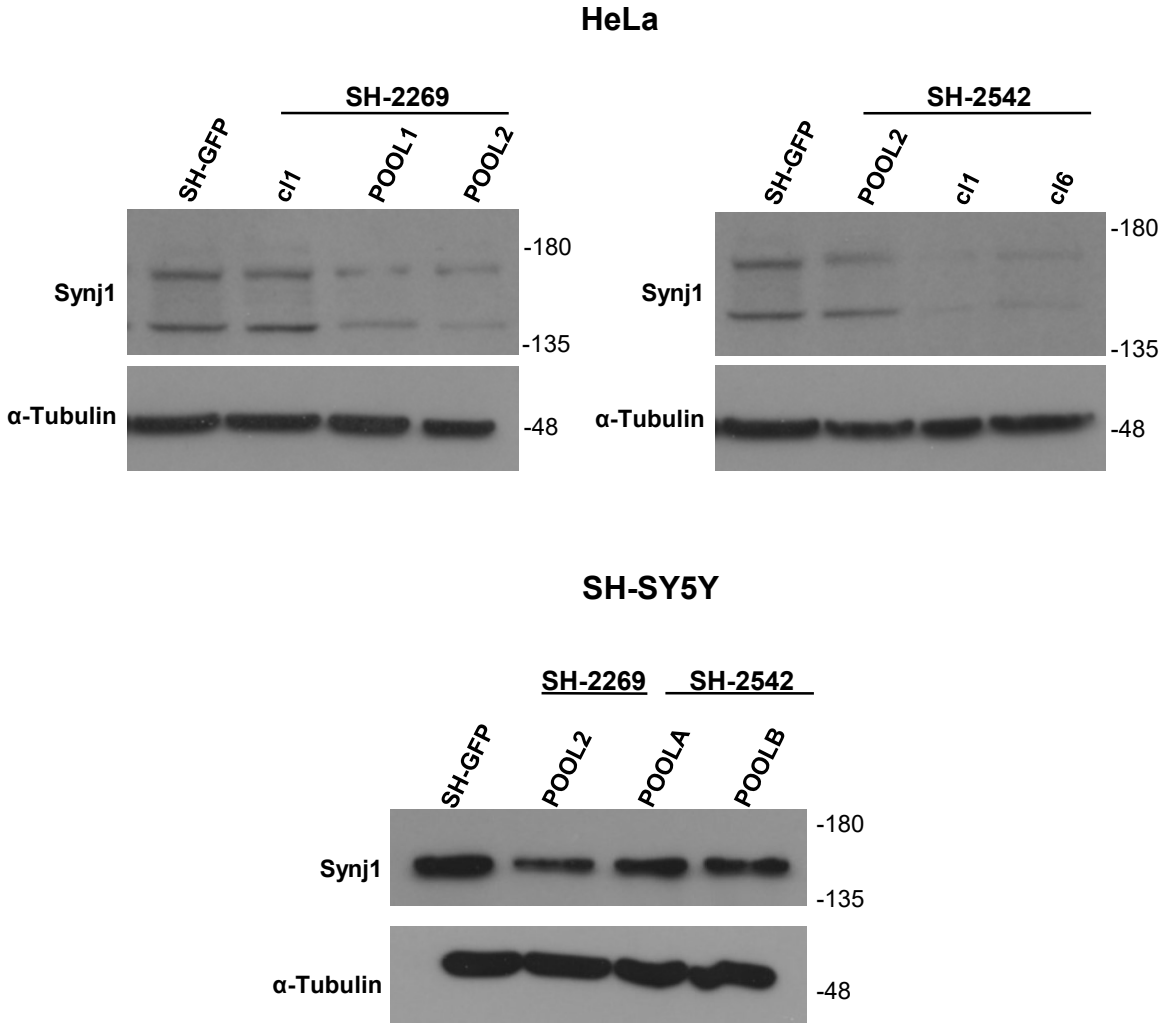

Fig. 41: Synj1 expression is silenced by using short hairpin RNAs in different cell lines. Lysates of Hela and SH-SY5Y cells transfected with shRNA anti Synj1 (SH-2542, SH-2269), shRNA scramble (SH-GFP) were immunoblotted with an anti-Synj1 antibody. We used α-tubulin as loading control. Molecular weights of standard proteins are indicated.

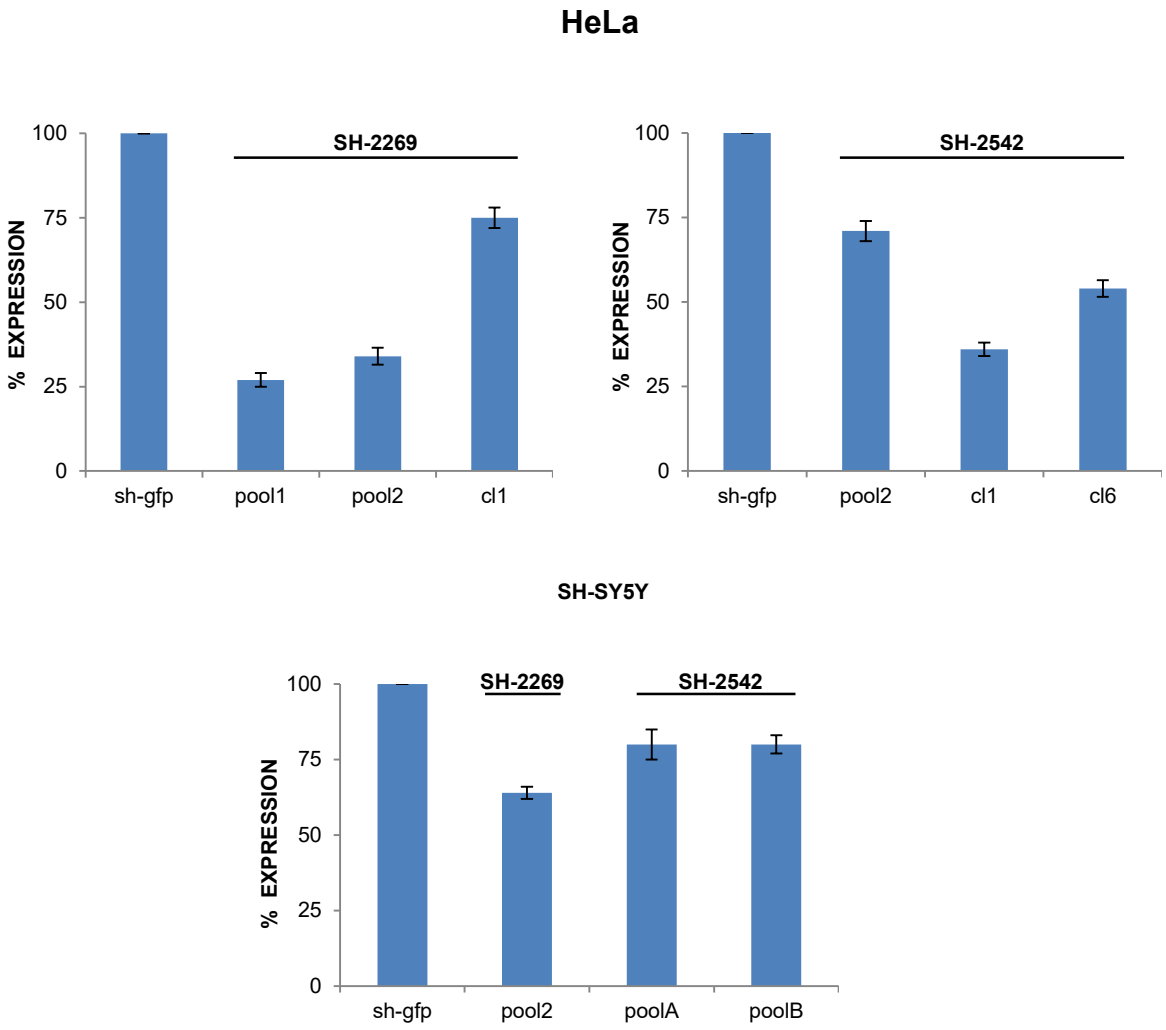

Fig. 42: Quantitation of silencing of the pool or clones in different cell lines. Densitometric analysis of bands was performed with ImageJ. Percentage of Synj1 expression in the different pools and clones respect to the amount of protein in scrambled cells (placed equal to 100). Quantification of three independent experiments are shown (Error bars ± SD).

is much more intense, as it is even more evident in the 3D reconstruction (Figs. 43, 44).

On the contrary, we observed that the silencing of Synj1 does not alter the morphology of late endosomes that were labelled with an anti-Rab7 antibody (Fig. 45).

We obtained the same results by analyzing the fluorescence of GFP-tagged Rab proteins (GFP-Rab5 and GFP-Rab 7) used to stain these compartments (data not shown).

These data clearly indicate that the loss of Synj1 alters exclusively the homeostasis of early endosomes. In addition, the fact that the silencing of Synj1 expression has similar effects in fibroblasts and neuronal cells suggests that the protein plays an essential role in the control of early endosomal compartments in all cell types.

The loss of Synj1 slightly alters lysosomal compartments

Then, we investigated the effect of silencing of Synj1 expression on the lysosomes labelling these organelles by using an anti-lamp1 antibody or the Lysotracker dye (Fig. 46).

We found that, with both staining, lysosomes appear more numerous and as fluorescent spots with more intense signal in HeLa and SH-SY5Y silenced cells (Fig. 46; upper and lower panels, respectively), indicating an expansion of this compartment. If this is due to the altered membrane trafficking from early endosomes or is a consequence of the increased level of autophagy (found in neurodegenerative disease) is to be clarified.

The loss of Synj1 affects the recycling trafficking

The above results indicate that Synj1 is critical for the homeostasis of the early endosomes. Thus, we asked if the loss of Synj1 inhibits the functions of these compartments. To this aim, through endocytosis assays we analyzed the trafficking of the transferrin receptor (TfR), which upon internalization recycled back to the cell surface.

In a first approach, the cells were incubated with AlexaFluor 546 conjugated-transferrin at 37°C for different time (5, 10, 15 and 30 min) and then fixed and observed. We observed that in Synj1-depleted HeLa cells TfR progressively

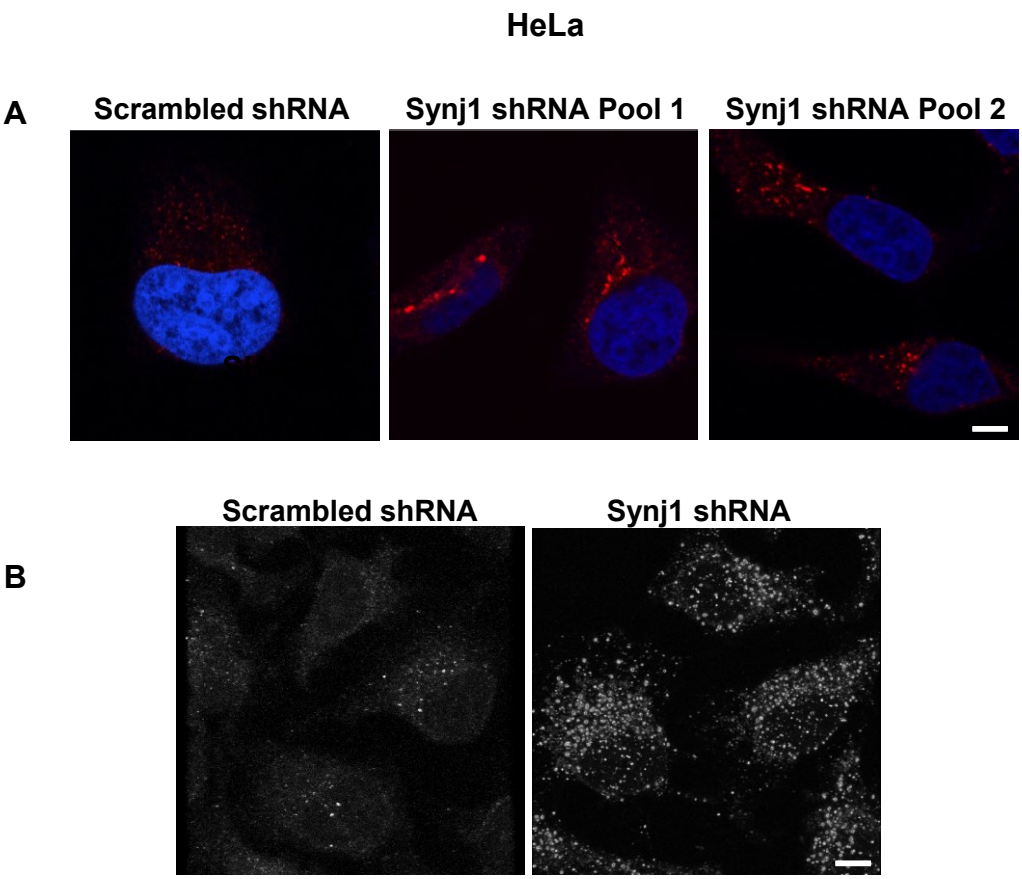

Fig. 43: Loss of Synj1 affects the morphology of early endosomes. Scrambled and silenced cells were fixed permeabilized and stained with EEA1 (early endosome antigen 1) revealed with Alexa Fluor 546-conjugated secondary antibody. Confocal images were acquired from the top to the bottom of cells by using the same settings (laser power, detector gain). Scale bar 5 µm. Single confocal sections (A) or 3D reconstruction (B) are showed.

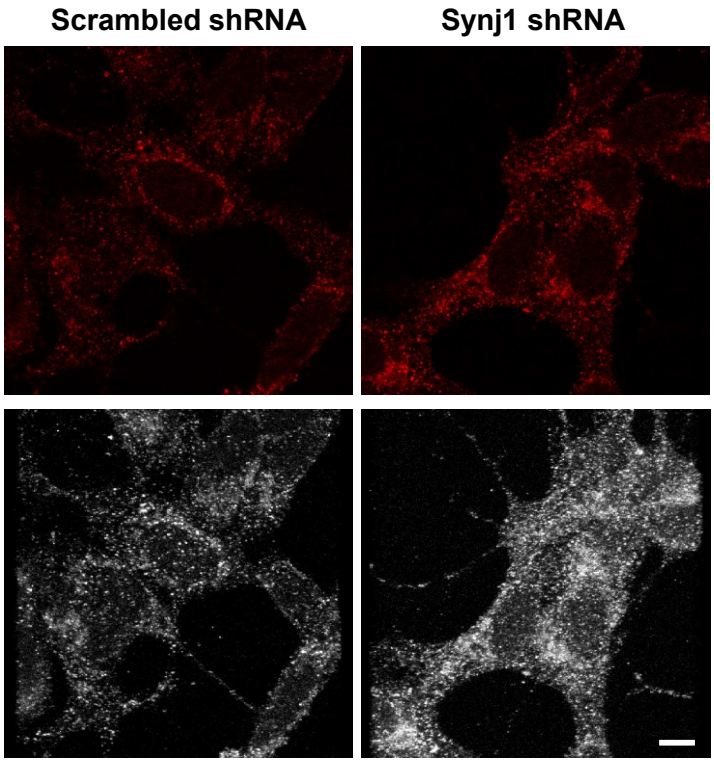

Fig. 44: Loss of Synj1 affects the morphology of early endosomes. Scrambled and silenced cells were fixed permeabilized and stained as in Fig.43. Confocal images were acquired from the top to the bottom of cells by using the same settings (laser power, detector gain). Scale bar 5 μm. Single confocal sections (upper panel) or 3D reconstruction are shown.

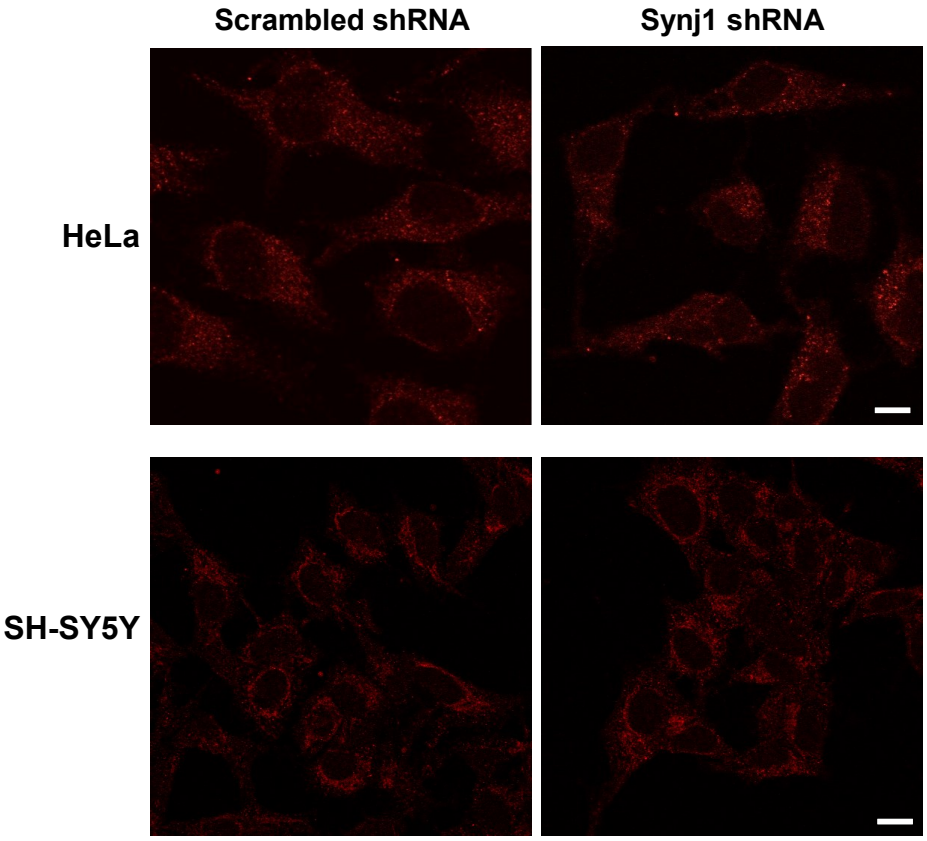

Fig. 45: Loss of Synj1 does not alter the morphology of late endosomes. After fixation cells were permeabilized and stained with Rab7 antibody revealed with Alexa Fluor 546-conjugated secondary antibody. Images were acquired by confocal microscopy by using the same settings (laser power, detector gain). Scale bar 5 µm.

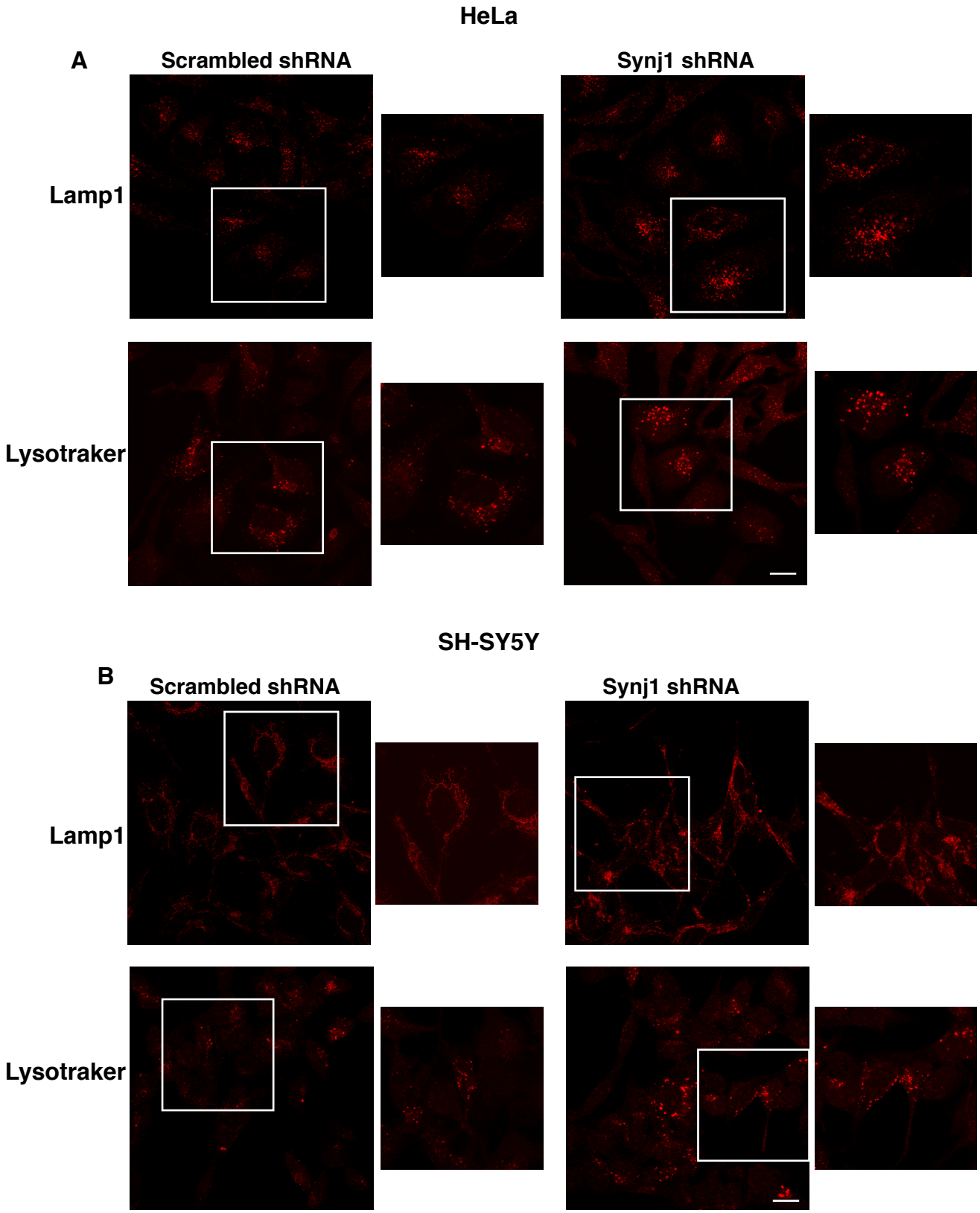

Fig. 46: Loss of Synj1 alters lysosomal compartments in HeLa and SH-SY5Y. Lysosomes of HeLA (A) and SH-SY5Y (B) were labeled by using an anti-Lamp1antibody revealed with Alexa-546 or Lysotracker Dye as described in Fig. 27. Images were acquired by confocal microscopy by using the same settings (laser power, detector gain). Scale bar 5 μm. The squares show magnification of image.

accumulate at the intracellular level, as more evident after 30 min of incubation (Fig. 47), indicating that its recycling to surface is impaired.
In a second approach, cells were incubated with transferrin at 37°C for 10' (pulse), washed to remove the unbound transferrin, and then incubated at 37°C for different times in the standard culture medium (chase). Also with this assay we found intracellular accumulation of transferrin as shown in the single confocal sections (Fig. 48, upper panels) and in the 3D reconstruction (Fig. 48, lower panels) both in HeLa and SH-SY5Y silenced cells.
Furthermore, we also investigated the trafficking of the EGF receptor upon ligand stimulation and we found that the kinetic of internalization is comparable between control and silenced cells (data not shown).
Altogether these results indicate that the activity of Synj1 is crucial for the function of early/recycling compartments.

Patient fibroblasts display the same alterations found in the cell lines

To determine whether the dysfunction of the early endocytic pathway is the cause of this genetic form of PD where Synj1 is mutated, we repeated the experiments on patients fibroblasts. First, we performed an immunofluorescence assay by using an anti-EEA1 antibody to label the early endosomes. In agreement with results obtained in the silenced cells, we found that in the patient fibroblasts early endosomes are expanded, as shown by the presence of larger and more intense fluorescent spots (Fig. 49, upper panel).
Moreover, we observed that the recycling to the surface of the transferrin is impaired in patient fibroblasts (Fig. 49, lower panel). Indeed, the transferrin is greatly accumulated inside the cells of patients respect control fibroblasts (Fig. 49, lower panels).
Altogether these results indicate that the loss of Synj1 or the presence of a mutated form of the protein (in patients) causes an alteration in the early/recycling endosomal compartments. Therefore, these data highlighted that an alteration of homeostasis of endosomal compartments might cause the disease.

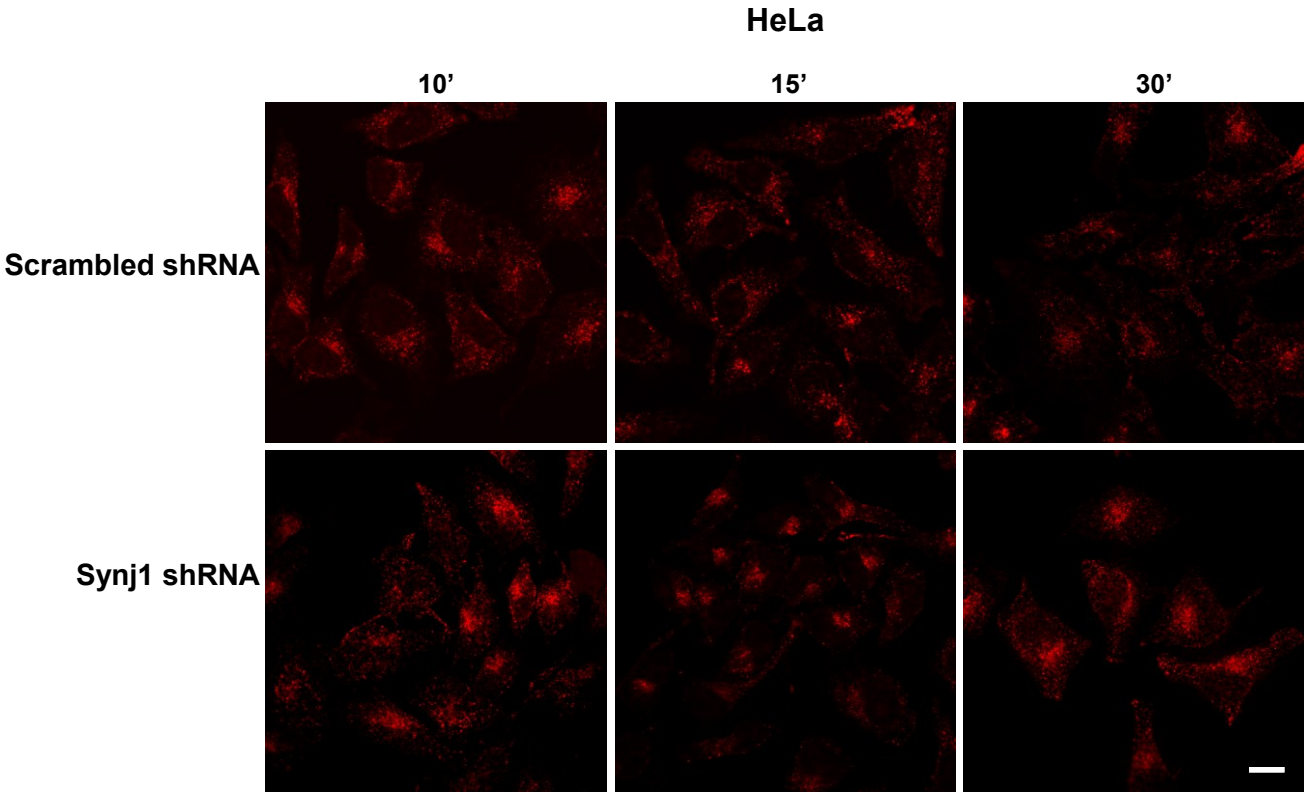

Fig. 47: The loss of Synj1 affects the trafficking of TfR in Hela cells. Internalization assay of Alexa Fluor 546 conjugated transferrin (Tf) in scrambled and Synj1 silenced cells. After incubation with Tf the cells were fixed at the indicated times. Images were acquired by confocal microscopy by using the same settings (laser power, detector gain). Scale bar 5μm.

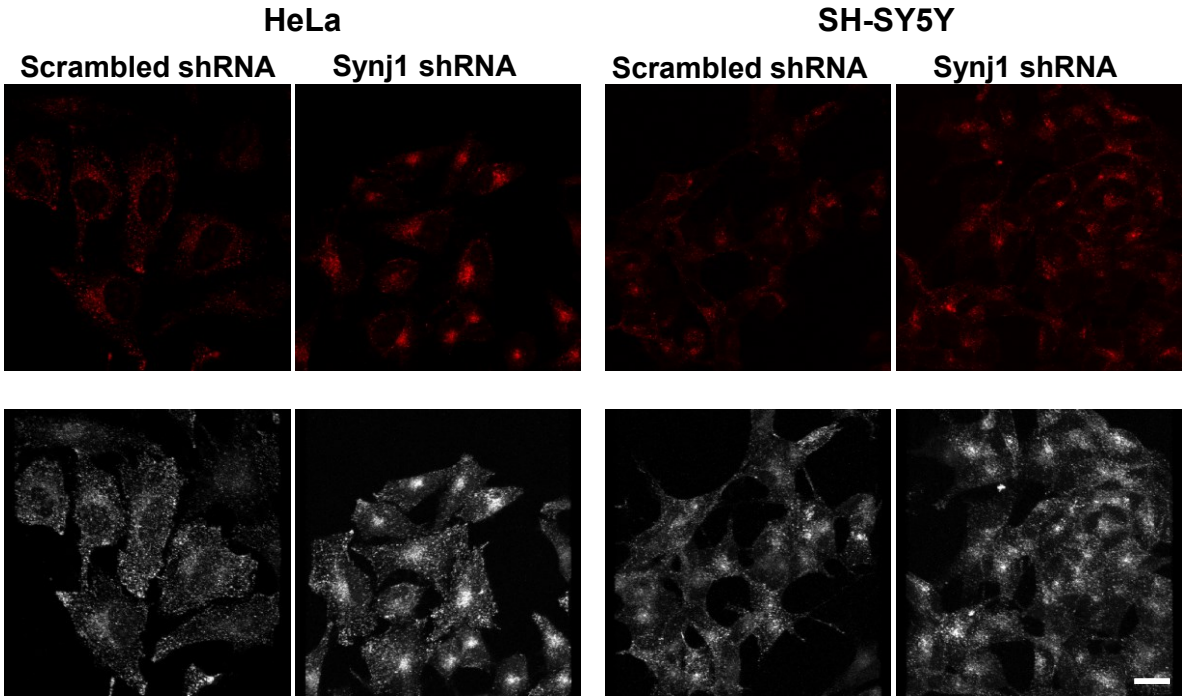

Fig. 48: The loss of Synj1 leads to intracellular accumulation of Transferrin. Cells were incubated with Alexa Fluor 546 conjugate transferrin at 37°C for 10 min (pulse), washed, and incubated in the standard culture medium at 37°C for different times (chase). In the figure single confocal section (xy) or 3D reconstruction of pictures token after 10 min of chase are shown. Were used the same settings (laser power, detector gain). Scale bar 5 μm.

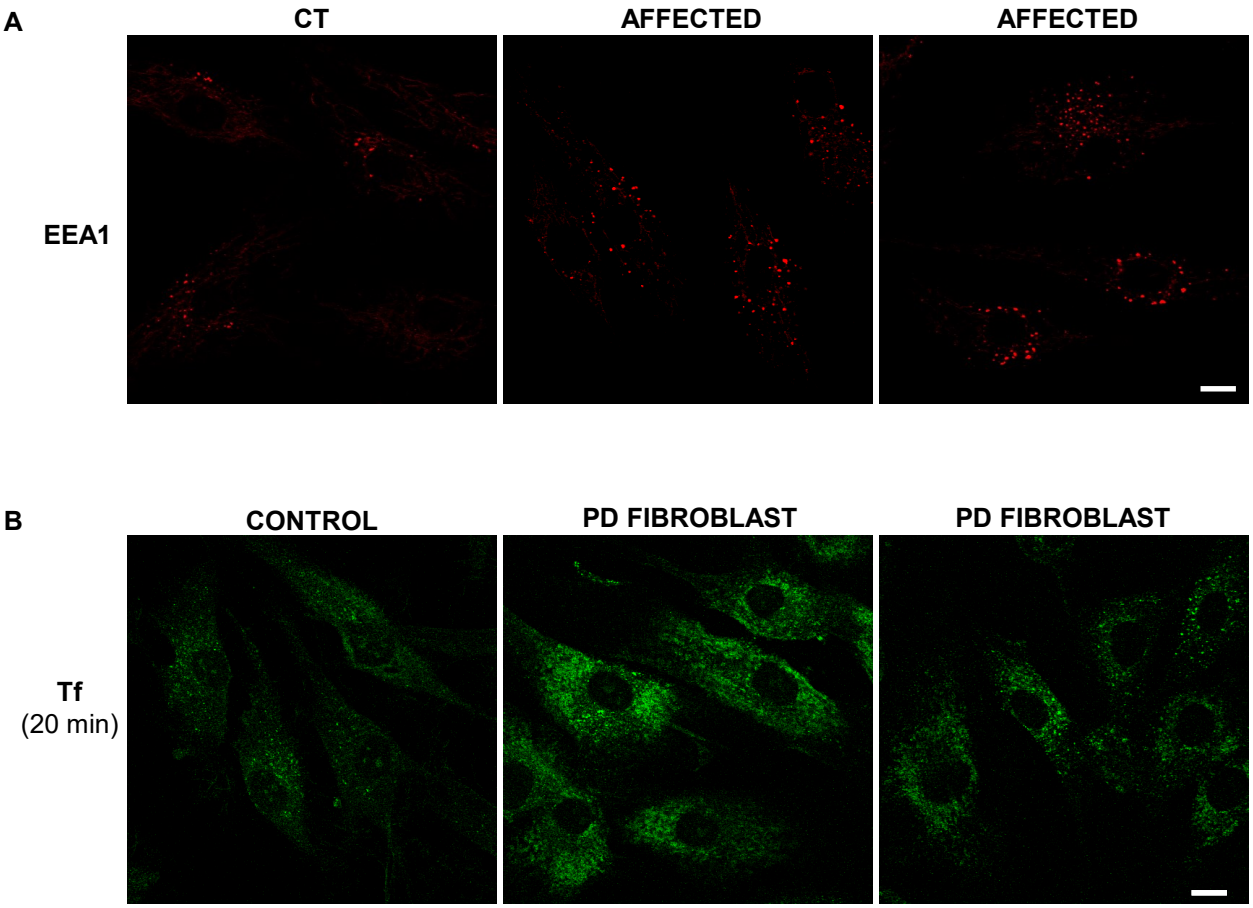

Fig. 49: In patient fibroblasts early endosome are alterated as well as the trafficking of transferrin. Health control (left panel) and patient fibroblast (middle and right panels) and healthy control were fixed, permeabilized and stained with EEA1 antibody and revealed by Alexa Fluor 546-conjugated secondary antibody (A). The fibroblasts were incubated with FITC-conjugated transferrin (Tf) for different times and fixed. The image after 20 min of Tf incubation are shown. The images were acquired by confocal microscopy by using the same settings (laser power, detector gain. Scale bar 5 µm.

DISCUSSION

DISCUSSION

PROJECT 1: MOLECULAR BASIS OF CMT4J

Mutations in the in the inositol-phosphatase Fig4 cause the rare autosomal recessive Charcot-Marie-Tooth peripheral neuropathy type 4J. FIG4 is ubiquitously expressed and remove the 5 phosphate of PI(3,5)P_2, which is enriched in late endosomes and lysosomes (Di Palo and De Camilli, 2006; Takatori et al, 2015).

During my PhD program, we explored the properties and functions of of Fig4 as wells as its role in the membrane trafficking in order to get insights on the molecular mechanism of CMT4J.

Localization and dynamics of Fig4

The strict control of the subcellular distribution, membrane association and activity state of inositol kinases and phosphatases is crucial for the localized phosphoinositides signalling and functions.

We found that Fig4 is localized mainly in the cytoplasm into discrete punctate structures that at least partially co-localize with Rab7 indicating that Fig4 is enriched/recruited in these compartments. Therefore, they can be the main sites where Fig4 acts as supported by the fact that the PIKfyve kinase is also enriched in Rab7-compartments (Ikonomov et al, 2006) as well as the PI(3,5)P_2 (Di Palo and De Camilli, 2006; Takatori et al, 2015). Importantly, Fig4 has comparable distribution in neural and in non-neural indicating that it undergoes to similar regulation in different cell types.

In contrast to wild-type protein, we found that both pathological mutants, I41T and L17P, displayed a more diffuse intracellular signal suggesting that they are unable to be recruited on intracellular compartments. Thus, the punctate appearance of Fig4 is connected with its association to intracellular membranes and this correlates with the functions of the protein.

Which is the molecular defect of these mutant proteins? Why they are unable to be recruited on intracellular membranes? One possibility is that mutant proteins have a fast turn over. Several findings showed that Fig4I41T appears to be unstable as consequence of the impairment of its interaction with ArPIKfyve, although there are conflicting data (Ikonomov et al, 2010; Lenk et

al, 2011). By crystallographic analysis and computational modeling it has been shown that the two mutations are surface exposed and located in flexible loop regions that may be involved in protein-protein interactions (Manford et al, 2010). Thus, mutations could affect putative interactions with factors promoting the association and/or stabilization of Fig4 with membranes. Overall, these data indicate that the activity of Fig4 is strictly regulated through its localization.

Interestingly, beyond to the cytosolic signal, we found that Fig4 appears also distributed in a nuclear structure that resembles the typical nuclear bodies. Although at different extent, this distribution is observed in different cell types supporting that there is nuclear pool of this enzyme. Some studies suggest that the PI(5)P, which is mostly generated from PI(3,5)P2, plays a regulatory role in the nucleus through binding ING2 (Gozani et al, 2003; Jones et al, 2006). Thus, we can postulate that nuclear Fig4 could be implicated in the thin regulation of these PIs in the nucleus. It will be interesting to understand whether the loss of the putative nuclear function of Fig4 is implicated in the CMT4J pathogenesis. We are currently investigating this aspect.

Fig4 regulates the homeostasis of endosomal compartments

The loss of Fig4 leads to drastic changes in the endo-lysosome system. In agreement with observations in plt mice and CMT4J patient fibroblasts (Chow et al, 2007; Zhang et al, 2008), we found that in Fig4-silenced cells lysosomes are enlarged and more abundant. In addition, also late endosomes appears as large dots upon Fig4 silencing. Although this could be expected because $PI(3,5)P_2$ is enriched in these compartments, these data indicate that proper concentration of this PI is essential for the homeostasis of these organelles. Strikingly, we found that the loss of Fig4 also affects early endosomes as well as recycling pathways dependent on them. Instead, no alteration of exocytic organelles, endoplasmic reticulum and Golgi apparatus, have been observed, indicating that Fig4 is not implicated in the regulation of these membrane compartments.

All these data indicate that the absence of Fig4 affects the homeostasis of whole endo-lysosomal axis, highlighting that $PI(3,5)P_2$ plays a key role in the endocytic pathway.

The lower basal levels found in plt mice (Chow et al, 2007) might impair the bulk trafficking of membranes in and out late endosomes with consequent enlargements of both later and earlier compartments of endocityc route. In yeast, it has been shown that $PI(3,5)P_2$ regulates vacuole fission (Bonangelino et al. 2002). On the other hands, always in yeast it has been found that the activity of the vacuolar pump V-ATPae, which control the lumen acidification and volume, requires the $PI(3,5)P_2$ (Li et al, 2014). Therefore, both mechanisms could contribute to the aberrant alteration of endosomal compartments.

Moreover, upon Fig4 loss there is a dysfunction of whole endosomal system. Indeed, the trafficking of two receptors (trasnferrin and EGF), which follow different fates, is altered in Fig4-depleted cells. For both receptors, we observed that there is a protein accumulation inside the cells. In the case of transferrin receptor, these results clearly indicate that the recycling pathway is impaired, and possibly both the fast (directly from early endosomes) and more slowly (passing trough recycling endosomes) route. In the case of EGFR, its accumulation may be due to its failure degradation because of dysfunction of lysosomes or the impairment of fusion between late endosomes and lysosomes, thus preventing to the receptor to reach its final destination.

Importantly, the activity of Fig4 is crucial for homeostasis and function of endocytic compartments in all cells types since we have found the same results in different cell lines.

Thus, all these data indicate that the loss of Fig4 could lead to a dysfunction of endosomal compartments and this likely might be the pathogenic mechanism in the CMT4J. It is likely that the impairment of the trafficking of specific neural proteins (e.g., growth factor and neurotransmitter receptors, proteins implicated in neuritogenesis like tag1 etc.) is critical for the development of disease. This would explain the sensitivity of different neurons. A recent study showing that Fig4-regulated endo-lysosomal trafficking is essential for myelin formation in Schwann cells (Vaccari et al, 2014) supports this hypothesis. Therefore, in the near future it will be important to unravel which pathways are altered in neurons.

Role of Fig4 in neural differentiation

We showed that Fig4 is expressed in stem cells and then in differentiated cells. Interestingly, in neural cells the Fig4 expression is higher than in mesdormal-derived cells, suggesting that Fig4 plays a critical role in the nervous system. In addition, while during mesodermal differentiation the levels of Fig4 decrease respect to the ESCs and remain stable over time, during neural differentiation Fig4 transcripts and proteins follow a peculiar kinetic going down and going up at early and late phase of differentiation, respectively. These data suggest that for the correct differentiation the Fig4 levels have to be finely controlled. Consistently, we found that the loss of Fig4 correlates with altered temporal expression of stemness and early neural markers with consequent earlier induction of neural differentiation. This could affect the proper development of the nervous system and, therefore, could be related with the pathogenesis of the disease.

PROJECT 1: MOLECULAR BASIS OF PARKINSON'S DISEASE

Synj1 was discovered long time ago (McPherson, 1994), while very recently it is implicated in a monogenic form of Parkinson (Krebs et al, 2013 Quadri et al, 2013; Olgiati et al, 2014).

There is mounting evidence that vesicle trafficking pathways are implicated in PD mechanisms since most of the proteins involved in autosomal dominant PD as well as those responsible for autosomal recessive form are part, directly or indirectly, of the molecular machinery regulating the membrane trafficking (Thomas and Beal, 2007; Bonifati et al, 2013). The knockout mice for Synj1 gene die early after birth and have neurological defects such as severe weakness, ataxia, spontaneous seizures, poor motor coordination (Cremona et al., 1999). The neurons of these mice have impaired the endocytic process, although it is not entirely clear the molecular defect.

To understand the molecular basis of this genetic form of Parkinson we analyzed i) its localization in neural and non-neural since the spatiotemporally regulation is crucial for this type of enzymes as aforementioned; ii) the effects of the silencing of its expression on the regulation of membrane trafficking.

In agreement with previous data (Ramjaun and McPherson, 1996; Haffner et al, 1997) we found that Synj1 is expressed in different cell types and while in neuronal cells is present only the 145 kDa isoform, two isoforms, 145 kDa and 170 kDa, are expressed at different extent in other cells of different origin. The pathological mutation mapped in a common region to the two isoforms, therefore this cannot explain the sensitivity of neurons respect to the other cells. Although 170 kDA isoform has an additional short PRD domain allowing the binding with other proteins (Ramjaun and McPherson 1996; De Heuvel et al, 1997; Drouet et al, 2014), it is still unknown if the two isoforms play different roles.

Moreover, we found that both in neural and in non-neural cells Synj1 is localized in the cytoplasm mainly along the plasma membrane in agreement with the previous findings showing that it interacts with molecules involved in the endocytic machinery (such as amphysin, endophilin) and is recruited in coated pits (McPherson et al, 1994; McPherson, Takei, et al, 1994; Milosevic et al, 2011). In addition, Synj1 is also present in intracellular discrete punctate structures more distant from surface, which could be other sites where the enzyme acts. Interestingly, in differentiated neuronal cells Synj1 is abundant in neurites suggesting that the protein may have a role in neurogenesis and/or in preserving neuronal plasticity and, on the other hands, the absence of its activity could alter these processes. The fact that Synj1 has been shown implicated in synaptic vesicles turn over (MacPherson et al, 1996; Mani et al. 2007) supports this hypothesis.

We found that the loss of Synj1 causes a drastic alteration of the early endosomes, which result expanded, while does not affect late endosomes. Moreover, in absence of Synj1 the trafficking of the transferrin receptor is inhibited, but not that to lysosomes of the EGF receptor. Altogether these data indicate that the loss of Synj1 causes a dysfunction of the early endosomal compartments. On the other hands, these data indicate that Synj1 plays a crucial role in regulating the homeostasis and functions of these organelles and this role is essential in all cells because we found that the silencing of Synj1 expression has similar effects in fibroblasts and neuronal cells.

Importantly, in patient fibroblasts early endosomal compartments result enlarged and the recycling of transferrin is impaired. Thus, these results

indicate that the loss of Synj1 as well as the presence of a mutated form of the protein (as it occurs in patients) leads to the dysfunction of early endosomes. Hence, altogether, these data highlighted that an alteration of homeostasis of endosomal compartments might cause the disease.

While the conversion of $PI(4,5)P_2$ to PI(4) has been shown to be required for the removal of clathrin coating and vesicle endocytosis (Cremona et al., 1999; Mani et al., 2007), it is likely that phosphatase activity of Synj1 on PIs monophosphates (such PI3P and PI4P) may be the cause of the alteration of endosomal compartments. Consistently, it has been found that disease-linked mutation almost entirely eliminates both the 3- and 4-phosphatse activity, but does not affect the activity on $PI(4,5)P_2$ (Krebs et al, 2013).

Furthermore, we also observed an enlargement of lysosomes in Synj1-silenced cells. This could be a consequence of the altered membrane trafficking from early endosomes. However, the late endosomes are not altered as well as the trafficking of EGFR. Otherwise, lysosome alteration could be the consequence of the increase of autophagy levels. Our preliminary data showed increased levels of autophagy in Synj1 silenced cells supporting this hypothesis. Moreover many studies have revealed increased autophagy levels in neurodegenerative diseases including Parkinson (Pan et al, 2008; Ferguson et al, 2009) supporting this hypothesis.

CONCLUSIONS

In the last years, an increasing number of human genetic diseases including neuropathies have discovered to be associated to mutations in enzymes regulating the turnover of PIs, highlighting the central role of these lipids in cell homeostasis.

Our data clearly confirmed that the levels of phosphoinostides might be finely regulated and specifically they are critical for membrane homeostasis. Indeed, our findings clearly demonstrate that the loss of the activity of two inositol phosphatases drastically affects the homeostasis of endo-lysosomal compartments, although in different manner. Moreover, our study confirm an emerging concept that endosome-lysosome system covers a critical role in cellular homeostasis by controlling the degradation of materials from the phagocytic, endocytic, autophagic pathways as well as by finely regulating the

recycling of proteins back to plasma membrane or their transport toward early secretory compartments. In this context, the endosomal PIs play an important role.

Furthermore, our findings indicate that beyond the catalytic activity the subcellular distribution and membrane association of phosphatases and kinases is critical for metabolism of PI and their functions.

The proper balance between synthesis and degradation of PIs poses special challenges in nervous system that, indeed, appears more sensitive to alterations of PI metabolism and, as consequence, to disturbances of membrane remodeling and trafficking pathways.

On this line, our data suggest that the dysfunction of endo-lysosome system correlated with the neurodegeneration.

In conclusion, this study highlighted the cellular defect underlying the pathogenesis of CMT4J and Synj1-related PD. Further studies aimed to understanding the specific molecular cascades involved (altered in the disease) are will necessary and will open the door to the development of new therapies.

REFERENCES

REFERENCES

Arnold, A., Mcentagart, M., & Younger, D. S. (2005). Psychosocial Issues That Face Patients With Charcot-Marie-Tooth Disease : The Role of Genetic Counseling, 14(4). http://doi.org/10.1007/s10897-005-0760-z

Balla A, Tuymetova G, Tsiomenko A, Várnai P, Balla T. A plasma membrane pool of phosphatidylinositol 4-phosphate is generated by phosphatidylinositol 4-kinase type-III alpha: studies with the PH domains of the oxysterol binding protein and FAPP1. Mol Biol Cell. 2005 Mar;16(3):1282-95.

Bharadwaj R, Cunningham KM, Zhang K, Lloyd TE. FIG4 regulates lysosome membrane homeostasis independent of phosphatase function. Hum Mol Genet. 2016 Feb 15;25(4):681-92. doi: 10.1093/hmg/ddv505. Epub 2015 Dec 11.

Begley MJ, Dixon JE. The structure and regulation of myotubularinphosphatases. Curr Opin Struct Biol. 2005 Dec;15(6):614-20.

Ben, G. T., Loeb, V., Israeli, E., Altschuler, Y., Selkoe, D. J., & Sharon, R. (2009). Alpha-synuclein and polyunsaturated fatty acids promote clathrin mediated endocytosis and synaptic vesicle recycling. Traffic, 10(2), 218–234. http://doi.org/10.1111/j.1600-0854.2008.00853.x.

Berg, D., Schweitzer, K. J., & Leitner, P, Zimprich A., Lichtner P., Belcredi P., Brussel T., Schulte C., Maass S., Nagele T., Wszolek Z., and Thomas Gasser (2005). Type and frequency of mutations in the LRRK2 gene in familial and sporadic Parkinson's disease*. Brain, 128, 3000–3011. http://doi.org/10.1093/brain/awh666

Billcliff PG, Lowe M. Inositol lipid phosphatases in membrane trafficking and human disease. Biochem J. 2014 Jul 15;461(2):159-75. doi: 10.1042/BJ20140361.Review.

Birkeland HC, Stenmark H. Protein targeting to endosomes and phagosomes via FYVE and PX domains. Curr Top Microbiol Immunol. 2004;282:89-115. Review.

Bonifacino, J. S., & Hurley, J. H. (2008). Retromer. Current Opinion in Cell Biology, 20(4), 427–436. http://doi.org/10.1016/j.ceb.2008.03.009

Bonifati V. Genetics of parkinsonism Parkinsonism and Related Disorders 13 (2007) S233–S241

Bonifati, V. (2014). Genetics of Parkinson's disease – state of the art, 2013. Parkinsonism & Related Disorders, 20, S23–S28. http://doi.org/10.1016/S1353-8020(13)70009-9

Bonifati, V., Rizzu, P., van Baren, M. J., Schaap, O., Breedveld, G. J., Krieger, E., Dekker M. C. J., Squitieri F, Ibanez P., Joosse M., Dongen J. W., Vanacore N.

van Swieten J.C., Brice A., Meco G., van Duijn M., Oostra B. A., Heutink, P. (2003). Mutations in the DJ-1 gene associated with autosomal recessive early-onset parkinsonism. Science (New York, N.Y.), 299(5604), 256–259. http://doi.org/10.1126/science.1077209

Bonifati V, Rohé CF, Breedveld GJ, Fabrizio E, De Mari M, Tassorelli C,Tavella A, Marconi R, Nicholl DJ, Chien HF, Fincati E, Abbruzzese G, Marini P, De Gaetano A, Horstink MW, Maat-Kievit JA, Sampaio C, Antonini A, Stocchi F, Montagna P, Toni V, Guidi M, Dalla Libera A, Tinazzi M, De Pandis F, Fabbrini G, Goldwurm S, de Klein A, Barbosa E, Lopiano L, Martignoni E, Lamberti P, Vanacore N, Meco G, Oostra BA; Italian Parkinson Genetics Network. Early-onsetparkinsonism associated with PINK1 mutations: frequency, genotypes, and phenotypes. Neurology. 2005 Jul 12;65(1):87-95.

Botelho R. J., Efe J. A., Teis D., and Emr S. D. Assembly of a Fab1 Phosphoinositide Kinase Signaling Complex Requires the Fig4 Phosphoinositide Phosphatase Moulecular Biology of the Cell Vol. 19, 4273–4286, October 2008

Choudhury, R. R., Hyvola, N., & Lowe, M. (2005). Phosphoinositides and membrane traffic at the trans-Golgi network. Biochem Soc Symp, (72), 31–38

Chow, C. Y., Zhang, Y., Dowling, J. J., Jin, N., Adamska, M., Shiga, K., Shy M. E., Li J., Zhang X., Lupski J. R., Weisman L. S., and Meisler, M. H. (2007). Mutation of FIG4 causes neurodegeneration in the pale tremor mouse and patients with CMT4J. Nature, 448(7149), 68–72. http://doi.org/10.1038/nature05876

Collins B, Constant J, Kaba S, Barclay CL, Mohr E. Dementia with lewy bodies: implications for clinical trials Clin Neuropharmacol. 2004 Nov-Dec;27(6):281-92.

.Cremona, O., Di Paolo, G., Wenk, M. R., Luthi, A., Kim, W. T., Takei, K., Daniell L., Nemoto Y., Shears S. B., Flavell R. A. McCormick D. A., De Camilli, P. (1999). Essential role of phosphoinositide metabolism in synaptic vesicle recycling. Cell, 99(2), 179–188. http://doi.org/10.1016/S0092-8674(00)81649-9

D'Angelo G, Vicinanza M, Di Campli A, De Matteis MA. The multiple roles of PtdIns(4)P -- not just the precursor of PtdIns(4,5)P2. J Cell Sci. 2008 Jun 15;121(Pt 12):1955-63. doi: 10.1242/jcs.023630. Review.

Dauer, W., & Przedborski, S. (2003). Parkinson's Disease. Neuron, 39(6), 889–909. http://doi.org/10.1016/S0896-6273(03)00568-3

David C, McPherson PS, Mundigl O, de Camilli P. A role of amphiphysin in synaptic vesicle endocytosis suggested by its binding to dynamin in nerve terminals. Proc Natl Acad Sci U S A. 1996 Jan 9;93(1):331-5.

De Heuvel, E., Bell, A. W., Ramjaun, A. R., Wong, K., Sossin, W. S., & McPherson, P. S. (1997). Identification of the major synaptojanin-binding proteins in brain.

Journal of Biological Chemistry, 272(13), 8710–8716. http://doi.org/10.1074/jbc.272.13.8710

De Lau LM, Koudstaal PJ, Hofman A, Breteler MM. Subjective complaints precede Parkinson disease: the rotterdam study. Arch Neurol. 2006 Mar;63(3):362-5.

De Matteis MA, D'Angelo G. The role of the phosphoinositides at the Golgi complex. Biochem Soc Symp. 2007;(74):107-16. Review.

Di Fonzo A, Dekker MC, Montagna P, Baruzzi A, Yonova EH, Correia Guedes L, Szczerbinska A, Zhao T, Dubbel-Hulsman LO, Wouters CH, de Graaff E, Oyen WJ, Simons EJ, Breedveld GJ, Oostra BA, Horstink MW, Bonifati V. FBXO7 mutations cause autosomal recessive, early-onset parkinsonian-pyramidal syndrome. Neurology. 2009 Jan 20;72(3):240-5. doi: 10.1212/01.wnl.0000338144.10967.2b.

Di Paolo, G., & De Camilli, P. (2006). Phosphoinositides in cell regulation and membrane dynamics. Nature, 443(7112), 651–657. http://doi.org/10.1038/nature05185

Dong XP, Shen D, Wang X, Dawson T, Li X, Zhang Q, Cheng X, Zhang Y, Weisman LS, Delling M, Xu H. PI(3,5)P(2) controls membrane trafficking by direct activation of mucolipin Ca(2+) release channels in the endolysosome. Nat Commun. 2010 Jul 13;1:38. doi: 10.1038/ncomms1037.

Dove, S. K., Cooke, F. T., Douglas, M. R., Sayers, L. G., Parker, P. J., & Michell, R. H. (1997). Osmotic stress activates phosphatidylinositol-3,5-bisphosphate synthesis. Nature, 390(6656), 187–192. http://doi.org/10.1038/36613

Drouet, V., & Lesage, S. (2014). Synaptojanin 1 mutation in Parkinson's disease brings further insight into the neuropathological mechanisms. BioMed Research International, 2014, 289728. http://doi.org/10.1155/2014/289728

Duex, J. E., Tang, F., & Weisman, L. S. (2006). The Vac14p-Fig4p complex acts independently of Vac7p and couples PI3,5P2 synthesis and turnover. Journal of Cell Biology, 172(5), 693–704. http://doi.org/10.1083/jcb.200512105

Edvardson, S., Cinnamon, Y., Ta-Shma, A., Shaag, A., Yim, Y. I., Zenvirt, S., Jalas C., Lesage S., Brice A., Taraboulos A., Kaestner K. H., Greene L. E., Elpeleg, O. (2012). A deleterious mutation in DNAJC6 encoding the neuronal-specific clathrin-uncoating Co-chaperone auxilin, is associated with juvenile parkinsonism. PLoS ONE, 7(5), 4–8. http://doi.org/10.1371/journal.pone.0036458

Efe JA, Botelho RJ, Emr SD. The Fab1 phosphatidylinositol kinase pathway in the regulation of vacuole morphology. Curr Opin Cell Biol. 2005 Aug;17(4):402-8. Review. PubMed PMID: 15975782.

Erdmann KS, Mao Y, McCrea HJ, Zoncu R, Lee S, Paradise S, Modregger J, Biemesderfer D, Toomre D, De Camilli P. A role of the Lowe syndrome protein OCRL in early steps of the endocytic pathway. Dev Cell. 2007 Sep;13(3):377-90.

Falasca M, Maffucci T. Rethinking phosphatidylinositol 3-monophosphate. Biochim Biophys Acta. 2009 Dec;1793(12):1795-803. doi: 10.1016/j.bbamcr.2009.10.003. Epub 2009 Oct 21. Review.

Falkenburger, B. H., Jensen, J. B., Dickson, E. J., Suh, B. C., & Hille, B. (2010). Phosphoinositides: lipid regulators of membrane proteins. J Physiol, 588(Pt 17), 3179–3185. http://doi.org/10.1113/jphysiol.2010.192153

Ferguson, C. J., Lenk, G. M., & Meisler, M. H. (2009). Defective autophagy in neurons and astrocytes from mice deficient in PI(3,5)P2. Human Molecular Genetics, 18(24), 4868–4878. http://doi.org/10.1093/hmg/ddp460

Gasser, T. (2007). Update on the genetics of Parkinson's disease. Movement Disorders, 22(SUPPL. 17). http://doi.org/10.1002/mds.21676

George, A. A., Hayden, S., Holzhausen, L. C., Ma, E. Y., Suzuki, S. C., & Brockerhoff, S. E. (2014). Synaptojanin 1 is required for endolysosomal trafficking of synaptic proteins in cone photoreceptor inner segments. PLoS ONE, 9(1). http://doi.org/10.1371/journal.pone.0084394

Gong, L.-W., & De Camilli, P. (2008). Regulation of postsynaptic AMPA responses by synaptojanin 1. Proceedings of the National Academy of Sciences of the United States of America, 105(45), 17561–17566. http://doi.org/10.1073/pnas.0809221105

Gozani O, Karuman P, Jones DR, Ivanov D, Cha J, Lugovskoy AA, Baird CL, Zhu H, Field SJ, Lessnick SL, Villasenor J, Mehrotra B, Chen J, Rao VR, Brugge JS,Ferguson CG, Payrastre B, Myszka DG, Cantley LC, Wagner G, Divecha N, Prestwich GD, Yuan J. The PHD finger of the chromatin-associated protein ING2 functions as a nuclear phosphoinositide receptor. Cell. 2003 Jul 11;114(1):99-111.

Gray P, Hildebrand K. Fall risk factors in Parkinson's disease. J Neurosci Nurs. 2000 Aug;32(4):222-8.

Greenamyre, J. T., & Hastings, T. G. (2004). Biomedicine. Parkinson's--divergent causes, convergent mechanisms. Science (New York, N.Y.), 304(5674), 1120–2. http://doi.org/10.1126/science.1098966

Guo, S., Stolz, L. E., Lemrow, S. M., & York, J. D. (1999). SAC1-like domains of yeast SAC1, INP52, and INP53 and of human synaptojanin encode polyphosphoinositide phosphatases. Journal of Biological Chemistry, 274(19),

12990–12995. http://doi.org/10.1074/jbc.274.19.12990

Gupta, A., Dawson, V. L., & Dawson, T. M. (2008). What causes cell death in Parkinson's disease? Annals of Neurology, 64(SUPPL. 2), 1–4. http://doi.org/10.1002/ana.21573

Haffner, C., Takei, K., Chen, H., Ringstad, N., Hudson, A., Butler, M. H., … De Camilli, P. (1997). Synaptojanin 1: Localization on coated endocytic intermediates in nerve terminals and interaction of its 170 kDa isoform with Eps15. FEBS Letters, 419(2-3), 175–180. http://doi.org/10.1016/S0014-5793(97)01451-8

Harding, A. E., & Thomas, P. K. (1980). Genetic aspects of hereditary motor and sensory neuropathy (types I and II). J Med Genet, 17(5), 329–336. Retrieved from http://www.ncbi.nlm.nih.gov/entrez/query.fcgi?cmd=Retrieve&db=PubMed&dopt=Citation&list_uids=7218272

Hely, M. A., Reid, W. G. J., Adena, M. A., Halliday, G. M., & Morris, J. G. L. (2008). The Sydney Multicenter Study of Parkinson's disease: The inevitability of dementia at 20 years. Movement Disorders, 23(6), 837–844. http://doi.org/10.1002/mds.21956

Herdmann J, Reiners K, Freund HJ. Motor unit recruitment order in neuropathic disease. Electromyogr Clin Neurophysiol. 1988 Jan;28(1):53-60.

Hyvola N, Diao A, McKenzie E, Skippen A, Cockcroft S, Lowe M. Membrane targeting and activation of the Lowe syndrome protein OCRL1 by rab GTPases. EMBO J. 2006 Aug 23;25(16):3750-61.

Ho CY, Alghamdi TA, Botelho RJ. Phosphatidylinositol-3,5-bisphosphate: no longer the poor PIP2. Traffic. 2012 Jan;13(1):1-8. doi: 10.1111/j.1600-0854.2011.01246.x.

Holzhausen, L. C., Lewis, A. A., Cheong, K. K., & Brockerhoff, S. E. (2009). Differential role for synaptojanin 1 in rod and cone photoreceptors. Journal of Comparative Neurology, 517(5), 633–644. http://doi.org/10.1002/cne.22176

Hughes, W. E., Cooke, F. T., & Parker, P. J. (2000). Sac phosphatase domain proteins. Biochem J, 350 Pt 2, 337–352. http://doi.org/10.1042/0264-6021:3500337

Ibáñez P, Lesage S, Lohmann E, Thobois S, De Michele G, Borg M, Agid Y, Dürr A, Brice A; French Parkinson's Disease Genetics Study Group. Mutational analysis of the PINK1 gene in early-onset parkinsonism in Europe and North Africa. Brain. 2006 Mar;129(Pt 3):686-94. Epub 2006 Jan 9.

Ikonomov, O. C., Sbrissa, D., Fligger, J., Delvecchio, K., & Shisheva, A. (2010).

ArPIKfyve regulates Sac3 protein abundance and turnover disruption of the mechanism by Sac3I41T mutation causing charcot-marie-tooth 4J disorder. Journal of Biological Chemistry, 285(35), 26760–26764. http://doi.org/10.1074/jbc.C110.154658

Ikonomov OC, Sbrissa D, Shisheva A. Localized PtdIns 3,5-P2 synthesis to regulate early endosome dynamics and fusion. Am J Physiol Cell Physiol. 2006 Aug;291(2):C393-404.

Itoh, T., Erdmann, K. S., Roux, A., Habermann, B., Werner, H., & De Camilli, P. (2005). Dynamin and the actin cytoskeleton cooperatively regulate plasma membrane invagination by BAR and F-BAR proteins. Developmental Cell, 9(6), 791–804. http://doi.org/10.1016/j.devcel.2005.11.005

Jin N, Chow CY, Liu L, Zolov SN, Bronson R, Davisson M, Petersen JL, Zhang Y, Park S, Duex JE, Goldowitz D, Meisler MH, Weisman LS. VAC14 nucleates a protein complex essential for the acute interconversion of PI3P and PI(3,5)P(2) in yeast and mouse. EMBO J. 2008 Dec 17;27(24):3221-34. doi: 10.1038/emboj.2008.248.

Kalinderi, K., Bostantjopoulou, S., & Fidani, L. (2016). The genetic background of Parkinson's disease: current progress and future prospects. Acta Neurologica Scandinavica, (7), n/a–n/a. http://doi.org/10.1111/ane.12563

Katona I, Zhang X, Bai Y, Shy ME, Guo J, Yan Q, Hatfield J, Kupsky WJ, Li J.Distinct pathogenic processes between Fig4-deficient motor and sensory neurons.Eur J Neurosci. 2011 Apr;33(8):1401-10. doi: 10.1111/j.1460-9568.2011.07651.

Kim, W. T., Chang, S., Daniell, L., Cremona, O., Di Paolo, G., & De Camilli, P. (2002). Delayed reentry of recycling vesicles into the fusion-competent synaptic vesicle pool in synaptojanin 1 knockout mice. Proceedings of the National Academy of Sciences of the United States of America, 99, 17143–17148. http://doi.org/10.1073/pnas.222657399

Kitada T, Asakawa S, Hattori N, Matsumine H, Yamamura Y, Minoshima S, Yokochi M, Mizuno Y, Shimizu N. Mutations in the parkin gene cause autosomal recessive juvenile parkinsonism. Nature. 1998 Apr 9;392(6676):605-8.

Koyano, F., Okatsu, K., Kosako, H., Tamura, Y., Go, E., Kimura, M., … Matsuda, N. (2014). Ubiquitin is phosphorylated by PINK1 to activate parkin. Nature, 510(7503), 162–6. http://doi.org/10.1038/nature13392

Köroğlu Ç, Baysal L, Cetinkaya M, Karasoy H, Tolun A. DNAJC6 is responsible for juvenile parkinsonism with phenotypic variability. Parkinsonism Relat Disord. 2013 Mar;19(3):320-4. doi: 10.1016/j.parkreldis.2012.11.006.

Krebs CE, Karkheiran S, Powell JC, Cao M, Makarov V, Darvish H, Di Paolo

G,Walker RH, Shahidi GA, Buxbaum JD, De Camilli P, Yue Z, Paisán-Ruiz C. The Sac1 domain of SYNJ1 identified mutated in a family with early-onset progressive Parkinsonism with generalized seizures. Hum Mutat. 2013 Sep;34(9):1200-7. doi: 10.1002/humu.22372.

Kutateladze TG. Translation of the phosphoinositide code by PI effectors. Nat Chem Biol. 2010 Jul;6(7):507-13. doi: 10.1038/nchembio.390. Review.

Lecompte O, Poch O, Laporte J. PtdIns5P regulation through evolution: roles in membrane trafficking? Trends Biochem Sci. 2008 Oct;33(10):453-60. doi: 10.1016/j.tibs.2008.07.002.

Leevers SJ, Vanhaesebroeck B, Waterfield MD. Signalling through phosphoinositide 3-kinases: the lipids take centre stage. Curr Opin Cell Biol. 1999 Apr;11(2):219-25. Review.

Lemmon MA. Phosphoinositide recognition domains. Traffic. 2003 Apr;4(4):201-13. Review.

Lemmon MA, Ferguson KM. Signal-dependent membrane targeting by pleckstrin homology (PH) domains. Biochem J. 2000 Aug 15;350 Pt 1:1-18. Review.

Lenk GM, Ferguson CJ, Chow CY, Jin N, Jones JM, Grant AE, Zolov SN, Winters JJ, Giger RJ, Dowling JJ, Weisman LS, Meisler MH. Pathogenic mechanism of the FIG4 mutation responsible for Charcot-Marie-Tooth disease CMT4J. PLoS Genet. 2011 Jun;7(6):e1002104. doi: 10.1371/journal.pgen.1002104.

Li SC, Diakov TT, Xu T, Tarsio M, Zhu W, Couoh-Cardel S, Weisman LS, Kane PM. The signaling lipid PI(3,5)P_2 stabilizes V_1-V(o) sector interactions and activates the V-ATPase. Mol Biol Cell. 2014 Apr;25(8):1251-62. doi:10.1091/mbc.E13-10-0563.

Jun .Lesage, S., & Brice, A. (2009). Parkinson's disease: From monogenic forms to genetic susceptibility factors. Human Molecular Genetics, 18(R1), 48–59. http://doi.org/10.1093/hmg/ddp012

Lesage S, Brice A. Parkinson's disease: from monogenic forms to genetic susceptibility factors. Hum Mol Genet. 2009 Apr 15;18(R1):R48-59. doi:10.1093/hmg/ddp012. Review.

Levine TP, Munro S. Targeting of Golgi-specific pleckstrin homology domains involves both PtdIns 4-kinase-dependent and -independent components. Curr Biol. 2002 Apr 30;12(9):695-704.

Loi M. Lowe syndrome. Orphanet J Rare Dis. 2006 May 18;1:16. Review.

Lücking CB, Dürr A, Bonifati V, Vaughan J, De Michele G, Gasser T, Harhangi BS, Meco G, Denèfle P, Wood NW, Agid Y, Brice A; French Parkinson's Disease Genetics Study Group; European Consortium on Genetic Susceptibility in

Parkinson's Disease. Association between early-onset Parkinson's disease and mutations in the parkin gene. N Engl J Med. 2000 May 25;342(21):1560-7.

Macphee GJ, Stewart DA. Diagnosis of Parkinsonism in older patients receiving sodium valproate. Mov Disord. 2007 Jun 15;22(8):1211.

Mayinger, P. (2012). Phosphoinositides and vesicular membrane traffic. Biochimica et Biophysica Acta - Molecular and Cell Biology of Lipids, 1821(8), 1104–1113. http://doi.org/10.1016/j.bbalip.2012.01.002

Maguire-Zeiss K. and Federoff H: Convergent pathobiologic model of Parkinson's disease Ann N Y Acad Sci. 2003 Jun;991:152-66. Review.

Manford, A., Xia, T., Saxena, A. K., Stefan, C., Hu, F., Emr, S. D., & Mao, Y. (2010). Crystal structure of the yeast Sac1: implications for its phosphoinositide phosphatase function. The EMBO Journal, 29(9), 1489–1498. http://doi.org/10.1038/emboj.2010.57

Mani M, Lee SY, Lucast L, Cremona O, Di Paolo G, De Camilli P, Ryan TA. The dual phosphatase activity of synaptojanin1 is required for both efficient synaptic vesicle endocytosis and reavailability at nerve terminals. Neuron. 2007 Dec 20;56(6):1004-18.

McBride HM, Rybin V, Murphy C, Giner A, Teasdale R, Zerial M. Oligomeric complexes link Rab5 effectors with NSF and drive membrane fusion via interactions between EEA1 and syntaxin 13. Cell. 1999 Aug 6;98(3):377-86.

Miller RM1, Federoff HJ. Altered gene expression profiles reveal similarities and differences between Parkinson disease and model systems. Neuroscientist. 2005 Dec;11(6):539-49.

McPherson PS, Garcia EP, Slepnev VI, David C, Zhang X, Grabs D, Sossin WS, Bauerfeind R, Nemoto Y, De Camilli P. A presynaptic inositol-5-phosphatase. Nature. 1996 Jan 25;379(6563):353-7.

McPherson PS, Czernik AJ, Chilcote TJ, Onofri F, Benfenati F, Greengard P, Schlessinger J, De Camilli P. Interaction of Grb2 via its Src homology 3 domains with synaptic proteins including synapsin I. Proc Natl Acad Sci U S A. 1994 Jul 5;91(14):6486-90.

McPherson, P. S., Takei, K., Schmid, S. L., & De Camilli, P. (1994). p145, a major Grb2-binding protein in brain, is co-localized with dynamin in nerve terminals where it undergoes activity-dependent dephosphorylation. Journal of Biological Chemistry, 269(48), 30132–30139.

Milosevic, I., Giovedi, S., Lou, X., Raimondi, A., Collesi, C., Shen, H., … De Camilli, P. (2011). Recruitment of endophilin to clathrin-coated pit necks is required for efficient vesicle uncoating after fission. Neuron, 72(4), 587–601.

http://doi.org/10.1016/j.neuron.2011.08.029

Nemoto Y, Arribas M, Haffner C, DeCamilli P. Synaptojanin 2, a novel synaptojanin isoform with a distinct targeting domain and expression pattern. J Biol Chem. 1997 Dec 5;272(49):30817-21.

Narendra DP, Jin SM, Tanaka A, Suen DF, Gautier CA, Shen J, Cookson MR, Youle RJ. PINK1 is selectively stabilized on impaired mitochondria to activate Parkin. PLoS Biol. 2010 Jan 26;8(1):e1000298. doi: 10.1371/journal.pbio.1000298.

Nemani V. M, Lu W., Berge V., Nakamura K., Onoa B., Lee M. K., Chaudhry F. A., Nicoll R. A., and Edwards R. H. Increased Expression of Alpha-Synuclein Reduces Neurotransmitter Release by Inhibiting Synaptic Vesicle Reclustering After Endocytosis Neuron. 2010 January 14; 65(1): 66–79. doi:10.1016/j.neuron.2009.12.023

Nicholson G, Lenk GM, Reddel SW, Grant AE, Towne CF, Ferguson CJ, Simpson E, Scheuerle A, Yasick M, Hoffman S, Blouin R, Brandt C, Coppola G, Biesecker LG, Batish SD, Meisler MH. Distinctive genetic and clinical features of CMT4J: a severe neuropathy caused by mutations in the PI(3,5)P_2 phosphatase FIG4. Brain. 2011 Jul;134(Pt 7):1959-71. doi: 10.1093/brain/awr148.Nicot AS, Laporte J. Endosomal phosphoinositides and human diseases. Traffic. 2008 Aug;9(8):1240-9. doi: 10.1111/j.1600-0854.2008.00754.x. Epub 2008 Apr 21.Review.

Osborne SL, Wen PJ, Meunier FA. Phosphoinositide regulation of neuroexocytosis: adding to the complexity. J Neurochem. 2006 Jul;98(2):336-42. Review.

Owen, D. J., Collins, B. M., & Evans, P. R. (2004). ADAPTORS FOR CLATHRIN COATS: Structure and Function. Annual Review of Cell and Developmental Biology, 20(1), 153–191. http://doi.org/10.1146/annurev.cellbio.20.010403.104543

Parisi S, Cozzuto L, Tarantino C, Passaro F, Ciriello S, Aloia L, Antonini D, De Simone V, Pastore L, Russo T. Direct targets of Klf5 transcription factor contribute to the maintenance of mouse embryonic stem cell undifferentiated state. BMC Biol. 2010 Sep 27;8:128. doi: 10.1186/1741-7007-8-128.

Patzko, Agnes, & Shy, M. E. (2011). Update on Charcot-Marie-Tooth disease. Current Neurology and Neuroscience Reports, 11(1), 78–88. http://doi.org/10.1007/s11910-010-0158-7

Perera, R. M., Zoncu, R., Lucast, L., De Camilli, P., & Toomre, D. (2006). Two synaptojanin 1 isoforms are recruited to clathrin-coated pits at different stages. Proceedings of the National Academy of Sciences of the United States of America, 103(51), 19332–7. http://doi.org/10.1073/pnas.0609795104

Polymeropoulos MH, Lavedan C, Leroy E, Ide SE, Dehejia A, Dutra A, Pike B,Root H, Rubenstein J, Boyer R, Stenroos ES, Chandrasekharappa S, Athanassiadou A,Papapetropoulos T, Johnson WG, Lazzarini AM, Duvoisin RC, Di Iorio G, Golbe LI, Nussbaum RL. Mutation in the alpha-synuclein gene identified in families with Parkinson's disease. Science. 1997 Jun 27;276(5321):2045-7.

Praefcke GJ, Ford MG, Schmid EM, Olesen LE, Gallop JL, Peak-Chew SY, Vallis Y, Babu MM, Mills IG, McMahon HT. Evolving nature of the AP2 alpha-appendage hub during clathrin-coated vesicle endocytosis. EMBO J. 2004 Nov 10;23(22):4371-83.

Quadri M, Fang M, Picillo M, Olgiati S, Breedveld GJ, Graafland J, Wu B, Xu F, Erro R, Amboni M, Pappatà S, Quarantelli M, Annesi G, Quattrone A, Chien HF, Barbosa ER; International Parkinsonism Genetics Network, Oostra BA, Barone P, Wang J, Bonifati V. Mutation in the SYNJ1 gene associated with autosomal recessive, early-onset Parkinsonism. Hum Mutat. 2013 Sep;34(9):1208-15. doi:10.1002/humu.22373.

Raiborg C, Bache KG, Gillooly DJ, Madshus IH, Stang E, Stenmark H. Hrs sorts ubiquitinated proteins into clathrin-coated microdomains of early endosomes. Nat Cell Biol. 2002 May;4(5):394-8.

Ramirez A, Heimbach A, Gründemann J, Stiller B, Hampshire D, Cid LP, Goebel I, Mubaidin AF, Wriekat AL, Roeper J, Al-Din A, Hillmer AM, Karsak M, Liss B, Woods CG, Behrens MI, Kubisch C. Hereditary parkinsonism with dementia is caused by mutations in ATP13A2, encoding a lysosomal type 5 P-type ATPase. Nat Genet. 2006 Oct;38(10):1184-91

Ramjaun, A. R., & McPherson, P. S. (1996). Tissue-specific alternative splicing generates two synaptojanin isoforms with differential membrane binding properties. Journal of Biological Chemistry, 271(40), 24856–24861. http://doi.org/10.1074/jbc.271.40.24856

Reilly, M. M., Ead, S., Murphy, M., & Lau, M. (2011). Charcot-Marie-Tooth disease. J Peripher Nerv Syst, 16, 1–14. http://doi.org/10.1111/j.1529-8027.2011.00324.x

Robertson RG, Clarke CA, Boyce S, Sambrook MA, Crossman AR. The role of striatopallidal neurones utilizing gamma-aminobutyric acid in the pathophysiology of MPTP-induced parkinsonism in the primate: evidence from [3H]flunitrazepamautoradiography. Brain Res. 1990 Oct 29;531(1-2):95-104.

Roth, M. G. (2004). Phosphoinositides in constitutive membrane traffic. Physiological Reviews, 84(3), 699–730. http://doi.org/10.1152/physrev.00033.2003

Roy A, Levine TP. Multiple pools of phosphatidylinositol 4-phosphate detected using the pleckstrin homology domain of Osh2p. J Biol Chem. 2004 Oct

22;279(43):44683-9.

Rudge SA, Anderson DM, Emr SD. Vacuole size control: regulation of PtdIns(3,5)P2 levels by the vacuole-associated Vac14-Fig4 complex, a PtdIns(3,5)P2-specific phosphatase. Mol Biol Cell. 2004 Jan;15(1):24-36.

Saarikangas J, Zhao H, Lappalainen P. Regulation of the actincytoskeleton-plasma membrane interplay by phosphoinositides. Physiol Rev. 2010 Jan;90(1):259-89. doi: 10.1152/physrev.00036.2009. Review.

Saporta, A. S. D., Sottile, S. L., Miller, L. J., Feely, S. M. E., Siskind, C. E., & Shy, M. E. (2011). Charcot-marie-tooth disease subtypes and genetic testing strategies. Annals of Neurology, 69(1), 22–33. http://doi.org/10.1002/ana.22166

Sbrissa, D., Ikonomov, O. C., Fu, Z., Ijuin, T., Gruenberg, J., Takenawa, T., & Shisheva, A. (2007). Core protein machinery for mammalian phosphatidylinositol 3,5-bisphosphate synthesis and turnover that regulates the progression of endosomal transport: Novel Sac phosphatase joins the ArPIKfyve-PIKfyve complex. Journal of Biological Chemistry, 282(33), 23878–23891. http://doi.org/10.1074/jbc.M611678200

Sbrissa D, Ikonomov OC, Fenner H, Shisheva A. ArPIKfyve homomeric and heteromeric interactions scaffold PIKfyve and Sac3 in a complex to promote PIKfyve activity and functionality. J Mol Biol. 2008 Dec 26;384(4):766-79. doi: 10.1016/j.jmb.2008.10.009.

Shewan A, Eastburn DJ, Mostov K. Phosphoinositides in cell architecture. Cold Spring Harb Perspect Biol. 2011 Aug 1;3(8):a004796. doi:10.1101/cshperspect.a004796. Review.

Shimura, H., Hattori, N., Kubo, S. I., Mizuno, Y., Asakawa, S., Minoshima, S., … Suzuki, T. (2000). Familial Parkinson disease gene product, parkin, is a ubiquitin-protein ligase. Nature Genetics, 25(3), 302–

Shy ME, Blake J, Krajewski K, Fuerst DR, Laura M, Hahn AF, Li J, Lewis RA, Reilly M. Reliability and validity of the CMT neuropathy score as a measure of disability. Neurology. 2005 Apr 12;64(7):1209-14. 305. http://doi.org/10.1038/77060

Simon A. Rudge, Deborah M. Anderson, and Scott D. Emr Vacuole Size Control: Regulation of PtdIns(3,5)P2 Levels by the Vacuole-associated Vac14-Fig4 Complex, a PtdIns(3,5)P2-specific Phosphatase Molecular Biology of the Cell Vol. 15, 24–36, January 2004

Simonsen A, Gaullier JM, D'Arrigo A, Stenmark H. The Rab5 effector EEA1 interacts directly with syntaxin-6. J Biol Chem. 1999 Oct 8;274(41):28857-60.

Singleton, A. B., Farrer, M. J., & Bonifati, V. (2013). The genetics of Parkinson's

disease: progress and therapeutic implications. Movement Disorders : Official Journal of the Movement Disorder Society, 28(1), 14–23. http://doi.org/10.1002/mds.25249

Siskind, C. E., Panchal, S., Smith, C. O., Feely, S. M. E., Dalton, J. C., Schindler, A. B., & Krajewski, K. M. (2013). A review of genetic counseling for charcot marie tooth disease (CMT). Journal of Genetic Counseling, 22(4), 422–436. http://doi.org/10.1007/s10897-013-9584-4

Soda K, Balkin DM, Ferguson SM, Paradise S, Milosevic I, Giovedi S, Volpicelli-Daley L, Tian X, Wu Y, Ma H, Son SH, Zheng R, Moeckel G, Cremona O, Holzman LB, De Camilli P, Ishibe S. Role of dynamin, synaptojanin, and endophilin in podocyte foot processes. J Clin Invest. 2012 Dec;122(12):4401-11. doi: 10.1172/JCI65289.

Stefan CJ, Audhya A, Emr SD. The yeast synaptojanin-like proteins control the cellular distribution of phosphatidylinositol (4,5)-bisphosphate. Mol Biol Cell. 2002 Feb;13(2):542-57.

Sun, Y., Tawara, I., Zhao, M., Qin, Z. S., Toubai, T., Mathewson, N., … Reddy, P. (2013). Allogeneic T cell responses are regulated by a specific miRNA-mRNA network. Journal of Clinical Investigation, 123(11), 4739–4754. http://doi.org/10.1172/JCI70013

Takatori S, Tatematsu T, Cheng J, Matsumoto J, Akano T, Fujimoto T. Phosphatidylinositol 3,5-Bisphosphate-Rich Membrane Domains in Endosomes and Lysosomes. Traffic. 2016 Feb;17(2):154-67.

Tazir, M., Bellatache, M., Nouioua, S., & Vallat, J.-M. (2013). Autosomal recessive Charcot-Marie-Tooth disease: from genes to phenotypes. Journal of the Peripheral Nervous System, 18(2), 113–29. http://doi.org/10.1111/jns5.12026

Thomas, B., & Flint Beal, M. (2007). Parkinson's disease. Human Molecular Genetics, 16(R2), 183–194. http://doi.org/10.1093/hmg/ddm159

Tritarelli, A., Oricchio, E., Ciciarello, M., Mangiacasale, R., Palena, A., Lavia, P., … Cundari, E. (2004). p53 Localization at Centrosomes during Mitosis and Postmitotic Checkpoint Are ATM-dependent and Require Serine 15 Phosphorylation. Molecular Biology of the Cell, 15(April), 3751–3737. http://doi.org/10.1091/mbc.E03

Tronchère H, Laporte J, Pendaries C, Chaussade C, Liaubet L, Pirola L, Mandel JL, Payrastre B. Production of phosphatidylinositol 5-phosphate by the phosphoinositide 3-phosphatase myotubularin in mammalian cells. J Biol Chem. 2004 Feb 20;279(8):7304-12.

Vaccari I, Carbone A, Previtali SC, Mironova YA, Alberizzi V, Noseda R,Rivellini C,

Bianchi F, Del Carro U, D'Antonio M, Lenk GM,Wrabetz L, Giger RJ, Meisler MH, Bolino A. Loss of Fig4 in both Schwann cells and motor neurons contributes to CMT4J neuropathy. Hum Mol Genet. 2015 Jan 15;24(2):383-96. doi: 10.1093/hmg/ddu451.

Valente, E. M., Salvi, S., Ialongo, T., Marongiu, R., Elia, A. E., Caputo, V., … Bentivoglio, A. R. (2004). PINK1 mutations are associated with sporadic early-onset Parkinsonism. Annals of Neurology, 56(3), 336–341. http://doi.org/10.1002/ana.20256

Van Epps, H. A. (2004). The Zebrafish nrc Mutant Reveals a Role for the Polyphosphoinositide Phosphatase Synaptojanin 1 in Cone Photoreceptor Ribbon Anchoring. Journal of Neuroscience, 24(40), 8641–8650. http://doi.org/10.1523/JNEUROSCI.2892-04.2004

Vicinanza M, D'Angelo G, Di Campli A, De Matteis MA. Function and dysfunction of the PI system in membrane trafficking. EMBO J. 2008 Oct 8;27(19):2457-70. doi: 10.1038/emboj.2008.169.

Vicinanza M, Di Campli A, Polishchuk E, Santoro M, Di Tullio G, Godi A, Levtchenko E, De Leo MG, Polishchuk R, Sandoval L, Marzolo MP, De Matteis MA. OCRL controls trafficking through early endosomes via PtdIns4,5P_2-dependent regulation of endosomal actin. EMBO J. 2011 Oct 4;30(24):4970-85. doi: 10.1038/emboj.2011.354.

Vieira OV, Harrison RE, Scott CC, Stenmark H, Alexander D, Liu J, Gruenberg J, Schreiber AD, Grinstein S. Acquisition of Hrs, an essential component of phagosomal maturation, is impaired by mycobacteria. Mol Cell Biol. 2004 May;24(10):4593-604.

Vilariño-Güell C, Wider C, Ross OA, Dachsel JC, Kachergus JM, Lincoln SJ, Soto-Ortolaza AI, Cobb SA, Wilhoite GJ, Bacon JA, Behrouz B, Melrose HL, Hentati E, Puschmann A, Evans DM, Conibear E, Wasserman WW, Aasly JO, Burkhard PR, Djaldetti R, Ghika J, Hentati F, Krygowska-Wajs A, Lynch T, Melamed E, Rajput A, Rajput AH, Solida A, Wu RM, Uitti RJ, Wszolek ZK, Vingerhoets F, Farrer MJ. VPS35 mutations in Parkinson disease. Am J Hum Genet. 2011 Jul 15;89(1):162-7. doi:10.1016/j.ajhg.2011.06.001. Erratum in: Am J Hum Genet. 2011 Aug 12;89(2):347.

Watt SA, Kular G, Fleming IN, Downes CP, Lucocq JM. Subcellular localization of phosphatidylinositol 4,5-bisphosphate using the pleckstrin homology domain of phospholipase C delta1. Biochem J. 2002 May 1;363(Pt 3):657-66.

Waugh MG. PIPs in neurological diseases. Biochim Biophys Acta. 2015

Aug;1851(8):1066-82. doi: 10.1016/j.bbalip.2015.02.002. Epub 2015 Feb 11. Review

Wenk, M. R., & De Camilli, P. (2004). Protein-lipid interactions and phosphoinositide metabolism in membrane traffic: insights from vesicle recycling in nerve terminals. Proceedings of the National Academy of Sciences of the United States of America, 101(22), 8262–9. http://doi.org/10.1073/pnas.0401874101

Whiteford CC, Brearley CA, Ulug ET. Phosphatidylinositol 3,5-bisphosphate defines a novel PI 3-kinase pathway in resting mouse fibroblasts. Biochem J. 1997 May 1;323 (Pt 3):597-601.

Yin HL, Janmey PA. Phosphoinositide regulation of the actin cytoskeleton. Annu Rev Physiol. 2003;65:761-89. Epub 2002 May 1. Review.

Zhang, X., Chow, C. Y., Sahenk, Z., Shy, M. E., Meisler, M. H., & Li, J. (2008). Mutation of FIG4 causes a rapidly progressive, asymmetric neuronal degeneration. Brain, 131(8), 1990–2001. http://doi.org/10.1093/brain/awn114

Zhang, Y., McCartney, A. J., Zolov, S. N., Ferguson, C. J., Meisler, M. H., Sutton, M. a, & Weisman, L. S. (2012). Modulation of synaptic function by VAC14, a protein that regulates the phosphoinositides PI(3,5)P2 and PI(5)P. The EMBO Journal, 31(16), 3442–3456. http://doi.org/10.1038/emboj.2012.200

Zhang Y, Zolov SN, Chow CY, Slutsky SG, Richardson SC, Piper RC, Yang B, Nau JJ, Westrick RJ, Morrison SJ, Meisler MH, Weisman LS. Loss of Vac14, a regulator of the signaling lipid phosphatidylinositol 3,5-bisphosphate, results in neurodegeneration in mice. Proc Natl Acad Sci U S A. 2007 Oct 30;104(44):17518-23. Epub 2007 Oct 23.Zigmond MJ, Burke RE (2002) Pathophysiology of parkinson's disease.In: Fifth generation of progress (Davis KL, Coyle J, Charney D, Nemeroff C, eds), pp 1781–1794. American College of Neuropsychopharmacology. Philadelphia: Lippincott, Williams and Wilkens.

Zimprich A, Biskup S, Leitner P, Lichtner P, Farrer M, Lincoln S, Kachergus J, Hulihan M, Uitti RJ, Calne DB, Stoessl AJ, Pfeiffer RF, Patenge N, Carbajal IC, Vieregge P, Asmus F, Müller-Myhsok B, Dickson DW, Meitinger T, Strom TM, Wszolek ZK, Gasser T. Mutations in LRRK2 cause autosomal-dominant parkinsonism with pleomorphic pathology. Neuron. 2004 Nov 18;44(4):601-7

Zimprich A, Benet-Pagès A, Struhal W, Graf E, Eck SH, Offman MN, Haubenberger D, Spielberger S, Schulte EC, Lichtner P, Rossle SC, Klopp N, Wolf E, Seppi K, Pirker W, Presslauer S, Mollenhauer B, Katzenschlager R, Foki T, Hotzy C, Reinthaler E, Harutyunyan A, Kralovics R, Peters A, Zimprich F, Brücke T, Poewe W, Auff E, Trenkwalder C, Rost B, Ransmayr G, Winkelmann J, Meitinger T, Strom TM. A mutation in VPS35, encoding a subunit of the retromer complex, causes late-onset Parkinson disease. Am J Hum Genet. 2011 Jul 15;89(1):168-75. doi: 10.1016/j.ajhg.2011.06.008.